Final Report for Period 1999-2001

Basic and Applied Studies of the Ram Accelerator as a High Performance Launcher

ARO Grant No.:
DAAG55-97-0131

Carl Knowlen, Research Scientist
Adam P. Bruckner, Principal Investigator

Aerospace and Energetics Research Program
University of Washington, Box 352250

Submitted to:

U.S. Army Research Office
P.O. Box 12211
Research Triangle Park, NC 27709-2211

June 28, 2001

APPROVED FOR PUBLIC RELEASE;
DISTRIBUTION UNLIMITED

REPORT DOCUMENTATION PAGE

Form Approved
OMB NO. 0704-0188

1. AGENCY USE ONLY (Leave Blank)	2. REPORT DATE	3. REPORT TYPE AND DATES COVERED
	28 June 2001	Final 01 Apr 97 – 28 Feb 01

4. TITLE AND SUBTITLE
Basic and Applied Studies of the Ram Accelerator as a High Performance Launcher

5. FUNDING NUMBERS
DAAG55-97-1-0131

6. AUTHOR(S)
Carl Knowlen, Adam Bruckner

7. PERFORMING ORGANIZATION NAME(S) AND ADDRESS(ES)

8. PERFORMING ORGANIZATION REPORT NUMBER

9. SPONSORING / MONITORING AGENCY NAME(S) AND ADDRESS(ES)
U. S. Army Research Office
P.O. Box 12211
Research Triangle Park, NC 27709-2211

10. SPONSORING / MONITORING AGENCY REPORT NUMBER
37211-EG

11. SUPPLEMENTARY NOTES
The views, opinions and/or findings contained in this report are those of the author(s) and should not be construed as an official Department of the Army position, policy or decision, unless so designated by other documentation.

12 a. DISTRIBUTION / AVAILABILITY STATEMENT
Approved for public release; distribution unlimited.

12 b. DISTRIBUTION CODE

13. ABSTRACT (Maximum 200 words)

The ram accelerator is a hypervelocity launch concept that uses a confined, in-tube ramjet propulsive cycle to generate thrust for the acceleration of a projectile. Key technical issues involving the starting and operation of the ram accelerator were investigated at fill pressures up to 200 atmospheres. The research was initiated to evaluate the feasibility of using a ram accelerator of limited length for specific applications, e.g. mobile or ship-based. In particular, it was determined that modification to both projectile materials and configurations were necessary to ensure operation at the highest mixture fill pressures. The report summarizes the results of that investigation.

14. SUBJECT TERMS	15. NUMBER OF PAGES
	16. PRICE CODE

17. SECURITY CLASSIFICATION OR REPORT	18. SECURITY CLASSIFICATION ON THIS PAGE	19. SECURITY CLASSIFICATION OF ABSTRACT	20. LIMITATION OF ABSTRACT
UNCLASSIFIED	UNCLASSIFIED	UNCLASSIFIED	UL

Table of Contents

Summary of Ram Accelerator Research for Period: 1999 - 2000

Introduction

Key technical issues involving the starting and operation of the ram accelerator at fill pressures up to 200 atm have been theoretically and experimentally investigated at the University of Washington over the two year period from January 1999 to December 2000. This research was initiated to evaluate the feasibility of fielding ship-based ram accelerator launching systems for direct fire support. The primary results of this investigation are summarized and the pertinent technical publications produced in the course of this effort are included as appendices. Two aspects of high pressure operation were discovered that may not warrant a patent application in their own right, but are sufficiently obscure that withholding publication of their details would significantly impair any potential competitors in developing high performance ram accelerator capabilities.

The ram accelerator is a hypervelocity launcher that uses in-tube ramjet propulsive cycles to generate thrust for projectiles [1-5]. The thrust is proportional to the fill pressure and increases with increasing heat release from propellant combustion. Highest possible performance for a given projectile mass is thus obtained by using the maximum fill pressure the facility can accommodate along with the most energetic propellant that will sustain ram acceleration. Dense gaseous propellants impose severe structural and aerothermal heating concerns for the projectile in addition to logistical issues of penetrating thick diaphragms and starting the ram accelerator. Whereas the real gas effects alter the sound speed and kinetic rates of the propellant which cause the chemical energy release as a function of projectile velocity to be quite different than predicted from ideal gas calculations. Since naval ram accelerator weapon systems are expected to require fill pressures in the 150-300 atm range [6], it is imperative to understand the impact of the real gas effects on ram accelerator operation. Thus the University of Washington 38-mm-bore ram accelerator facility was modified to enable experimentation at fill pressures up to 200 atm; a pressure level at which real gas effects are very significant yet within the bounds of what can be safely handled in the laboratory without having to make extensive facility modifications. The details of the UW facility upgrade can be found in Appendix A and drawings of the projectiles used in the experiments are attached as Appendix E.

Projectile design modifications that enable ram accelerator operation with fill pressures up to 200 atm have been determined. A summary of the key findings is presented in this section of the report along with some experimental data at 200 atm that have not yet been publicly disseminated. A complete list of all ram accelerator technical papers published by the UW research team during this reporting period is also included. The details of the experimental procedures and results from the early phase of the research program in which the goal was to achieve operation in 150 atm propellant are presented in Appendix B. The subsequent research which ultimately led to understanding the projectile geometry requirements for 200 atm operation is discussed in detail in Appendix C, and the primary results of 4-m-long experiments in 200 atm propellant are presented in Appendix D. The data log of all high pressure experiments conducted during the reporting time frame are included in Appendix F.

Experimental Results Leading to Operation at 150 atm

It was found that projectiles having a throat diameter of 29 mm could be started in the ram accelerator at entrance velocities of 1120-1150 m/s in propellants having fill pressures up to 77 atm. At fill pressures greater than 85 atm, however, the entrance velocity had to be at least 1270 m/s before the ram accelerator could be successfully started [7]. The term "successfully started" is used here to indicate that the projectile accelerated at least 1 m beyond the entrance diaphragm to the test section. Due to structural limitations (thin-walled nosecone and afterbody) of the low-mass projectiles used in the higher entrance velocity experiments, immediate nosecone collapse is suspected to be the primary cause of start attempt failures at fill pressures greater than 110 atm. Schematics showing the external geometry of these projectiles are in Appendix A and more detailed drawings showing internal configurations are in Appendix E.

It was also observed during the course of these experiments that the acceleration level in the first meter of operation was relatively weak when compared to the real gas calculations for the thermally choked ram accelerator. After about a meter of travel the projectile acceleration would then increase significantly and behave in a manner much closer to that expected for thermally choked operation. This starting "lag" was not very sensitive to chemistry changes, however, it was affected by the perforation ratio of the obturator (open area of obturator to tube bore area). A series of 75 atm experiments was conducted in which the perforation ratio was reduced from 42% until a successful start could not be achieved. Ultimately a 23% perforation ratio was found to be reliable for starting the ram accelerator and reducing the starting lag, as shown in Appendix B. This obturator configuration (16 gm perforated cylinder plus 3 gm solid disk) was then used in all experiments below 150 atm.

Successful starts at fill pressures in the 100-150 atm range at an entrance velocity of 1300 m/s were achieved with magnesium alloy projectiles having both a solid nosecone and a throat diameter that was reduced to 25 mm (Drawings 1017, 1020, 1024, and 1025 in Appendix E). No attempt to conduct high pressure experiments with solid nosecone, low mass projectiles having 29 mm throat diameter have been made, thus the minimum entrance velocity requirement for this particular external geometry at fill pressures above 110 atm has not yet been determined. Conclusions from this phase of the work are that the minimum starting velocity of the ram accelerator increases with increasing fill pressure and that reducing the projectile throat diameter may enable a lower entrance velocity for starting at elevated pressure. The two most likely explanations for this outcome are; 1) the sound speed increases in a non-linear manner with increasing fill pressure, 2) the obturator-to-propellant density ratio decreases with increasing fill pressure. Why these effects are significant is addressed later, more details on the experimental results of this phase of the research program can be found in Appendix B.

Experimental Results at 150 - 200 atm

After establishing the need for smaller throat diameter and higher entrance velocity for starting the ram accelerator at fill pressures of 150 atm, titanium alloy projectiles having a 25 mm throat diameter, 12.5° half angle nosecone, and 51 mm afterbody length were fabricated and tested to determine their operating characteristics over the 4 m length of the test section (Drawing 1026 in Appendix E; note that nosecone angle was modified from 10° to 12.5°). It was found that the solid nosecone Ti projectiles would only operate for a distance of about 3 m in 150 atm

propellant before becoming too severely canted to continue accelerating. In subsequent experiments using a Ti projectile afterbody that was lengthened from 51 mm to 76 mm to enhance stability (Drawing 1034 in Appendix E), continuous acceleration throughout the 4 m long test section in 150 atm propellant was readily achieved. Details of these experiments can be found in Appendix C.

In order to launch massive Ti projectiles to the desired entrance velocity for 150 atm experiments, the breech pressure was maximized (400 atm) and the perforated obturators were found to be not strong enough to withstand the launch loads. Therefor a solid 18 gm polycarbonate obturator was employed. The solid obturator was used with all the Ti projectiles in the 150 atm experiments and a 0.5-1.0 m lag in the starting process was always observed. It should be noted that even though there is a lag present in the starting process, the acceleration is still on the order of 10,000 g during this period (theoretical acceleration is ~100,000 g). This initial acceleration at 150 atm could not be significantly increased by decreasing the propellant inert dilution (i.e., increasing heat release and reducing induction time) because the start process would immediately fail.

Experiments with Mg alloy projectiles in 150-200 atm propellants demonstrated them to be durable enough to examine geometry and entrance velocity variation effects on the starting process at these fill pressures. This enabled rapid prototyping of different projectile configurations and the determination of the minimum conditions necessary to effect starting of the ram accelerator at 200 atm. The primary outcomes of these experiments were to find that the projectile throat diameter had to be reduced to 23 mm and that the entrance velocity could be reduced to ~1200 m/s while still enabling starting of ram accelerator in 200 atm propellant. This phase of the research program is discussed in more detail in Appendix C.

Ram Accelerator Operation at 200 atm

Having previously determined; the minimum starting velocity (1200 m/s), maximum throat diameter (23 mm), and the need for as long of afterbody as possible (for stability purposes) to enable ram accelerator operation at 200 atm for at least 1 m, Ti alloy and bimetallic (titanium/aluminum) projectiles were fabricated which had the maximum afterbody length feasible while being constrained to not be more massive than 118 gm. This resulted in the all Ti alloy projectile having an afterbody length of 76 mm (118 gm) and the Ti/Al bimetallic projectile having a length of 94 mm (114 gm), as shown in Drawings 1034 and 1037, respectively (see Appendix E). The throat and base diameters of both projectiles were 23 mm and 18 mm, respectively, thus the taper angle of the bodies were slightly different (which proved to not be significant). The front half of the bimetallic projectile (Drawing 1035-1) was manufactured from Ti alloy with the same nosecone half angle (12.5°) and leading edge fin geometry (20° rake angle, 15° knife edge) as the all Ti projectiles. The rear afterbody (Drawing 1036-1) was manufactured from Al alloy to allow for longer fins for enhanced stability without incurring any mass penalty. The disadvantage of the bimetallic projectile is that the intense aerothermal environment at high pressure would erode the aluminum fins more quickly than those made of titanium; however, it allows a significant increase in fin length without any increase in mass. When the afterbody length of the bimetallic projectile was reduced to 76 mm, it had a mass of approximately 102 gm.

The first experiment with the all Ti projectile demonstrated that it would easily operate for 4 m in 150 atm propellant with an entrance velocity of ~1200 m/s (exit velocity was 1860 m/s). Subsequent experiments at 200 atm with the same entrance velocity were unsuccessful in starting the ram accelerator. Reducing the afterbody length to lower projectile mass to 105 gm and allow higher entrance velocities of 1230-1240 m/s produced some performance improvement, however, stable ram accelerator operation much beyond 1 m of the test section entrance was still not achieved under these conditions.

Since increasing the entrance velocity only marginally increased the distance over which the projectile could be accelerated, two-stage experiments were carried out in which the first meter of the test section contained 150 m propellant and the last 3 m were filled to 200 atm. With entrance velocities of 1200-1220 m/s, the 118 gm Ti alloy projectiles ran smoothly throughout the test section and had exit velocities of ~2100 m/s (~46,000 g in second stage). Thus the 76 mm long Ti alloy projectile could readily sustain ram accelerator operation at 200 atm, if it could somehow first get started. Details of these experiments are presented in Appendix D.

Unpublished Bimetallic Projectile Experiments

Two-stage experiments using 1 m of 150 atm and 3 m of 200 atm propellant were carried out with the Ti/Al bimetallic projectiles having an afterbody length of 76 mm and mass of 102 gm for comparison purposes. In the first bimetallic experiment, the projectile entered at 1250 m/s and accelerated throughout the 4 m long test section, reaching an exit velocity of 2340 m/s (63,000 g in second stage). Velocity-distance data from this experiment and the corresponding one using the Ti projectile are shown in Fig. 1. The bimatallic performance was ~20% better over 4 m of operation than that achieved with the all Ti projectile when the 15% difference in mass is included (102 vs. 118 gm). Subsequent experiments showed this extraordinary performance was repeatable over the first 3 m of the test section; however, it would only accelerate throughout the last meter 33% of the time without unstarting. Tube wall electromagnetic data indicated that these projectiles were severely canted before experiencing an

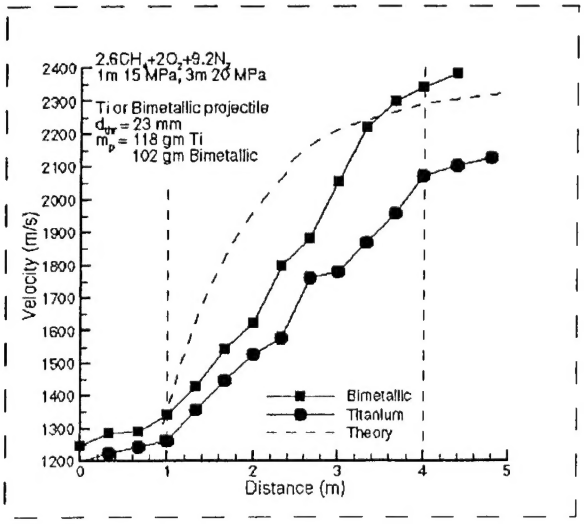

Fig. 1 Velocity-distance data from two stage experiments using Ti and Ti/Al bimetallic projectiles with 18 gm solid obturator.

unstart. The average acceleration of the bimetallic projectiles over the first 2 m of the 200 atm stage was ~70,000 g, about 50% higher than that achieved by the corresponding Ti alloy projectile over the distance.

Even though only 3 m of reliable ram accelerator operation with the two-stage, 150/200 atm test section configuration were demonstrated with the Ti/Al bimetallic projectile, the extraordinary acceleration is very significant. This is direct evidence that the Al alloy is reacting with the propellant. Since this large difference in experimental thrust has not been seen in experiments with Al alloy projectiles at fill pressures below 50 atm, it is surmised that the rate at which the aluminum is oxidized must be increased significantly at 200 atm fill pressure. It was shown that Ti fins will maintain their integrity under 200 atm operating conditions, thus if titanium-finned projectiles with aluminum surfaces could be manufactured, then it may well be possible to realize the performance enhancement benefits of aluminum combustion without sacrificing the durability of the projectile. For example, in the 4 m long test section of the UW ram accelerator facility, this kind of performance would enable a muzzle velocity of ~2700 m/s to be reached with an entrance velocity of only 1200 m/s. In military applications, the projectile afterbody would probably be coated with aluminum (or any other energetic solid propellant candidate) and the substrate would be of a material that can withstand the rigors of the high pressure ram accelerator operation.

The UW research team [8] and others [9,10] have noted the potential benefits of using metal-enhanced combustion for the ram accelerator, however, no one has yet realized that the performance could be so significantly enhanced using aluminum bodies at high fill pressure. Researchers at ISL have conducted experiments in their 30 mm and 90 mm bore ram accelerators with magnesium afterbody extensions attached to the base of aluminum projectiles and found 40% improvement in thrust at Mach numbers greater than 4, without reducing the time duration in which the aluminum component would maintain its structural integrity. The increased thrust seen in the UW experiments at 200 atm using Al afterbodies begins around Mach 3, thus the overall performance of the ram accelerator is significantly increased over those fabricated from titanium. Based on the ISL results, it is very probable that magnesium afterbody extensions would also be effective in enhancing performance these circumstances. Since the unanticipated discovery of extraordinary thrust at low Mach number using Ti/Al bimetalltic projectiles was a direct consequence of conducting high fill pressure experiments, the experimental data are not being published at this time until a better understanding of the nature of the combustible projectile propulsive cycle is reached and the potential ramifications of these results have been more fully considered.

Unpublished High Pressure Starting Experiments

The last mystery of this phase of ram accelerator research was to determine why the starting process is so difficult at high fill pressures. It turns out that the clues were present in the succession of experiments leading up to operation at 150 atm. The "lag" in starting does not become obvious in the UW ram accelerator facility until the fill pressure exceeds 60 atm; whereas the 30 and 90 mm bore facilities at ISL have reported [10] that a starting lag is always present at any fill pressure they are capable of operating (up to 50 atm). One factor contributing to this difference is the use of a light gas gun pre-launcher in the UW facility versus powder gun launchers used elsewhere. The higher ballistic efficiency of the light gas gun means there is less

stress on the payload and thus a lower obturator mass can be used. A low-mass obturator is kicked back quicker upon entrance to the test section which allows the first stage propellant to be more energetic and possibly more reactive (i.e., shorter induction time, lower ignition energy, etc.). The propellants used in the first stage of the UW facility have generally been tuned to maximize projectile acceleration performance for a given obturator configuration without sacrificing reliability. The ability to use a relatively high energetic propellant in the starting stage enables the ram accelerator process to start very quickly, thus, to within the resolution of the instrument port spacing, no starting lag is observed during routine ram accelerator operations in the UW 38-mm-bore facility at fill pressures less than 60 atm.

The ISL 30-mm-bore facility can successfully start with the same propellant used at the UW, however, it requires a more complicated obturator which undoubtedly affects the starting process and may well account for the starting lag seen in these circumstances [11]. Otherwise, all propellants used in the ISL 30 and 90-mm-bore ram accelerators are much less energetic than those used at the UW, thus some greater degree of lag in the starting process is to be expected. Conversely, ram accelerator experiments in the 25 mm bore facility at Tohoku University do not undergo any lag in the start process when using a similar obturator configuration and the same propellant as that used in the UW facility at fill pressures in the range of 25-50 atm [12]. Thus the starting lag does seem to be strongly correlated with the obturator configuration and propellant heat release.

Within the capabilities of the UW facility, experiments exploring variations in propellant chemistry, projectile geometry, and entrance velocity were successful at initiating and stabilizing ram acceleration directly in 200 atm propellant for 1-2 m of the test section while using the solid 18 gm obturator. Even though the projectile could be readily accelerated in 200 atm propellant for distances somewhat greater than 1 m, the average acceleration was 30% less within the first meter of operation than typically observed under similar circumstances in 150 atm propellant. Why was the higher pressure not generating greater thrust during the start process, even when the propellant had less diluent and thus more heat release? Since prior lower pressure experiments had shown that under some circumstances a minimum amount of propellant heat release was required to effect a successful start in the ram accelerator [13], maybe the combustion process was not being initiated quick enough?

A sequence of 200 atm experiments was commenced in which the solid obturator mass was increased and the projectile length decreased to maintain the same test section entrance velocity (1240-1280 m/s). Successful starts and 4 m operating capability were realized with both the Ti and Ti/Al bimetallic projectiles, as shown in Fig. 2, once the obturator mass was increased by 56% to 28 gm. The starting lag was still evident for the first meter of operation beyond the entrance to the test section; however, the average acceleration (~20,000 g) during this period was nearly 3 times greater than observed in previous 200 atm experiments using less massive obturators. Upon reaching a velocity of 1400 m/s, the thrust suddenly increases for both projectiles as evident by the kink their velocity-distance data. The bimetallic projectile shows significantly enhanced performance from this point onward, and reaches a higher velocity (2400 m/s) at the end of the 4 m long test section. Since these experiments were conducted with the last available projectiles at the end of the research program, the reliability of bimetallic projectiles operating for the whole length of the 4 m long test section in 200 atm propellant has not yet been determined; however, the repeatability of attaining acceleration levels of 70,000 g

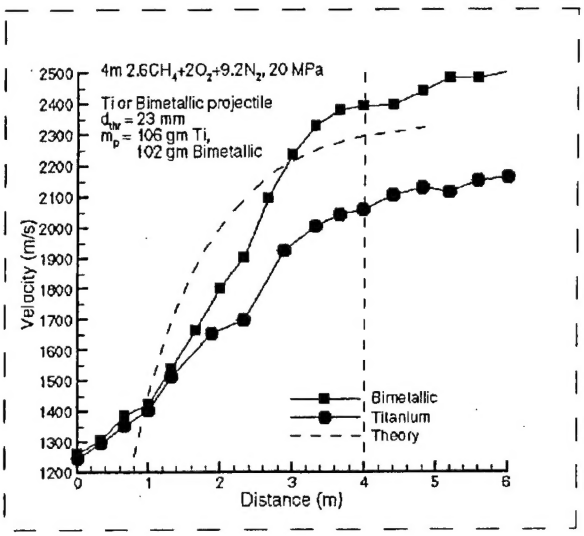

Fig. 2 Velocity-distance data from single stage experiments at 200 atm using Ti and Ti/Al bimetallic projectiles with 28 gm solid obturator.

for at least another 2 m once the projectile gets beyond the effects of the starting process is remarkably good (86% success rate in 7 Ti/Al bimetallic projectile experiments). The limitations of the all Ti projectiles having an afterbody length greater than 58 mm in 200 atm propellant have not yet been determined because they always accelerate throughout the test section once the ram accelerator process has been fully established.

Experiments showed that the projectile would weakly accelerate for 1 m in 200 atm propellant before unstarting when using an 18 gm obturator; however, over 4 m of ram accelerator operation became possible with a significantly more massive obturator. Since the obturator driven shock wave remains on the projectile for a longer period of time in this situation, these results imply that the propellant ignition must be more fully enacted during the starting process before stable ram accelerator operation at 200 atm could be realized. At lower pressures, "weak" ignition was associated with prolonged starting delay, however, the stabilization of the ram accelerator process was not detrimentally affected. The need to rapidly ignite the propellant is a new insight into ram accelerator operation in general, and a key factor for high pressure operation. Consequently, no public dissemination of this aspect of high pressure ram accelerator operation has been released until the program sponsor has had sufficient time to consider the ramifications of these results. Other ways to more quickly ignite the propellant are certainly possible (e.g., ignitors on the tube wall or carried onboard the projectile, higher entrance velocity, short ignition stage, etc.) and reducing or even eliminating the starting lag is a probable outcome of investigating these concepts.

Theoretical Considerations

At fill pressures greater than 50 atm, it becomes necessary to use a real gas equation of state to accurately model the ram accelerator thrust-Mach number performance [14-16]. When real gas effects are accounted for by a non-ideal equation of state, the sound speed of the quiescent propellant varies with fill pressure and thus affects many parameters required for starting the ram accelerator. The variation of sound speed with fill pressure for a typical propellant modeled with

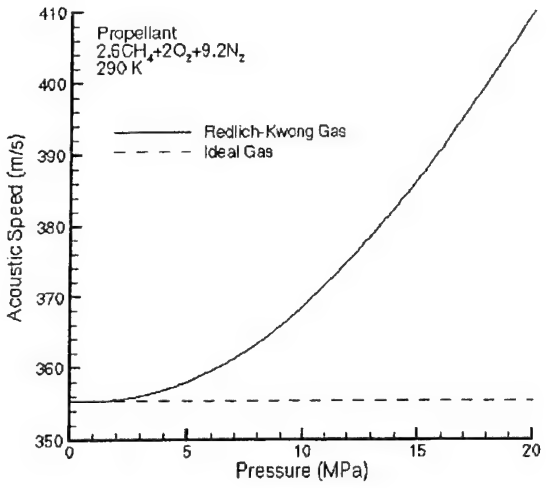

Fig. 3 Variation of $2.6CH_4+2O_2+9.2N_2$ acoustic speed with pressure at 290 K.

the Redlich- Kwong equation of state is shown in Fig. 3. The ideal gas sound speed is also shown in the figure for comparison. The real gas calculations for sound speed account for both the enthalpy deviation from non-ideal gas behavior and the variation of the specific heat capacity with pressure and temperature [17].

The sound speed of the quiescent propellant begins to deviate by 10% from that of an ideal gas at fill pressures above 150 atm. Consequently, the actual flight Mach number is much lower than expected in propellants with high fill pressure which has 3 major impacts on ram accelerator operation. 1) This increases the minimum velocity at which a projectile can travel while maintaining supersonic in its throat, thus the "sonic diffuser unstart" Mach number increases with increasing fill pressure. 2) The minimum entrance velocity must increase to have the projectile enter at above Mach 3, the generally accepted minimum Mach number found in lower pressure experiments at which starting can be accomplished in $CH_4/O_2/N_2$ propellant without the aid of an onboard ignitor. 3) The thrust modeling for high pressure thermally choked ram accelerator operation does not account for the compressibility of the unreacted propellant which leads to an overprediction of the thrust-velocity dependence at high pressure.

The increase in sound speed with increasing fill pressure accounts for the need of higher entrance velocity and reduction in throat diameters. Lower entrance Mach number may also play a role in the need for a more massive obturator to initiate and stabilize the ram accelerator process. It is not yet certain how much of the discrepancy between theoretical and experimental thrust (see Figs. 1 and 2) is due to the compressibility of the quiescent propellant, this is currently being evaluated. Recent theoretical modeling efforts which incorporate unsteady effects into the one-dimensional thrust equation indicate that unsteadiness is a major factor to be considered at acceleration levels over 20,000 g. The theoretical aspects of high pressure ram accelerator operation are still under investigation.

References

1. Hertzberg, A., Bruckner, A.P., and Bogdanoff, D.W., "Ram Accelerator: A New Chemical Method for Accelerating Projectiles to Ultrahigh Velocities," *AIAA J.*, Vol. 26, 1988, pp. 195-203.

2. Bruckner, A.P., Knowlen, C., Hertzberg, A., and Bogdanoff, D.W., "Operational Characteristics of the Thermally Choked Ram Accelerator," *J. Propulsion and Power*, Vol. 7, No. 5, 1991, pp. 828-836.

3. Hertzberg, A., Bruckner, A.P., and Knowlen, C., "Experimental Investigation of Ram Accelerator Propulsion Modes," *Shock Waves*, Vol. 1, 1991, pp. 17-25.

4. Higgins, A.J., Knowlen, C., and Bruckner, A.P., "Ram Accelerator Operating Limits, Part 1: Identification of Limits," *J. Propulsion and Power*, Vol. 14, 1998, pp. 951-958.

5. Higgins, A.J., Knowlen, C., and Bruckner, A.P., "Ram Accelerator Operating Limits, Part 1: Nature of Observed of Limits," *J. Propulsion and Power*, Vol. 14, 1998, pp. 959-966.

6. Kruczynski, D., Liberatore, F., and Nusca, M., "NAVRAM5 - An Analysis of Ram Accelerator for Specific Naval Applications," ARL-TR-1073, April 1996.

7. Shultz, E., Knowlen, C., and Bruckner, A.P., "Starting Envelope of the Subdetonative Ram Accelerator," *J. Propulsion and Power*, Vol. 16, 2000, pp. 1040-1052.

8. Auzias de Turenne, J., "An Analysis of Ram Accelerator Projectile Materials," AIAA Paper 92-0262, 1992.

9. Liberatore, F., "A Preliminary Study of the Solid Fuel In-Bore Ram Accelerator," AIAA Paper 96-2679, 1996.

10. Legendre, J.F. and Giraud, M., "Enhanced RAMAC Performance in Subdetonative Propulsion Mode with Semi-Combustible Projectile," *J. Physique IV*, Vol. 10, 2000, pp. Pr11-23 to Pr11-30.

11. Giraud, M., Legendre, J.F., and Henner, M., "RAMAC in Subdetonative Propulsion Mode: State of the ISL Studies," in *Ram Accelerators*, Takayama, K., and Sasoh, A. (eds), Springer-Verlag, Heidelberg, 1998, pp. 65-78.

12. Sasoh, A., Hamate, Y., and Takayama, K., "Small-Bore Ram Accelerator Operation," *J. Propulsion and Power*, Vol. 17, No. 3, 2001, pp. 622-628.

13. Stewart, J.F., Bruckner, A.P., and Knowlen, C., "Effects of Launch Tube Shock Dynamics on Initiation of Ram Accelerator Operation," in *Ram Accelerators*, Takayama K., and Sasoh, A. (eds), Springer-Verlag, Heidelberg, 1998, pp.181-189.

14. Bauer, P., Legendre, J.-F., Henner, M., and Giraud, M. "Real Gas Effects in Ram Accelerator Propellant Mixtures: Theoretical concepts and Applied Numerical Codes," in *Ram Accelerators*, Takayama K., and Sasoh, A. (eds), Springer-Verlag, Heidelberg, 1998, pp. 39-52.

15. Buckwalter, D.L., Knowlen, C., and Bruckner, A.P., "Real Gas Effects on Thermally Choked Ram Accelerator Performance," in *Ram Accelerators*, Takayama K., and Sasoh, A. (eds), Springer-Verlag, Heidelberg, 1998, pp.125-134.

16. Bundy, C., Knowlen, C., and Bruckner, A.P., "Ram Accelerator Operating Characteristics at Fill Pressures Greater than 10 MPa," AIAA Paper 99-2261, June 1999.

17. Cengel, Y., and Boles, M., *Thermodynamics: An Engineering Approach, 2nd Edition,* McGraw-Hill, New York, 1994, pp. 629-690.

Ram Accelerator Publications from January 1999 to December 2000

Schultz, E., Knowlen, C., and Bruckner, A.P., "Obturator and Detonation Experiments in the Subdetonative Ram Accelerator," *Shock Waves*, Vol. 9, 1999, pp 181-191.

Bundy, C., Knowlen, C., and Bruckner, A.P., "Ram Accelerator Operating Characteristics at Fill Pressures Greater than 10 MPa," AIAA Paper 99-2261, June 1999.

Kruczynski, D., Knowlen, C., Bundy, C., and Bruckner, A.P., "Low Velocity Start of Ram Accelerator: Obturator and Ignitor Effects," AIAA Paper 99-2265, June 1999.

Knowlen, C., Bundy, C., Schwab, R, and Bruckner, A.P., "University of Washington Ram Accelerator Facility," 50th Meeting of the Aeroballistic Range Association, Pleasanton, CA, October 1999.

Bundy, C., Knowlen, C., and Bruckner, A.P., "Investigation of Ram Accelerator Operation at Fill Pressures up to 20 MPa," AIAA Paper 2000-3231, July 2000.

Bundy, C., Knowlen, C., and Bruckner, A.P., "Ram Accelerator Operating Characteristics at Elevated Fill Pressures," *J. Physique IV*, Vol. 10, 2000, pp. Pr11-11 to Pr11-21.

Knowlen, C., Bundy, C., Bruckner, A.P., and Kruczynski, D., "Investigation of Obturator and Ignitor Effects on Low Velcoity Starting of the Ram Accelerator," *J. Physique IV*, Vol. 10, 2000, pp. Pr11-49 to Pr11-58.

Bauer, P, Knowlen, C., Bruckner, A.P., Henner, M., Legendre, J.F., and Giraud, M. , "Determination of the Choke Pressure of a Ram Accelerator Projectile in subdetonative Regime," *J. Physique IV*, Vol. 10, 2000, pp. Pr11-59 to Pr11-67.

Schultz, E., Knowlen, C., and Bruckner, A.P., "Starting Envelope of the Subdetonative Ram Accelerator," *J. Propulsion and Power*, Vol. 16, No. 6, 2000, pp.1040-1053.

Knowlen, C. and Bruckner, A.P., "Direct Space Launch Using Ram Accelerator Technology," Space Technology and Applications International Forum 2001, Albuquerque, NM, February 11-14, 2001.

Appendix A

University of Washington High Pressure Ram Accelerator Facility

Presented at the 50th Meeting of the Aeroballistic Range Association, November 8-12, 1999, Pleasanton, CA

University of Washington High Pressure Ram Accelerator Facility

C. Knowlen, C. Bundy, R. Schwab and A.P. Bruckner
Aerospace and Energetics Research Program
University of Washington, Box 352250
Seattle, WA 98195-2250

Abstract

The 38 mm bore ram accelerator facility at the University of Washington has been upgraded to enable experimentation at fill pressures up to 20 MPa. High strength, thick-walled tubes were incorporated into the first 4 m of the ram accelerator test section. A new gas handling system has been installed which can prepare and deliver 20 MPa propellant from commercially available gas cylinders. Multistage experiments showed that reinforcement of the nose cone was essential to enable ram accelerator operation at fill pressures over 10 MPa. Modifications to the external projectile geometry were also found necessary to achieve successful starting at fill pressures above 11 MPa with Mg projectiles. Details of the facility upgrade and a summary of preliminary experimental results at pressures up to 15 MPa are presented.

Introduction

The ram accelerator is a hypervelocity mass launcher in which projectiles, shaped similarly to the centerbody of a ramjet engine, are accelerated through a tube containing gaseous fuel and oxidizer mixtures.[1,2] In the thermally choked propulsive mode, shown in Fig. 1, the propellant flows at supersonic velocity over the nose of the projectile (in the projectile frame of reference) and is compressed by a series of reflected conical shock waves.[3] The flow passes the projectile throat (the minimum cross-sectional area of flow), and expands supersonically over the tapering aft body. The flow is recompressed by a normal shock wave system on the aft body, and then releases its chemical energy in a subsonic combustion zone just behind the projectile. This heat release causes the flow to thermally choke at some distance further down the tube, which stabilizes the normal shock wave system on the body. In principle, the thermally choked ram accelerator operates at velocities up to the Chapman-Jouguet (CJ) detonation speed of the propellant.[3,4] As the projectile velocity approaches the theoretical limit, however, the combustion

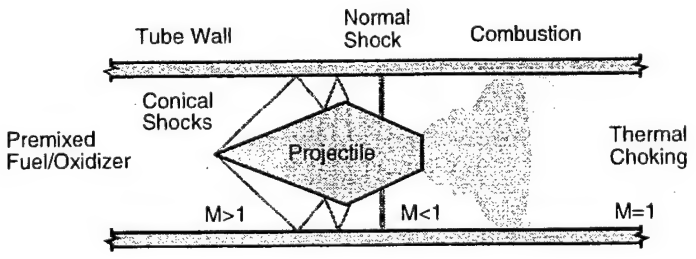

Fig. 1 Ram accelerator thermally choked propulsive mode.

process is observed to move up on to the body which enables acceleration of the projectile beyond the CJ speed.[5,6] Details of ram accelerator operation in the transdetonative and superdetonative velocity regimes can be found in the cited references.[7-12] The experiments discussed in this paper only involve projectiles operating in the subdetonative velocity regime, i.e., at velocities less than the CJ speed of the quiescent propellant.

A ram accelerator system consists of an initial launcher (typically a powder or light gas gun) and a tube containing gaseous propellant. The initial launcher accelerates the projectile to a velocity supersonic with respect to the ram accelerator propellant, which is necessary to "gas dynamically start" the projectile, i.e, establish supersonic flow in its throat passage. The ram accelerator "starting process" is defined as the period between when the projectile is accelerated from rest by the initial launcher to the instant when the flow field illustrated in Fig. 1 is established and stabilized.[13] A "successful start" is a projectile launch which satisfies the following criteria: supersonic flow is obtained behind the projectile throat, the obturator drives a normal shock wave onto the projectile body behind the throat, the normal shock wave is stabilized through ignition of the propellant in a combustion zone which remains on or behind the projectile, and the obturator has been completely isolated from the process.

Ram accelerator technology has the potential to launch massive projectiles at high velocity from relatively short length tubes.[14] Since the ram accelerator operates with a ramjet-like propulsive cycle, the amount of thrust generated is proportional to the fill pressure and increases with increasing heat release of the propellant. Thus the highest acceleration performance for a given projectile mass will be achieved by operating at the highest fill pressure feasible, within the constraints of the propellant delivery system and the strength of the accelerator tube, and with the most energetic propellant that will sustain ram acceleration. These operating conditions subject the projectile to a severe aerothermal heating environment and introduce significant logistical challenges to initiating the ram accelerator process itself. Addressing these issues is the primary focus of the high pressure research program currently in progress at the University of Washington. Details of the facility upgrade and recent experimental results are presented in this paper.

Experimental Facility

The 38 mm bore ram accelerator facility at the University of Washington, shown in Fig. 2, consists of a 168 caliber single-stage light gas gun, light gas vent section, 105 calibers high pressure test section followed by 316 calibers of a lower pressure test section, muzzle blast dump tank, and projectile catcher tube. A new gas handling system has been installed which is capable of loading the test section with a three component propellant at fill pressures up to 20 MPa from commercially available gas cylinders. The light gas gun vent section, low pressure ram accelerator test section, muzzle blast dump tank, projectile catcher tube, and data acquisition system are described in Refs. 15 and 16. Facility enhancements, including procedures for improving the light gas gun performance, installation of thick-walled tubes, electronic control of the high pressure propellant delivery system, sensor upgrades to the gas chromatography equipment, and projectile design modifications, are discussed in this section.

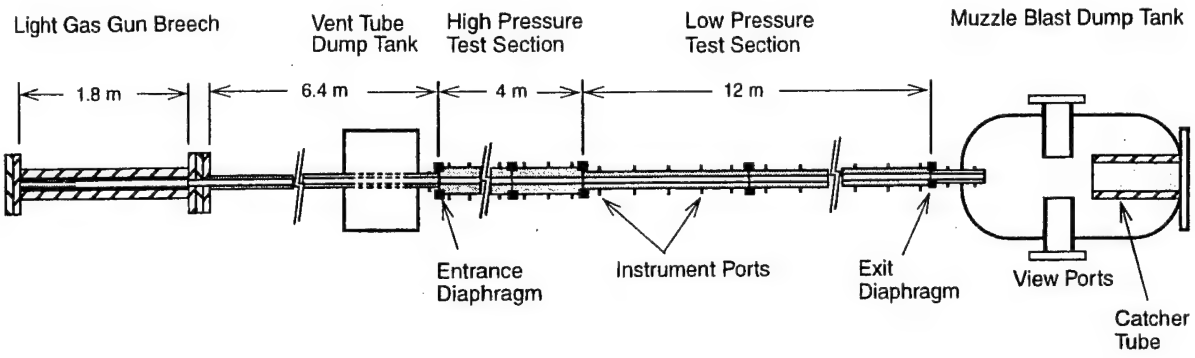

Fig. 2 Ram accelerator 38 mm bore experimental facility.

Light Gas Gun

The light gas gun breech shown in Fig. 3 has been hydro-tested to 52 MPa. Approximately 30% of the available breech volume is occluded with aluminum breech blocks (shaded regions in Fig. 3) to reduce light gas consumption when launching relatively low mass payloads. A Corblin diaphragm pump having a peak output pressure of 40 MPa is used to load the breech. Peak launch gun performance comes from first filling the breech volume with hydrogen from commercial cylinders (10 MPa maximum), then pressurizing the breech to 40 MPa with pumped helium. The total quantity of propellant loaded into the test section is limited when using hydrogen in the breech so that total dump volume of the facility remains sub-atmospheric after the experiment. Residual gases are pumped out after every firing prior to cleaning and recycling the system. Using the maximum breech load of hydrogen and helium allows a payload of 130 gm to be launched to 1200 m/s.

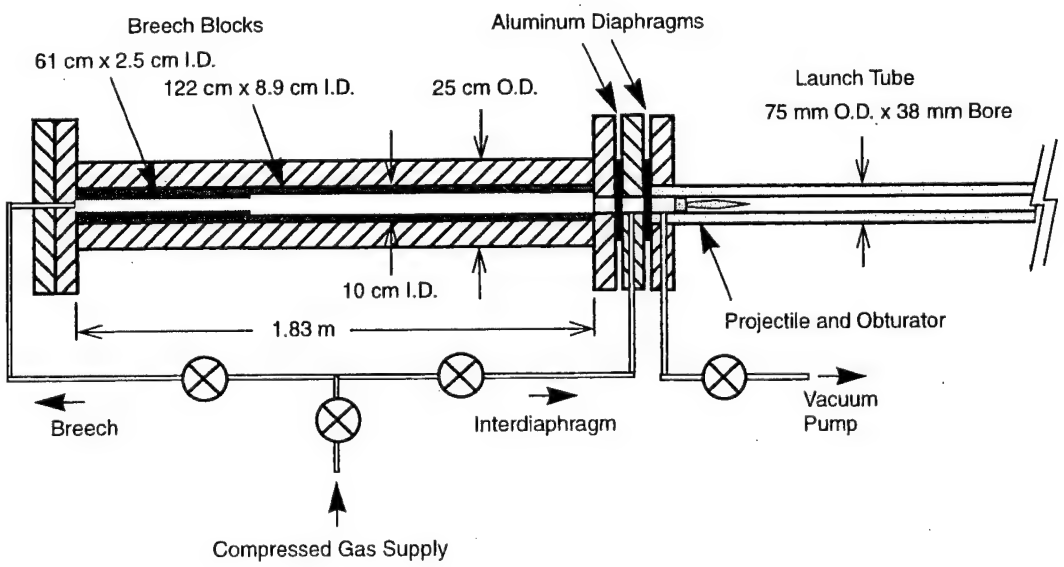

Fig. 3 Light gas gun breech configuration.

Dead-soft aluminum sheets of various thicknesses are sheared into hexagons and a cross is coined into their center with a hydraulic press to produce reliable gas gun diaphragms (burst pressure repeatability is ±3%). A double diaphragm arrangement is used to control the launch. The small interdiaphragm volume can be vented to ambient to initiate launch by breaking the breech diaphragm. Alternately, the breech gas itself can be routed to the interdiaphragm volume to burst of the interdiaphragm and launch the projectile without venting any gas to the laboratory. When hydrogen is used in the breech the launch process is initiated by either the latter approach or by pumping helium into the breech until its diaphragm bursts. Very repeatable muzzle velocities (±1%) are attained with these techniques.

Ram Accelerator Test Section

In the original facility configuration, the 38 mm bore ram accelerator test section was 16 m long, consisting of 8 tubes manufactured from AISI 4140 RC 32-36 steel, each 2 m in length, with outer diameters of 102 mm. These tubes were designed to withstand a static load of up to 550 MPa[16] and have been used with propellants at fill pressures as high as 7.5 MPa.[17] Instrument stations have 2, 3, or 4 ports for electromagnetic (EM) probes and piezoelectric pressure transducers (PCB model A119A11, 550 MPa maximum pressure rating) are spaced at 400 mm intervals. In between each tube, Mylar diaphragms are inserted to separate the propellants, enabling the use of multiple ram accelerator stages. The remainder of the test section not closed by diaphragms is evacuated for the experiments. More details about this part of the facility can be found in Ref. 15.

The high pressure upgrade to the ram accelerator test section, shown in Fig. 4, was accomplished by replacing the first two 2-m-long, 102 mm O.D. ram accelerator tubes with two 1-m-long and one 2-m-long high strength tubes having outer diameters of 152 mm and 38 mm bore. These tubes are manufactured from AISI 4340 AMS 6414 RC 36-40 steel (1170 MPa tensile yield), and are designed for a maximum static load of 1000 MPa. The 1-m-long tubes have three 2-port instrument stations which are equipped with opposing EM probes and pressure

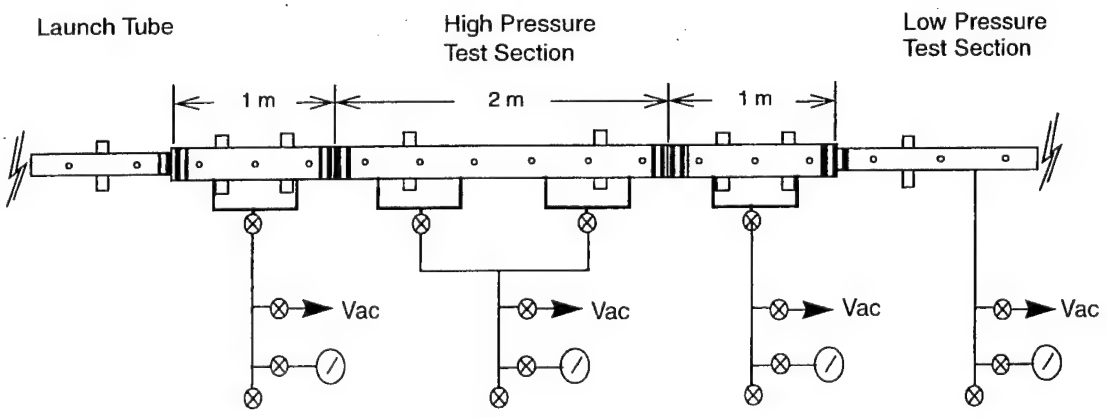

Fig. 4 High pressure test section of UW ram accelerator facility.

transducers (PCB model A119A12, 800 MPa maximum pressure rating), whereas the 2-m-long tube has six instrument stations. When these 3 tubes are joined together the instrument stations in the 4-m-long high pressure test section are equally spaced at 333 mm. The first and last instrument stations are located 167 mm from the ends of the tubes.

Each of the low pressure 2-m long tubes have a centrally located fill port through which the propellant is loaded by opening the corresponding air actuated isolation valve. In the upgraded high pressure test section, the thicker-walled tubes each have two fill ports per meter of length, as shown in Fig. 4. This enables a better axial distribution of gas should partial pressure mixing be required for a desired propellant composition. Each pair of fill ports is isolated from the fill lines by air actuated valves rated at 300 MPa to protect the gas handling system from the intense pressure surges generated in the experiments.

High Pressure Instrumented Insert

In order to observe high pressure ram accelerator phenomena just before or after a test section diaphragm, a 2 caliber insert, shown in Fig. 5, having two pairs of diametrically opposed instrument ports is installed at the tube joint. The insert is machined from the same steel alloy used for the high pressure tubes and the instrument ports enable flush mounting of the pressure transducers. The insert is installed at the entrance to the test section to better observe the pressure wave phenomena on the upstream side of the entrance diaphragm arising from the light gas gun launch process and to examine the projectile flow field during the ram accelerator starting process from a location 1 caliber beyond the diaphragm. The insert is also used at the end of the first stage to observe the projectile flow field 1 caliber before it enters the next stage. It is important to determine the operating condition of the projectile just prior to transition because its status can change very quickly in the high pressure experiments.

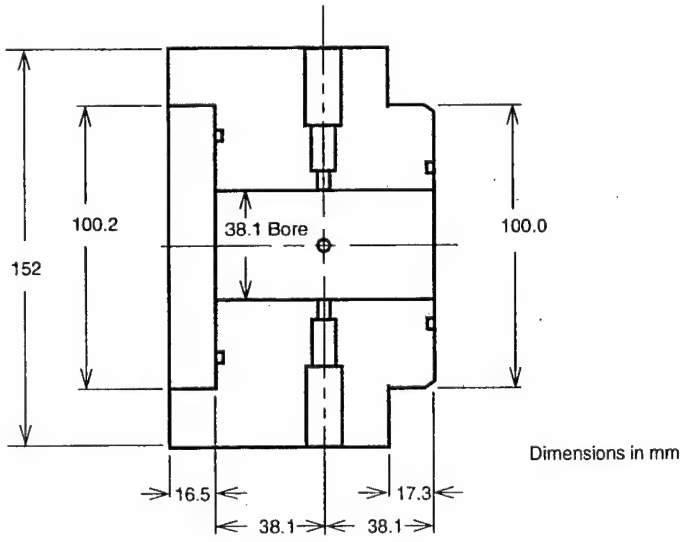

Fig. 5 High pressure, 38 mm bore, 2 caliber, 4-port instrumented insert.

Propellant Delivery System

Applying choked-orifice flow control for preparing gas mixtures at fill pressures greater than 8 MPa is impractical due the extreme supply pressure requirements. Consequently, a new propellant delivery system, shown in Fig. 6, has been installed which is based on electronically controlled mass flow controllers. Each constituent gas is run through a mass flow controller (Brooks model 5850TR), which can accept an inlet pressure of 30 MPa and maintain flow rates up to 20 standard liters per minute. The mass flow controllers are operated with a four-channel Brooks 0154E master controller, where the setpoint for the individual flow rates of the constituent gases are programmed as a percentage of the maximum flow rate of the controller. Inside the mass flow controllers, the gas is heated and a temperature differential is created between two temperature sensors. The temperature differential causes a voltage differential in a bridge circuit, which controls a flow valve inside the mass flow controller. When equilibrium is established, the bridge circuit voltage matches the command voltage from the master controller, and the flow rate is that of the programmed setpoint. The actual mass flow rates at various controller settings are calibrated by timing the filling of a fixed length of test section to 1.4 MPa.

The maximum flow rate through each regulator at a given setpoint is a function of the pressure of the incoming flow and the pressure differential across the mass flow controller. A Grove model 15LHX pressure reducing dome regulator (Fig. 6), with a maximum pressure rating

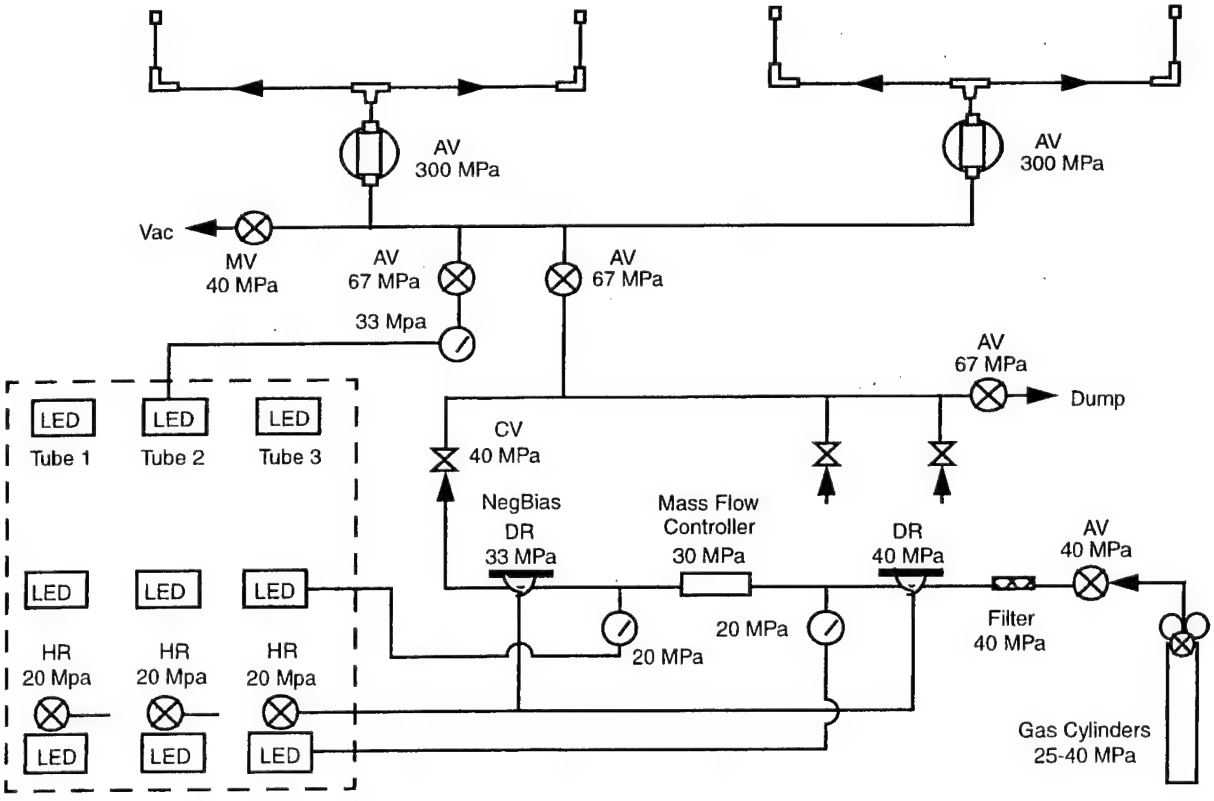

Fig. 6 High pressure propellant flow control system.

of 40 MPa, controls the pressure upstream of each mass flow controller. The downstream pressure is regulated with a Tescom model 26-1722-24-209 negative bias back pressure regulator, which has a 33 MPa maximum pressure rating. Barksdale model 425H3-13 pressure transducers, with a 20 MPa range, are installed upstream and downstream of each mass flow controller to monitor the pressure differentials.

A check valve is placed downstream of each flow controller to protect them from inadvertent pressure surges. The individual lines are then interconnected to permit in-line mixing of the constituent gases. The flow is routed out a dump line until the mass flow controllers have stabilized, after which the isolation valve for a given tube is opened and the propellant is loaded. This filling system is capable of delivering the desired propellant to the ram accelerator tube with less than 2% variation in the relative molar concentrations at fill pressures up to approximately 0.5 MPa less than the pressure of the lowest gas cylinder supply.

Gas Chromatography

Analysis of propellant by gas chromatography is used to validate the mixture composition. The primary analysis hardware consists of a Scientific Research Instruments (SRI) model 8610 gas chromatograph (GC) controlled by an IBM compatible computer. A four-element thermal conductivity detector (TCD) in a Wheatstone Bridge configuration has a sensitivity of 100 ppm to the gases typically used for ram accelerator propellant. Integration of detected peaks is computed with interactive software provided by SRI. The relative amounts of each constituent detected by the GC are repeatable to within 1%; multiple sample runs provide better statistical results.

The propellant sample bottles are 75 cm^3 stainless steel cylinders having a maximum pressure rating of 12 MPa, however, the sample pressure is usually limited to 200 KPa for GC equipment safety concerns. Multiple samples can be drawn from the dump line and the fill line leading to the second tube of the high pressure test section. Two samples per stage are usually taken for each experiment. The first sample is drawn from the dump line just prior to routing the propellent into the desired tubes of the test section. The second sample is drawn from same location after the stage has been loaded and the propellant flow has been switched back to the dump line. Determining the difference in the molar concentrations before and after the fill indicates how steadily the mass flow controllers behaved and provides a limit to the uncertainty of the propellant composition in the tube.

The VALCO 10-port sampling valve used for injecting the gas samples into the GC has a sample loop volume of 0.5 cm^3 and is typically loaded to 30-60 kPa. The sample pressure is monitored with a Barksdale model 402H2-03 pressure transducer having an absolute pressure range of 345 KPa. The separation column is a stainless steel 60/80 Molesieve-5A, 2.74 m x 3.2 mm, maintained at 40° C. Helium carrier gas is used for most analyses, however, argon is used as a carrier when the propellant has helium and/or hydrogen components. Typical run times are 5 minutes per sample when analyzing for oxygen, nitrogen, and methane.

The accuracy of the analysis is limited by the certainty of the gas calibration standard composition, the thoroughness of the GC calibration, and the number of times a sample is analyzed. The gas calibration standard for $CH_4/O_2/N_2$ propellant is prepared by partial pressure

filling of a 3.8 liter stainless steel cylinder with medical purity bottle air (21% O2 and 79% N2) and Grade 4 methane (99.97% purity) to approximately 1 MPa. The filling process is monitored with a 0.25% accurate dial gauge and the standard is set aside for at least a week to let the gases diffusively mix. The GC is calibrated by determining its response to a range of sample volumes of the gas calibration standard. Each propellant sample is then analyzed at least two times and the results are averaged. This approach allows resolving molar concentration differences between samples of less than 1% with an absolute accuracy of 2%.

Projectile and Obturator Configuration

Several different projectile geometries and materials have been used in this investigation. Five-finned projectiles having the standard throat dimension (29 mm diameter) and body length (71 mm), as shown in Fig. 7a, were fabricated from Al 7075-T6 and Ti 6Al-4V alloys in two pieces, a nose cone and body, which thread together at the throat. Both Al and Ti alloy projectiles of this configuration were manufactured on computer numerically controlled (CNC) machines with material removed from the interior in a manner that resulted in them all having about the same mass (110-120 gm). Shorter-bodied, low mass (50-60 gm), four-finned Al alloy projectiles, shown in Fig. 7b, were used to investigate the effects of entrance velocity on starting at fill pressures greater than 8.5 MPa. Since the throat and thread dimensions were the same for these CNC projectiles, all nose cone and body components were interchangeable.

One-piece Mg ZK60A-T5 alloy projectiles having 10^{o} solid nose cones with variations in throat diameter and fin leading edge configuration were used to determine how throat flow area ratio affects the starting process at pressures greater than 10 MPa and to eliminate concerns of nose cone buckling. A one-piece projectile having the standard external geometry (103 gm) is shown in Fig. 8a. A ceramic magnet was held in position at the projectile throat with a threaded Mg plug and the clearance hole was left open to reduce mass. The one piece projectile configuration having a 25 mm throat diameter and mass of ~60 gm is shown in Fig. 8b. A variant of this projectile with knife-edged fins at a 20^{o} rake angle, used in 15 MPa starting experiments, is illustrated in Fig. 8c (magnet installation not shown).

The two-piece polycarbonate obturator, shown in Fig. 8, is placed behind the projectile base to prevent gas blow-by from the light gas gun initial launcher and to facilitate ignition of the propellant in the ram accelerator tube. The perforated component of the obturator was found to be more effective in starting the ram accelerator at high pressure when its total open area was reduced to 23% (from 42%). This was accomplished by drilling the outer 12 holes at 3.2 mm diameter and the inner 7 holes at 5.6 mm. This geometry of the perforated obturator has a mass of 16 gm and the solid disk mass is 3 gm. The two-piece combination is glued to the base of projectile with cyanoacrylate adhesive for the process of loading them into the light gas gun.

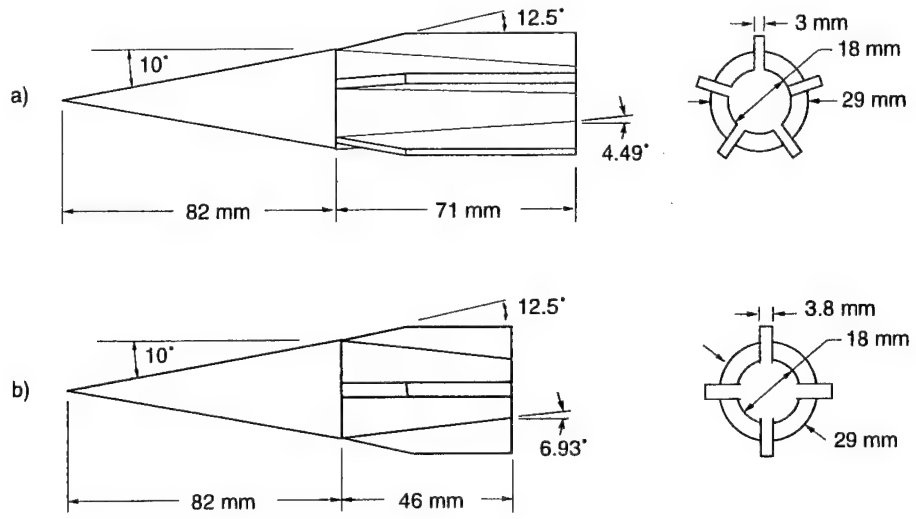

Fig. 7 Two-piece Al and Ti alloy projectiles with standard 29 mm throat diameter: a) standard body 5-fin. b) short body 4-fin.

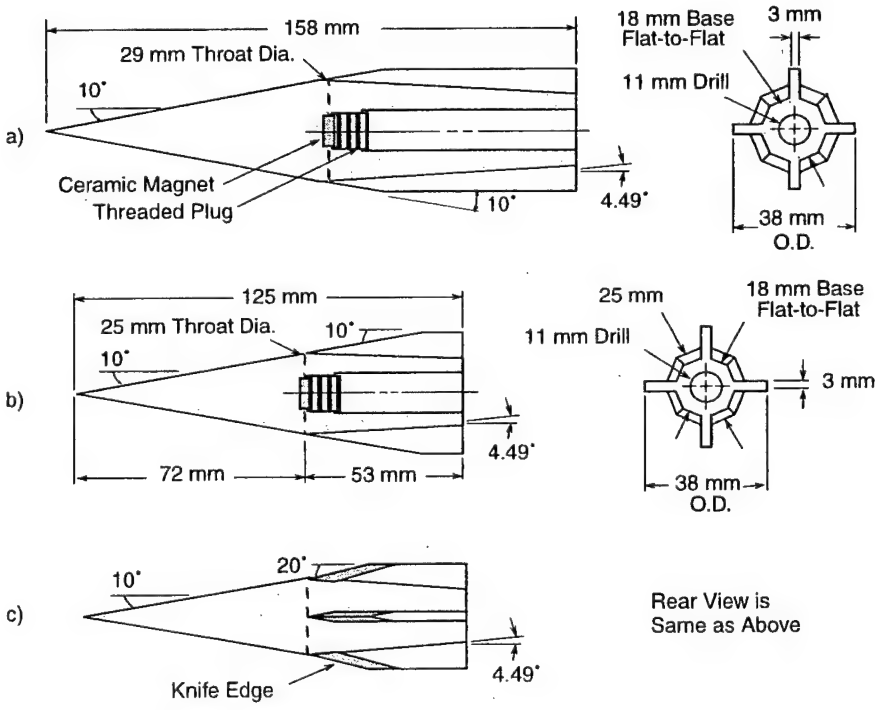

Fig. 8 Solid Mg alloy projectiles: a) standard 29 mm throat. b) reduced 25 mm throat. c) reduced 25 mm throat with knife-edged fins and 20^0 fin rake angle.

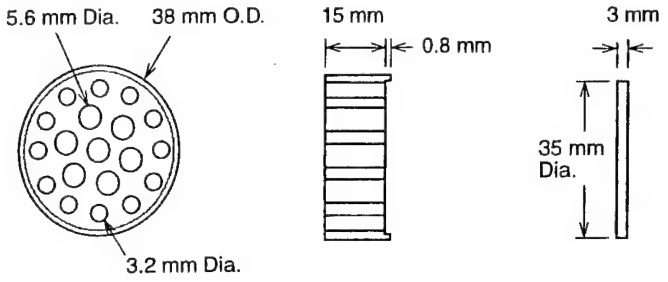

Fig. 9 Perforated obturator and disk configuration.

High Pressure Experimental Results

Preliminary experiments, using the "standard" projectile configuration (Fig. 7a), had investigated the efficacy of starting the ram accelerator in 1-m-long stage of 5 MPa propellant and then making a transition into a second stage at higher pressure. This approach worked well with second stage fill pressures up to 10 MPa, as reported in Ref. 17. Directly starting the ram accelerator with the standard projectile at an entrance velocity of 1120-1160 m/s in $3CH_4+2O_2+6.5N_2$ propellant was accomplished at fill pressures up to 7.7 MPa.[18] Careful review of the existing UW ram accelerator data base and subsequent experimentation found that the Mach number at which a decelerating projectile unstarts (sonic diffuser unstart[13]) increases with increasing fill pressure, indicating that higher starting velocity may be required for projectiles having the standard throat-to-tube flow area ratio.[19] More details of these earlier investigations can be found in the cited references.[17-19] A summary of recent experiments which further explored the phenomena of starting and operating the ram accelerator at elevated fill pressure is presented in this section.

Transition Velocity Effects on Operation Through a Pressure Discontinuity

A sequence of experiments was conducted to determine if the first-to-second stage transition velocity of standard geometry projectiles (Fig. 7a) was a significant variable when there is a pressure differential between stages. In this testing configuration, the first 1-m-long tube is evacuated, the adjacent 2-m-long tube contains a starting propellant of $3.1CH_4+2O_2+6.6N_2$ at 7.5 MPa, and the last 1-m-long tube contains a test propellant, such as $3CH_4+2O_2+7.5N_2$, at higher pressure. Using standard Al projectiles massing around 113 gm, the experiments demonstrated successful starting in the second tube and stable ram accelerator operation in the third tube at fill pressures up to 11 MPa. Similar results were achieved with standard Ti projectiles using a 3-m-long first stage followed by a 1-m-long high pressure stage. The velocity-distance data for the Ti projectiles are shown in Fig. 10. Because of the their thin walls, it proved necessary to drill a 9.5 mm hole into the projectile base to allow the high pressure gases in the combustion zone to internally pressurize it and help keep the nose cone from buckling under the compressive loads of the conical shock waves, when operating with fill pressures greater than

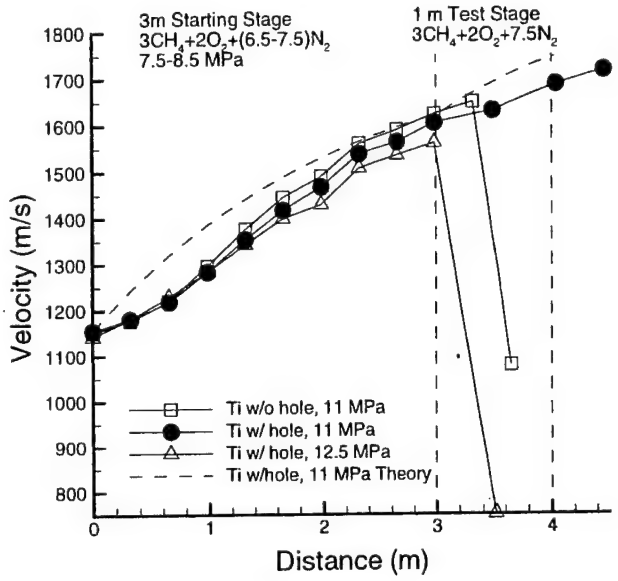

Fig. 10 Experimental results for standard 29 mm throat Ti projectile with base hole.

10 MPa. At propellant fill pressures greater than 12 MPa, however, even Ti projectiles with a base hole would immediately unstart upon entering the high pressure test stage. It has not yet been determined if this result is due to structural failure or reactive flow phenomena arising at the transition point.

Entrance Velocity Effects on Starting

The experimentally observed increase in sonic diffuser unstart Mach number with increasing pressure implies that higher entrance velocity is necessary for starting the ram accelerator at elevated pressure.[19] In order to achieve greater launch velocity, experiments were conducted with short-bodied Al projectiles (Fig. 7b) having the standard 29 mm throat diameter, 10^{o} nose cone, and a 9.5 mm hole drilled into their base. These relatively low mass projectiles (67 gm) were launched into the test section at entrance velocities ranging from 1270-1310 m/s, achieving successful starts in a 1-m-long stage of the $3.1CH_4+2O_2+6.6N_2$ propellant at 8.5 MPa. Successful starts were also achieved in 1-m-long stages of $3CH_4+2O_2+7.5N_2$ propellant at 10 and 11 MPa. The velocity-distance data from the 10 and 11 MPa experiments are shown in Fig. 11 along with the corresponding theoretical curves for the thermally choked propulsive mode. The theoretical curves were obtained using a numerical solver[20] which determines the chemical equilibria of the reacted flow using the Boltzmann equation of state.[21] Even though the average acceleration of these experiments was 30-40% lower than expected, the results indicate that projectiles having the standard throat diameter can be ram accelerated if they have sufficient initial velocity and their structural integrity is ensured.

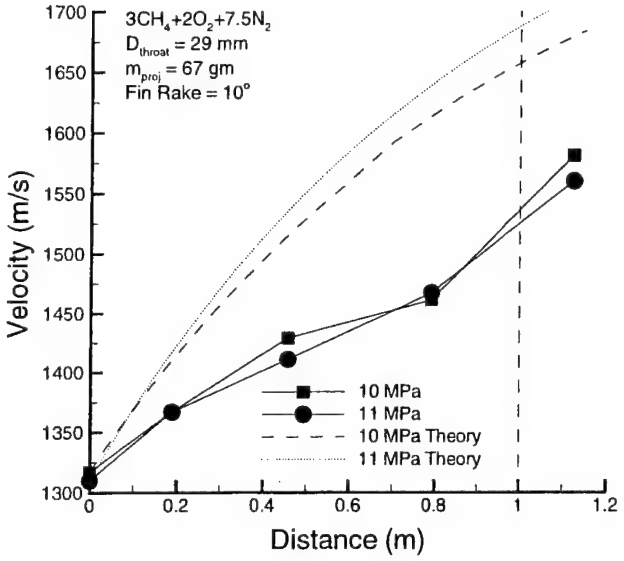

Fig. 11 Experimental results for standard 29 mm throat, short body, Al projectile with base hole.

Projectile Throat Diameter Effects on Starting

With the problems of starting the ram accelerator at fill pressures up to 11 MPa now clearly linked to entrance velocity and structural integrity, experimentation was directed toward achieving successful starts at higher fill pressures with one-piece Mg projectiles (see Fig. 8b). The results shown in Fig. 12 are from two experiments in a 1-m-long stage of $3CH_4+2O_2+7.5N_2$ propellant at

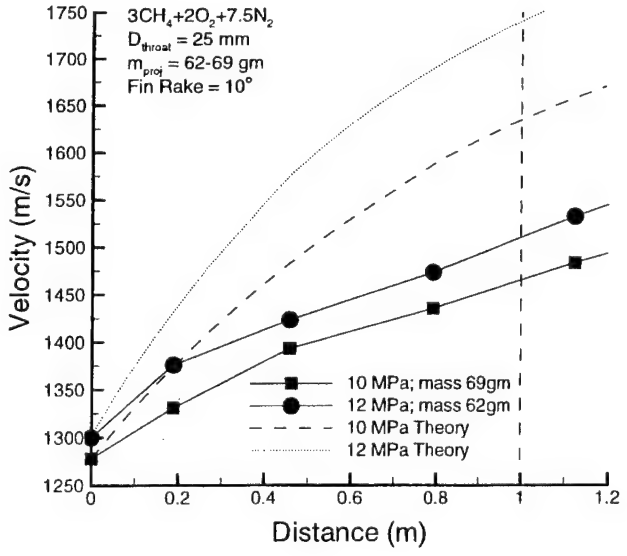

Fig. 12 Experimental results of starting experiments with 25 mm throat Mg projectile.

fill pressures up to 12 MPa. Reducing the throat diameter from 29 mm to 25.4 mm while maintaining the same 4.49° body taper angle and 18 mm base diameter resulted in a 25% shorter projectile body length. These one piece Mg projectiles with solid nose cones were able to be successfully started at entrance velocities of 1280-1300 m/s. Only 1 m of test section was used in these experiments to avoid tube damage from burning magnesium that could occur after prolonged ram accelerator operation at high Mach number. Again it can be seen that the acceleration during the first meter of ram accelerator operation is lower than expected for thermally choked propulsive mode. This infers that either the amount of heat release is less than expected or else there is a much longer induction time associated with the starting process under these conditions than observed in 5 MPa experiments.

The tube wall pressure data from experiments using different projectile geometries in a 1-m-long test stage of $3CH_4+2O_2+7.5N_2$ propellant at 10 MPa are presented in Figs. 13 and 14. In Fig. 13, the projectile had the standard throat diameter of 29 mm (Fig. 7b); in Fig. 14, the projectile throat diameter was 25.4 mm (Fig. 8b). In both cases, the wall pressure data are qualitatively similar to those associated with successful starting and operation in the thermally choked ram accelerator mode. The peak pressure ratio in the throat region of both projectiles is nearly the same (~4), however, there is a strong pressure rise just behind the throat of the larger projectile (Fig. 13) which may indicate the passage of a fin directly over the pressure transducer.[22] The peak pressure ratio behind the projectile having a 29 mm throat diameter was 30-40% higher than in the experiment with the 25 mm throat (Fig. 14), which suggests that the throat diameter may play a significant role in the combustion zone pressure rise during the starting process. On the other hand, the total velocity gains were very similar in both of these experiments which implies that the projectile throat diameter may have very little effect upon ram accelerator performance under these conditions. These phenomena are still under investigation.

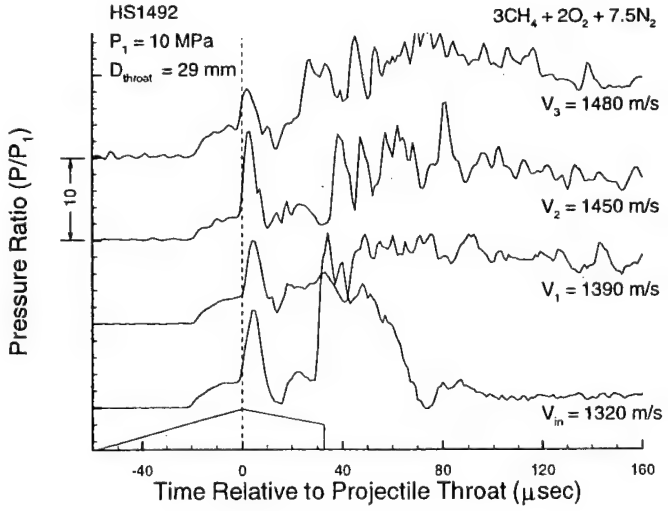

Fig. 13 Tube wall pressure data for standard 29 mm throat, short body, Al projectile with base hole.

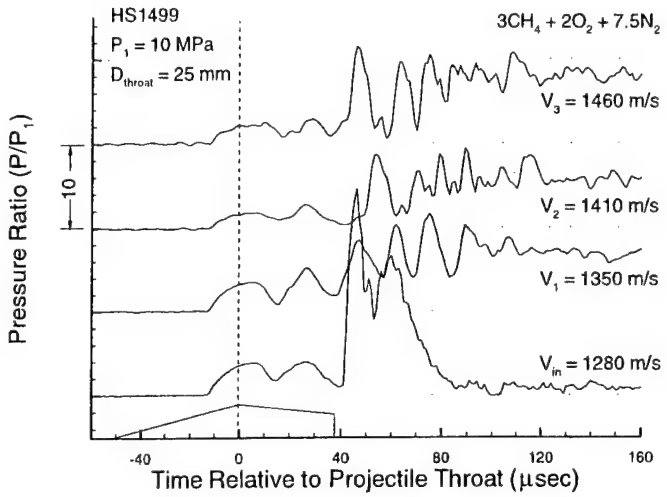

Fig. 14 Tube wall pressure data for 25 mm throat, solid nose cone Mg projectile.

Starting Experiments in 15 MPa Propellant

Experiments were conducted to investigate ram accelerator starting in propellants at 15 MPa using the reduced throat, solid nose cone, one-piece Mg projectiles with knifed-edged fins (Fig. 8c). Velocity-distance data from three of these experiments having entrance velocities of 1270-1305 m/s are shown in Fig. 15. A successful start was achieved in $3.3CH_4+2O_2+9.7N_2$ propellant as evident by the continuous acceleration of the projectile throughout the 1-m-long stage. This example of successful starting at 15 MPa represents the highest fill pressure yet in which ram accelerator operation has been demonstrated. Also shown in Fig. 15 are results from two of the "bounding" experiments. The less energetic $3.5CH_4+2O_2+9.8N_2$ propellant was not ignited under these conditions, resulting in the occurrence of a wave fall-off, typical for an unacceptably "cold" mixture. The more energetic $3CH_4+2O_2+9.5N_2$ propellant produced a wave unstart, which is to be expected for an excessively "hot" reactive mixture.

The corresponding theoretical velocity-distance curve for the successful 15 MPa start, using the Boltzmann equation of state, is shown in Fig. 15. The predicted average acceleration over the length of the 1-m-long stage is 80,000 g, whereas the average acceleration achieved was only 26,000 g. In all cases of successful starting at pressures of 10 MPa and greater, the thermally choked ram accelerator model overpredicts the average acceleration through a 1-m stage by a considerable margin. This discrepancy is currently attributed to a delay in starting process and is still under investigation.

Tube wall pressure data for the successful start at 15 MPa are shown in Fig. 16. These wave forms, in conjunction with the corresponding EM signals, positively confirm that the projectile was indeed being thrust ahead of the combustion waves, however, the flow field does not appear to be thermally choked. A peak pressure ratio of ~10 is observed behind the projectile when it is

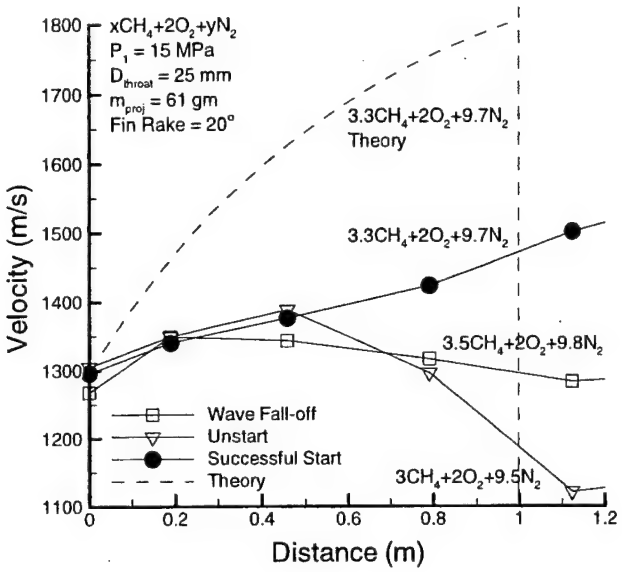

Fig. 15 Results of 15 MPa experiments using 25 mm throat Mg projectile with knife-edged fins.

operating at a velocity of 1460 m/s (Mach 4.0), whereas the peak pressure ratio at this velocity is normally ~15 when the fill pressure is 5 MPa. The pressure rise due to obturator impact, measured 1 caliber after the entrance diaphragm, is much less than that seen at the same location in the 10 MPa experiments (Fig. 13 and 14). This may be the consequence of a slower propellant ignition process or the effect of obturator structural failure induced by higher fill pressure. The large number of factors involved in the starting process necessitates the use of careful experimentation to determine the causes of these effects.

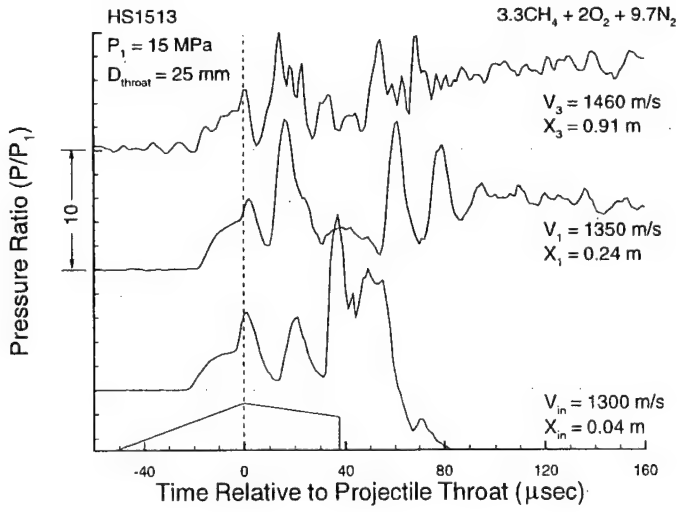

Fig. 16 Tube wall pressure data for 25 mm throat Mg projectile with knife-edged fins at 15 MPa.

Conclusions

The high pressure upgrade to the 38 mm bore ram accelerator facility enables experimentation with propellants at fill pressures up to 20 MPa. Preliminary experiments indicate that operating the ram accelerator at elevated fill pressures (above 7.5 MPa) requires a 150 m/s increase in entrance velocity for projectiles having the standard 29 mm throat diameter. The use of thick-walled Al and solid Mg nose cones was found necessary to prevent its abrupt collapse when entering propellant at fill pressure greater than 10 MPa. It was also shown that structural collapse can be avoided by drilling a hole into the projectile base to allow internal pressurization. Projectiles having a 29 mm diameter throat were not successfully started nor able to operate after making a transition through a pressure differential when the test propellant fill pressure was greater than 11 MPa. Reducing the throat diameter to 25.4 mm enabled successful ram accelerator starting with Mg alloy projectiles at fill pressures up to 15 MPa. The full operational entrance velocity range and endurance capability of the reduced throat Mg projectiles have yet to be determined. The next phase of the experimental program is to utilize Ti alloy projectiles having the 25.4 mm throat, knife-edged fin geometry to investigate their operational characteristics over a wide Mach number range at fill pressures up to 20 MPa.

Acknowledgments

The facility upgrade and experiments were supported under U.S. Army Research Office grant number DAAG55-97-1-0131. Thanks are due to Jesse Stewart, David Buckwalter and Andrew Shell for their assistance with the high pressure research program.

References

1. Hertzberg, A., Bruckner, A.P., and Bogdanoff, D.W., "Ram Accelerator: A New Chemical Method for Achieving Ultrahigh Velocities," 37th Meeting of Aeroballistic Range Association, Quebec, Canada, September 9-12, 1986

2. Hertzberg, A., Bruckner, A.P., and Bogdanoff, D.W., "Ram Accelerator: A New Chemical Method for Accelerating Projectiles to Ultrahigh Velocities", *AIAA Journal*, Vol. 26, 1988, pp. 195-203.

3. Bruckner, A.P., Knowlen, C., Hertzberg, A., and Bogdanoff, D.W., "Operational Characteristics of the Thermally Choked Ram Accelerator," *AIAA Journal of Propulsion and Power*, Vol. 7, 1991, pp. 828-836.

4. Knowlen, C. and Bruckner, A.P., "A Hugoniot Analysis of the Ram Accelerator," *Shock Waves*, Takayama, K. (ed), Springer-Verlag, Berlin, 1992, pp. 617-622.

5. Kull, A.E., Burnham, E.A., Knowlen, C., Bruckner, A.P., and Hertzberg, A., "Experimental Studies of Superdetonative Ram Accelerator Modes," AIAA Paper 89-2632.

6. Burnham, E.A., Kull, A.E., Knowlen, C., Bruckner, A.P. and Hertzberg, A., "Operation of the Ram Accelerator in the Transdetonative Velocity Regime," AIAA Paper 90-1985.

7. Hertzberg, A., Bruckner, A.P., and Knowlen, C., "Experimental Investigation of Ram Accelerator Propulsion Modes," *Shock Waves*, Vol. 1, 1991, pp. 17-25.

8. Brackett, D.C. and Bogdanoff, D.W., "Computational Investigation of Oblique Detonation Ramjet-in-Tube Concepts," *J Propulsion and Power*, Vol. 5, 1989, pp. 276-281.

9. Yungster, S. and Bruckner, A.P., "Computational Studies of a Superdetonative Ram Accelerator Mode," *J. Propulsion and Power*, Vol. 8, 1992, pp. 457-463.

10. Soetrisno, M., Imlay, S.T., and Roberts, D., "Numerical Simulation of the Superdetonative Ram Accelerator Combusting Flowfield," AIAA Paper 93-2185.

11. Knowlen, C., Higgins, A.J., Bruckner, A.P., and Bauer, P., "Ram Accelerator Operation in the Superdetonative Velocity Regime," AIAA Paper 96-0098, January 1996.

12. Knowlen, C., and Sasoh, A., "Ram Accelerator Performance Modeling," *Ram Accelerators*, Takayama K, Sasoh A (eds), Springer-Verlag, Heidelberg, 1998, pp. 25-37.

13. Schultz, E., Knowlen, C., and Bruckner, A.P., "Overview of the Subdetonative Ram Accelerator Starting Process," *Ram Accelerators*, Takayama K, Sasoh A (eds), Springer-Verlag, Heidelberg, 1998, pp. 189-203.

14. Kruczynski, D., Liberatore, F., and Nusca, M., "NAVRAM5 - An Analysis of Ram Acceleration for Specific Naval Applications," ARL-TR-1073, April 1996.

15. Knowlen, C., Li, J.G., Hinkey, J., and Dunmire, B., "University of Washington Ram Accelerator Facility," 42nd Meeting of the Aeroballistic Range Association, Adelaide, Australia, October 22-25, 1991.

16. Stewart, J.F., Knowlen, C., and Bruckner, A.P., "Effects of Launch Tube Gases on Starting of the Ram Accelerator," AIAA Paper 97-3175.

17. Bundy, C., Knowlen, C., and Bruckner, A.P., "Elevated Pressure Experiments in a 38-mm Bore Ram Accelerator," AIAA Paper 98-3144.

18. Bundy, C., Knowlen, C., and Bruckner, A.P., "Experiments in a 38-mm Bore Ram Accelerator at Pressures up to 12.5 MPa," 49th Meeting of the Aeroballistic Range Association, Scheveningen, The Netherlands, October 5-9, 1998.

19. Bundy, C., Knowlen, C., and Bruckner, A.P., "Ram Accelerator Operating Characteristics at Fill Pressures Greater Than 10 MPa," AIAA Paper 99-2261.

20. Buckwalter, D.L., Knowlen, C., and Bruckner, A.P., "Ram Accelerator Performance Analysis Code Incorporating Real Gas Effects," AIAA Paper 96-2945.

21. Bauer, P., Knowlen, C., and Bruckner, A.P., "Real Gas Effects on the Prediction of Ram Accelerator Performance," *Shock Waves*, Vol. 8, 1998, pp. 113-118.

22. Hinkey, J.B., Burnham, E.A., and Bruckner, A.P., "High Spatial Resolution Measurements of Ram Accelerator Gas Dynamic Phenomena," AIAA Paper 92-3244.

Appendix B

Summary of Experimental Results at 100 - 150 atm Fill Pressure

J. Phys. IV France **10** (2000)

Ram accelerator operating characteristics at elevated fill pressures

C. Bundy, C. Knowlen and A.P. Bruckner

University of Washington, AERP, Box 352250, Seattle, WA 98195, U.S.A.

Abstract : An experimental investigation of the starting and operational characteristics of a 38-mm bore ram accelerator with propellant fill pressures greater than 5 MPa is in progress. Successful starts with 60 – 124 gm projectiles have been achieved using methane/oxygen/nitrogen propellants at fill pressures ranging from 6 to 15 MPa. At fill pressures of 8.5 MPa and above, it was found that projectiles having the nominal throat diameter (29 mm) required a minimum entrance velocity of 1250 m/s, which is about 100 m/s faster than the minimum needed to successfully start the ram accelerator at fill pressures below 7.5 MPa. Projectiles with a reduced throat diameter (25 mm) and a solid magnesium nose cone were successfully started at fill pressures up to 15 MPa with entrance velocities around 1300 m/s. The average accelerations achieved using high pressure stages were in general less than predicted for thermally choked operation by the Boltzmann equation of state.

1. INTRODUCTION

Ram accelerator technology has the potential to launch massive projectiles at high velocity from relatively short length tubes [1]. Since the ram accelerator operates with a ramjet-like propulsive cycle [1,2], the amount of thrust generated is directly proportional to the fill pressure and increases with increasing heat release of the propellant. Thus the highest acceleration performance for a given projectile mass will be achieved by operating at the highest fill pressure feasible, within the constraints of the propellant delivery system and the strength of the accelerator tube, and with the most energetic propellant that will sustain ram acceleration. These operating conditions subject the projectile to a severe aerothermal environment and introduce significant logistical challenges to initiating the ram accelerator process itself. Addressing these issues is the primary focus of the high pressure ram accelerator research program currently in progress at the University of Washington.

Several different ram accelerator propulsive cycles have been identified which are characterized by the manner in which the propellant heat release occurs and by the velocity of the projectile relative to the Chapman-Jouguet (CJ) detonation speed [3]. Only high pressure operation in the thermally choked propulsive mode is discussed in this paper; details of the other propulsive modes can be found in Refs. 4 and 5, an overview of the ram accelerator starting process and possible results of that process are presented in Ref. 6, and the theoretical considerations of high pressure operation are discussed in Ref. 7. The facility upgrade for high pressure operation is described here in Section 2 and the key results from the most recent investigations and their implications are discussed in Section 3.

2. EXPERIMENTAL FACILITY

The ram accelerator facility at the University of Washington has been upgraded to enable experimentation at propellant fill pressures up to 20 MPa. Brief descriptions of the major modifications made to the facility and the various projectiles used in the experiments are provided in this section. Details of the light gas gun pre-launcher and other major system components can be found in Ref. 8.

2.1 High Pressure Test Section

The first 4 m of the ram accelerator test section, shown in Fig. 1, consist of two 1-m-long and one 2-m-long high pressure tubes, with an outer diameter of 152 mm and an inner diameter of 38 mm [9]. They are connected together using bolted flange joints. The high pressure tubes are manufactured from AISI 4340

steel, and are designed for a maximum static load of 1000 MPa. The remainder of the test section is comprised of 6 "low" pressure tubes manufactured from AISI 4140 steel, each 2 m in length, with outer diameters of 102 mm. These tubes are connected with threaded collars and are designed to withstand a static load of up to 550 MPa.

Each 1-m-long tube (Fig. 1) has three instrument stations with diametrically opposed ports, whereas the 2-m-long tube has six stations. These stations are spaced along the tubes at 333 mm intervals. The first instrument station in the high pressure test section is 167 mm from the entrance diaphragm and the last station is located 167 mm from the end of the high pressure section, and 396 mm from the first instrument port in the low pressure part of the test section. The instrument stations are spaced 400 mm apart throughout the low pressure section. The instrument ports can accommodate electromagnetic (EM) probes and PCB model A119A11 or A119A12 piezoelectric pressure transducers (550 or 800 MPa maximum pressure range, respectively).

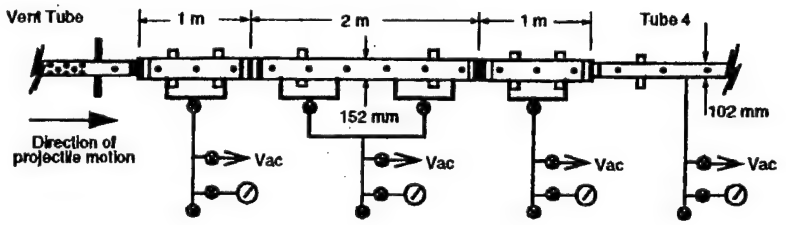

Figure 1: High pressure test section of the 38-mm bore ram accelerator facility.

All of the tubes in the high pressure test section have two fill ports per meter of length, as shown in Fig. 1. These fill ports are isolated from the fill lines by air-actuated valves (300 MPa rated), thus protecting the gas handling system, described in detail in Ref. 7, from the extreme pressure pulses generated in the experiments. The low pressure part of test section has fill ports placed every 2 m. Mylar diaphragms can be inserted between adjacent tubes to separate the propellants, enabling multiple stages of different propellants, and hence acoustic speeds, to be used. Any tubes not containing propellant are evacuated for the experiments.

2.2 Experimental Projectiles

Several different projectile geometries and materials were used in this investigation. Five-finned projectiles having the standard throat dimension (29 mm diameter) and body length (71 mm), as shown in Fig. 2a, were fabricated from Al 7075-T6 and Ti 6Al-4V alloys in two pieces, a nose cone and body, which thread together at the throat. Both Al and Ti alloy projectiles of this configuration were manufactured on computer numerically controlled machines with material removed from the interior in a manner that resulted in them all having about the same mass (110-120 gm). Shorter-bodied, low mass (60-70 gm), Al alloy, 4-fin projectiles, shown in Fig. 2b, were used to investigate the effects of entrance velocity on starting at fill pressures greater than 8.5 MPa. Since the throat and thread dimensions were the same for these projectiles, all nose cone and body components were interchangeable.

One-piece Mg ZK60A-T5 alloy projectiles having 10^{0} solid nose cones with variations in throat diameter and fin leading edge configuration were used to determine how throat flow area ratio affects the starting process at pressures greater than 10 MPa, and to eliminate concerns of nose cone buckling. A one-piece projectile having the standard external geometry (~103 gm) is shown in Fig. 2c. A ceramic magnet was held in position at the projectile throat with a threaded Mg plug and the clearance hole was left open to reduce mass. A one-piece projectile configuration having a 25 mm throat diameter and mass of ~60 gm is shown in Fig. 2d. A variant of this projectile with knife-edged fins at a 20^{0} rake angle, used in 15 MPa starting experiments, is illustrated in Fig. 2e (magnet installation not shown).

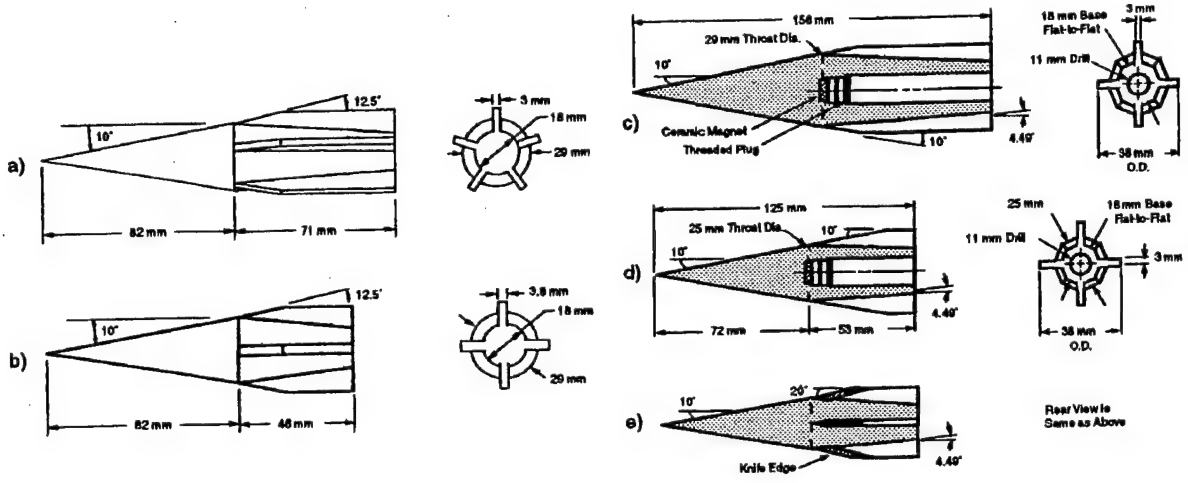

Figure 2: Two-piece Al and Ti projectiles with standard throat: a) standard length 5-fin, b) low mass 4-fin, solid Mg alloy projectiles: c) standard throat, d) reduced throat, e) reduced throat with knife-edged fins and 20° fin rake angle.

The obturator, shown in Fig. 3, is placed behind the projectile base to prevent gas blow-by from the light gas gun initial launcher and to drive a normal shock onto the projectile rear body upon entrance to the test section. The obturators are fabricated from polycarbonate in two pieces, a perforated cylinder and a solid backplate. The perforations consist of 19 holes of 6 mm diameter, giving an open area ratio of 42% (Fig. 3a) or 12 holes of 3.2 mm diameter and seven of 6 mm, giving an open area ratio of 23% (Fig 3b). The obturator and backplate have a combined mass of 16-18 gm and are glued to the projectile with cyanoacrylate adhesive for the process of loading the projectile/obturator combination into the light gas gun.

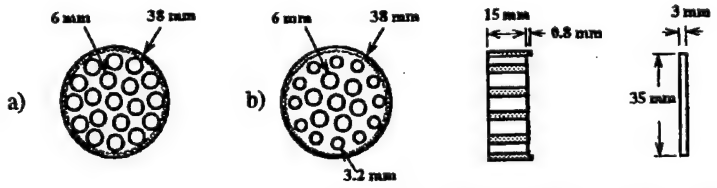

Figure 3: Obturators having a) 42% and b) 23% open area ratios.

3. HIGH PRESSURE EXPERIMENTAL RESULTS

3.1 Low Entrance Velocity Results

The first three ram accelerator experiments in the high pressure test section used a 1-m-long "starter" stage having 5 MPa fill pressure of $3CH_4+2O_2+5.7N_2$ propellant, followed by a 3-m-long stage having fill pressures of 5, 7.5, or 10 MPa [9]. The propellant used in the starter stage was also loaded into the second stage in the 5 and 7.5 MPa experiments. Due to an inadvertent deviation in the mass flow controller settings, which was not detected until after the third experiment via analysis of gas samples, the propellant used at 10 MPa was $4CH_4+2O_2+5.7N_2$. The 5-finned standard Al projectiles (Fig. 2a) used in this series had a mass of 113 gm and were launched with an entrance velocity in the first stage in the 1120 – 1140 m/s range. The velocity-distance data for these experiments are shown in Fig. 4. The projectiles gained about 150 m/s prior to entering the second stage. In each of these three experiments the projectile successfully started in the 5 MPa stage and continued to accelerate throughout the second stage. The total velocity gain in the second stage increased with increasing fill pressure, as expected, and the average acceleration across the second stage increased approximately linearly with fill pressure.

Attempts to establish ram accelerator operation in the second stage at pressures of 11 – 12.5 MPa, after having started in the 5 MPa propellant, resulted in unstarts by the time the projectile reached the first instrumentation station following the transition diaphragm. To investigate the effects of pressure ratio on the transition between stages, the pressure differential across the diaphragm was reduced by increasing the pressure of the first stage propellant while keeping the second stage at 11 MPa [9]. The propellant composition in both stages was $3CH_4+2O_2+6.5N_2$. The projectile entrance velocity in the first stage was 1120 - 1150 m/s and it entered the second stage at 1250 – 1300 m/s. It was found that ram accelerator operation could not be successfully established in the second stage using this propellant. The details of this experimental series are shown in Table A-1 in the Appendix.

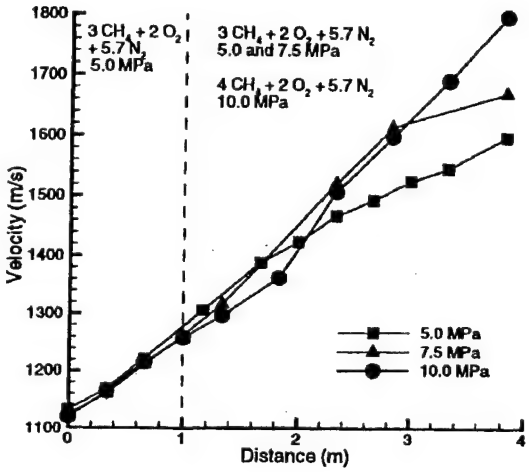

Figure 4: Results from high pressure experiments using 1-m-long starting stage.

Even when the second stage was filled with an inert gas mixture ($3CH_4+8.5N_2$), the projectile would be unstarted by the first instrument port, located 167 mm from the entrance diaphragm of the high pressure stage. It was uncertain whether these results were due to structural failure of the projectile or solely to gasdynamic mechanisms. While these experiments did not enable the continuous acceleration of a projectile at a fill pressure greater than 10 MPa, successful starts were attained in the first stage at fill pressures up to 7.7 MPa within the nominal entrance velocity range of 1120 – 1160 m/s. Attempts to inject these projectiles with this entrance velocity into inert mixtures at fill pressures greater than 7.7 MPa were not successful in gasdynamically starting the projectile. At the time of the investigation, it was uncertain if the experimentally determined limitation in fill pressure of the starting stage was due to structural failure of the projectile, excessive heat release, or insufficient entrance velocity.

3.2 Transition Velocity at a Pressure Discontinuity

A sequence of two-stage experiments using Al and Ti alloy projectiles was conducted to determine if the velocity at the transition point is a significant factor in whether positive acceleration can be maintained when there is a pressure differential between stages. In this testing configuration, the first 3 m of the ram accelerator contained a starting propellant of $3.1CH_4+2O_2+6.6N_2$ at 7.5 MPa, and the following 1 m contained a test propellant, usually $3CH_4+2O_2+7.5N_2$, at higher pressure.

Successful operation was demonstrated at a stage transition velocity of ~1600 m/s. Because of the thin wall of the Ti projectile, however, it proved necessary to drill a hole in its base to allow it to pressurize internally, in order to keep the nose cone from buckling at pressures greater than 10 MPa. At pressures greater than 11 MPa, the titanium projectiles unstarted upon entering the test stage, even with internal pressurization. The velocity-distance data for the titanium projectiles are shown in Fig. 5.

The wall pressure data for the experiment in which a titanium projectile made a successful transition from a 7.5 MPa starting stage and drove through an 11 MPa test propellant indicate pressure wave-forms

typical for a successfully established thermally choked flow field [11] and no flow field abnormalities caused by the hole in the projectile base [7]. This is one of several experiments that demonstrated ram accelerator operation at pressures up to 11 MPa when the entrance velocity to the high pressure stage is sufficiently high (>1400 m/s). The particular parameters for this series of experiments are shown in Table A-2 in the Appendix.

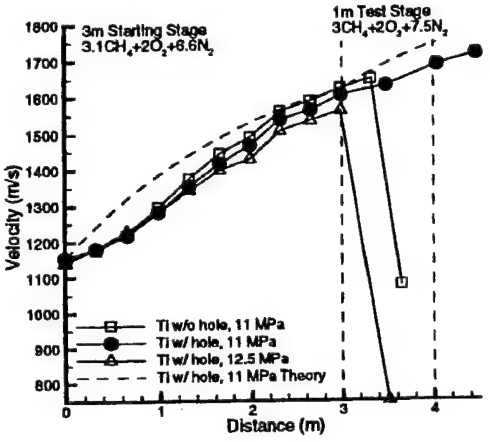

Figure 5: Results from Ti projectile pressure discontinuity experiments with 3-m, 7.5 MPa starting stage.

3.3 Obturator Geometry Effects

Some experiments in 7.5 MPa propellant using projectiles with a base hole generated relatively little thrust during the first meter of operation, until either the thermally choked propulsive mode was established or a wave unstart (i.e., the driving of a normal shock wave over the throat of the projectile, causing cessation of thrust) occurred. This "lag" in the starting process was attributed to a combination of factors, the most significant of which is the possibility that the obturator fragmented upon impact with the entrance diaphragm and did not provide sufficient occlusion of the flow to facilitate the starting process. Obturator fragments found in the vent tube during the clean-up between experiments supported this supposition. In order to alleviate this structural integrity problem, the obturator was strengthened by reducing the diameter of the perforations thus reducing its open area from 41% to 23%. The velocity-distance data for these experiments are shown in Fig. 6.

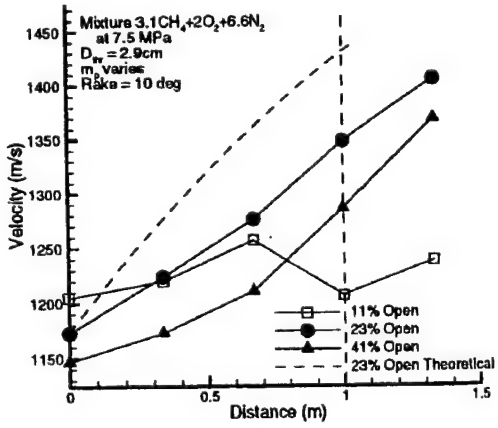

Figure 6: Velocity-distance data for obturator variation experimental series using Mg projectiles.

By reducing the open area ratio of the obturator (Figs. 3a and 3b), it was observed that the velocity lag the projectiles had been experiencing in the starting stage was reduced and high acceleration operation was established more quickly. When the open area was reduced to 13%, a wave unstart was experienced within 0.5 m of the entrance to the test section. These experiments showed that the strengthened obturator was more reliable in initiating a successful start of the ram accelerator at high fill pressure [7]. The particulars of the experimental setup in each case are shown in Table A-3 in the Appendix.

3.4 Sonic Diffuser Unstart at High Pressure

The experiments described in the previous section indicated that the standard projectile could not be gasdynamically started in inert propellant at entrance Mach numbers around 3.2. Prior experience had shown that the minimum projectile Mach number which can maintain supersonic flow through the projectile throat (sonic diffuser unstart limit) is approximately 2.6, when the propellant fill pressure is less than 5 MPa. Several experiments were conducted in which a projectile was launched into a 1-m-long starting stage of 7.5 MPa propellant, accelerated up to 1300 m/s, and then the combustion was stripped away and the projectile was allowed to decelerate through a 5-m-long stage of nitrogen at equal pressure. The standard 5-fin projectile (Fig. 2a) experienced a sonic diffuser unstart (SDU) at a higher velocity (~1220 m/s) in the 7.5 MPa propellant than that observed in similar experiments at 5 MPa (~960 m/s). Similarly, a standard geometry solid Mg projectile (Fig. 2c) experienced a sonic diffuser unstart at a velocity of ~1100 m/s in the same propellant and fill pressure. This increased sonic diffuser Mach number limit may indicate that starting the ram accelerator in propellants at elevated fill pressure requires a greater entrance velocity to the test section. The velocity-distance data for these two experiments are shown in Fig. 7a.

The data indicate two different values of the SDU velocity at the same fill pressure. To determine if this result is anomalous or indicative of unsteady flow field effects due to differing rates of deceleration, these data, along with those compiled from previous instances of sonic diffuser unstart, have been plotted as a function of SDU Mach number and fill-pressure-to-projectile-mass ratio in Fig. 7b. These data indicate that over the Mach number range shown the SDU Mach number is proportional to the ratio of the fill pressure to the projectile mass [7]. Thus the increase in SDU Mach number may be primarily due to increased deceleration once a wave fall-off has occurred. This topic is still under investigation.

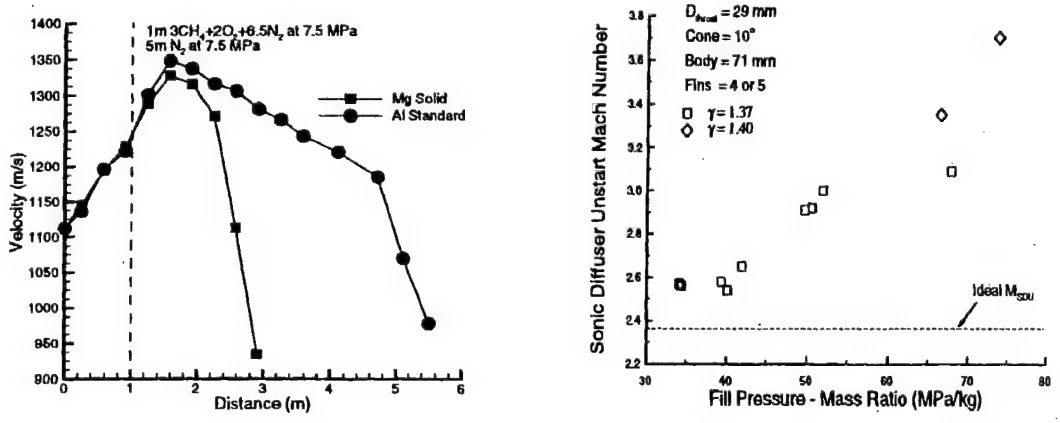

a) b)

Figure 7: a) Velocity-distance data from SDU determination experiments. b) SDU Mach number vs. P/m ratio data.

3.5 Entrance Velocity Effects on Starting

In order to achieve greater launch velocities, experiments were conducted with short-bodied Al projectiles (Fig. 2b) and 10° nose cones (total mass of 67 gm). These low mass projectiles were launched into the test section at entrance velocities in the range of 1270-1310 m/s, and achieved successful starts in a 1-m-long

stage of the $3.1CH_4+2O_2+6.6N_2$ propellant at 8.5 MPa, thus demonstrating entrance velocity to be a factor in successful starting at fill pressures greater than 8 MPa. Similar starting results were achieved in 1-m-long stages of $3CH_4+2O_2+7.5N_2$ propellant at 10 and 11 MPa, as shown in Fig. 8a.

Because of the thin walls of these projectiles, it proved necessary to drill a hole in the projectile base to allow it to pressurize internally and thus keep the nose cone from buckling. The success of these shots confirmed that projectiles having the standard throat diameter can be started at fill pressures up to 11 MPa as long as the entrance velocity is sufficiently high and the projectile integrity is maintained. At fill pressures greater than 11 MPa, however, wave unstarts occurred, even in inert propellant, indicating that structural failure could still be a significant factor affecting the start process under these conditions.

The theoretical velocity-distance curves for these experiments, using a real gas model with the Boltzmann virial equation of state [10], indicate average accelerations of 50,800 g at 10 MPa and 55,800 g at 11 MPa, considerably greater than the average accelerations achieved in the laboratory (34,700 g and 32,500 g, respectively). These discrepancies may be due to transient phenomena associated with the starting process at high pressure and are still under investigation.

Shown in Fig. 8b are the tube wall pressure data for the 10 MPa experiment. These data are typical for successful starting and operation of the ram accelerator in the thermally choked propulsive mode. The peak operating cycle pressure ratio is about 15, and the peak pressure appears behind the base of the projectile.

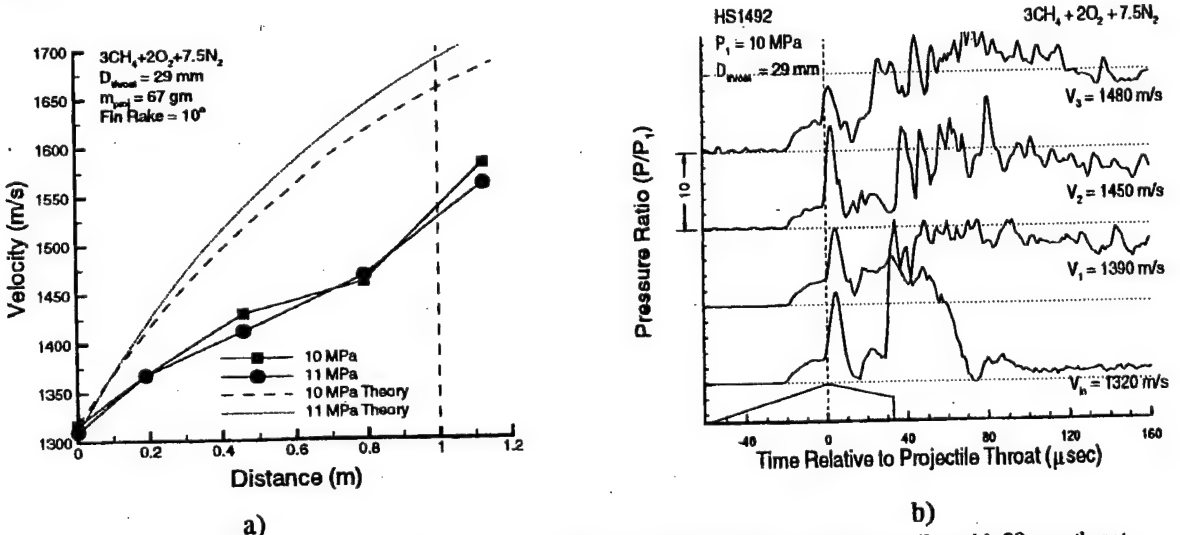

a) b)

Figure 8: a) Results of 10 and 11 MPa starting experiments using low mass aluminum alloy projectiles with 29 mm throat. b) Tube wall pressure data for the 10 MPa experiment.

3.6 Projectile Throat Diameter Effects on Starting

With the problem of starting at fill pressures greater than 7.5 MPa now clearly linked to entrance velocity, obturator open area, and the structural integrity of hollow projectiles, experimentation was directed toward achieving successful starts at higher fill pressure in the first tube using one-piece Mg alloy projectiles. These experiments used a 1-m-long stage of $3CH_4+2O_2+7.5N_2$ propellant, and fill pressures up to 12 MPa (only 1 m of test section was used in order to avoid the effects of burning magnesium that occur after prolonged ram acceleration at high Mach number). By reducing the throat diameter from 29 mm to 25 mm and reducing the overall length of the projectile to 125 mm (Fig. 2d), the one-piece magnesium projectiles with solid nose cones were able to be successfully started at fill pressures of 10 and 12 MPa within the entrance velocity range of 1280-1300 m/s, as shown in Fig. 9a. The wall pressure data from this experiment are presented in Fig 9b. In this case, the pressure data are similar to those indicating successful starting and operation in the thermally choked ram acceleration mode, and are similar in magnitude to the data of Fig. 8b. Thus the projectile throat diameter does not appear to affect ram accelerator operation at 10 MPa, but is significant in that it permits starting in 12 MPa propellants.

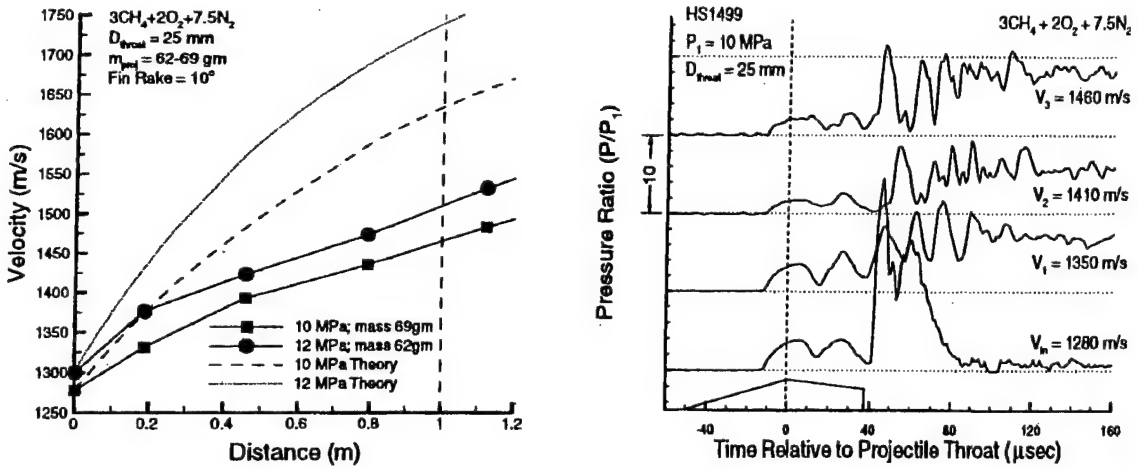

Figure 9: a) Results of 10 and 12 MPa starting experiments using solid magnesium alloy projectiles with 25 mm throat. b) Tube wall pressure data for the 10 MPa experiment.

3.7 High Pressure Starting Experiments

Because commercial gas cylinders of certain constituent gases at pressures above 17 MPa are not available, it was necessary to change the stoichiometry of the propellant to a range which could be obtained from the gases that were available at high pressure. By using 40 MPa air ($2O_2$+$7.52N_2$) and a 60/40 mixture of methane and nitrogen at 27 MPa, it was possible to prepare a high pressure propellant with a heat release and acoustic speed equivalent to that of the $3CH_4$+$2O_2$+$7.5N_2$ propellant.

One-piece Mg alloy projectiles with the reduced throat diameter and shortened body (Fig. 2d) were successfully started in 1-m-long stages of $2.5CH_4$+$2O_2$+$10N_2$ and $2CH_4$+$2O_2$+$9.5N_2$ propellant at a fill pressure of 12.5 MPa, and at entrance velocities of 1250-1320 m/s. These results indicate that there is a relatively wide range of allowable heat release for starting the ram accelerator at this fill pressure.

Additional experiments were conducted to investigate starting in propellants at 15 MPa using the reduced throat diameter, solid nose cone, one-piece Mg alloy projectiles. The projectiles used at 12.5 MPa (Fig. 2d) could not be successfully started at 15 MPa, regardless of the propellant chemistry. Due to concerns of possible projectile instability, the length of the fin in contact with the wall was increased by increasing the rake angle of the fins from 10^o to 20^o, and the fins were knife-edged (Fig. 2e) to reduce the influence of shock waves off the fins. These projectiles entered the test section in the velocity range of 1270-1305 m/s. Velocity-distance data from three experiments are shown in Fig. 10a. The projectile was able to successfully start in $3.3CH_4$+$2O_2$+$9.7N_2$ propellant and to accelerate throughout the 1-m-long stage. Also in this figure are results from two of the "bounding" experiments. A theoretical velocity-distance curve is also shown in Fig. 10a for the conditions of the successful 15 MPa start. The predicted average acceleration through the stage is 80,000 g, while the average acceleration experimentally achieved was only 26,000 g. It is not yet known if the deviation from theory is due to starting transients arising from high pressure and thick diaphragms, degradation of the projectile fin leading edges and nose tip, or other causes. Tube wall pressure data for the successful start at 15 MPa are shown in Fig. 10b. The first strong shock observed behind the throat is due to the intersection of shocks coming off the leading edges of the fins on the aft body of the projectile [11]. The combustion driven shock wave system seems to be just behind the base of the projectile, with a peak pressure ratio less than that expected for thermal choking. These waveforms do not provide conclusive evidence that a thermally choked flow field was fully established within the first 1-m of operation [11]. The low level of thrust achieved in this experiment may be an indication that the flow did not thermally choke within the stage. The overall results of the high pressure starting experimental series described in Sections 3.5 - 3.7 are shown in Table A-4.

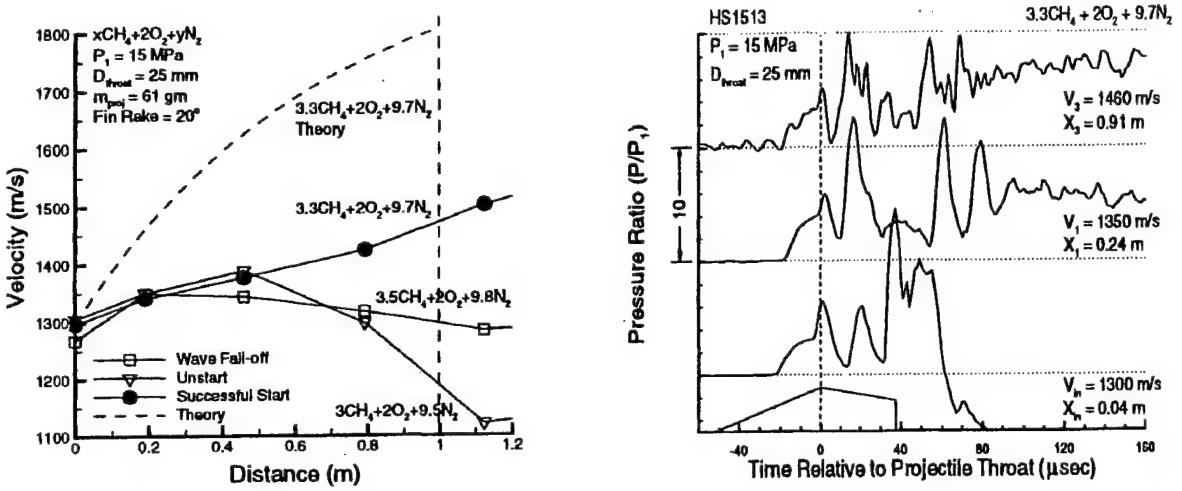

a) b)

Figure 10: a) Results from starting experiments at 15 MPa. b) Tube wall pressure data from successful start at 15 MPa

4. CONCLUSIONS

Experiments conducted in the 38-mm bore ram accelerator have demonstrated that successful starting of a projectile with a 29 mm-diameter throat at pressures greater than 7.5 MPa requires greater entrance velocity than 1200 m/s. The sonic diffuser unstart Mach number increases with fill pressure, and appears empirically to be proportional to the ratio of the fill pressure to the projectile mass, thus raising the lower limit of the entrance velocity at greater fill pressures. Successful starting and operation at fill pressures up to 11 MPa using hollow projectiles has been demonstrated when the projectiles are allowed to internally pressurize through a hole in the base. A strengthened obturator was found to be more reliable in initiating ram accelerator operation at high fill pressure. Solid magnesium projectiles with a reduced throat diameter of 25 mm have been successfully started at 10 MPa with no significant change in the flow field, and have enabled successful starting at pressures up to 15 MPa. The average acceleration in these experiments is generally overpredicted by the one-dimensional control volume theory using the Boltzmann equation of state, for reasons as yet undetermined.

Acknowledgments

These experiments were performed under U.S. Army Research Office grant number DAAG55-97-1-0131. The assistance of Ryan Schwab with the experiments and David Buckwalter with the real gas calculations is greatly appreciated.

References

1. A.P. Bruckner, C. Knowlen, A. Hertzberg, D.W. Bogdanoff, J. Prop. and Power, **7**, 828-836 (1991).
2. A. Hertzberg, A.P. Bruckner, D.W. Bogdanoff, AIAA J., **26**, 195-203 (1988).
3. A. Hertzberg, A.P. Bruckner, C. Knowlen, *Shock Waves*, **1**, 17-25 (1991).
4. E.A. Burnham, A.E. Kull, C. Knowlen, A.P. Bruckner, A. Hertzberg, AIAA 90-1985 (1990).
5. C. Knowlen, A.J. Higgins, A.P. Bruckner, P. Bauer, AIAA 96-0098 (1996).
6. E. Schultz, C. Knowlen, A.P. Bruckner, *Ram Accelerators*, edited by K. Takayama, A. Sasoh, (Springer-Verlag, Heidelberg, 1998), pp 189-203.
7. C. Bundy, C. Knowlen, A.P. Bruckner, AIAA 99-2261 (1999).
8. J.F. Stewart, A.P. Bruckner, C. Knowlen, *Ram Accelerators*, edited by K. Takayama, A. Sasoh, (Springer-Verlag, Heidelberg, 1998), pp 181-189.

9. C. Bundy, C. Knowlen, A.P. Bruckner, AIAA 98-3144 (1998).
10. D.L. Buckwalter, C. Knowlen, A.P. Bruckner, AIAA 96-2945 (1996).
11. J.B. Hinkey, E.A. Burnham, A.P. Bruckner, AIAA Paper 93-2186 (1993).

APPENDIX

Table A-1: Results of reducing pressure differential between stages using Al alloy projectiles (Fig. 2a).

Experiment Reference Number	Stage Length (m)	Propellant ($xCH_4+yO_2+zN_2$)	Fill Pressure (MPa)	Entrance Velocity (m/s)	Exit Velocity (m/s)	Average Acceleration (g)
HS1412	1	3/2/5.7	5	1133	1305	21,400
	3	3/2/5.7	5	1305	1597	14,400
HS1413	1	3/2/5.7	5	1125	1261	16,500
	3	3/2/5.7	7.5	1261	1669	20,300
HS1414	1	3/2/5.7	5	1120	1257	16,600
	3	4/2/5.7	10	1257	1796	28,000
HS1415	1	3/2/5.7	5	1120	1224	12,400
	3	3/2/5.7	12.5	1224	unstart	NA
HS1418	1	3/2/5.7	5	1143	1276	16,400
	3	3/2/5.7	11	1276	unstart	NA
HS1421	1	3/2/6.5	6	1150	1257	13,100
	3	3/2/6.5	11	1257	unstart	NA
HS1432	1	3/2/6.5	7.7	1145	1257	13,700
	3	3/2/6.5	11	1257	unstart	NA
HS1428	1	3/2/6.5	8.4	1116	unstart	NA
	3	3/2/6.5	11	NA	NA	NA

Table A-2: Results of stage transition velocity experiments using 3-m starting stages.

Experiment Reference Number	Stage Length (m)	Propellant ($xCH_4+yO_2+zN_2$)	Fill Pressure (MPa)	Entrance Velocity (m/s)	Exit Velocity (m/s)	Average Acceleration (g)	Projectile Design
HS1444	3	3.1/2/6.6	7.5	1173	1487	14,200	Fig. 2b (Al)
	1	3/2/7.5	10	1487	1692	33,200	
HS1469	3	3.1/2/6.6	7.5	1151	1623	22,200	Fig. 2b (Ti)
	1	3/2/7.5	11	1623	unstart	NA	
HS1473	3	3.1/2/6.6	7.5	1155	1604	21,000	Fig. 2b (Ti)
	1	3/2/7.5	11	1604	1687	13,900	w/ base hole
HS1471	3	3.1/2/6.6	7.5	1164	1623	22,200	Fig. 2b (Ti)
	1	3/2/7.5	12.5	1623	unstart	NA	w/ base hole

Table A-3: Results of obturator variation experiments using solid Mg projectiles (Fig. 2c).

Experiment Reference Number	Stage Length (m)	Propellant ($xCH_4+yO_2+zN_2$)	Fill Pressure (MPa)	Entrance Velocity (m/s)	Exit Velocity (m/s)	Average Acceleration (g)	Obturator Open Area
HS1475	1	3.1/2/6.6	7.5	1147	1286	17,200	42%
HS1479	1	3.1/2/6.6	7.5	1205	unstart	NA	13%
HS1480	1	3.1/2/6.6	7.5	1159	1343	23,500	23%

Table A-4: Starting results at fill pressures of 8.5 MPa and higher.

Experiment Reference Number	Stage Length (m)	Propellant ($xCH_4+yO_2+zN_2$)	Fill Pressure (MPa)	Entrance Velocity (m/s)	Exit Velocity (m/s)	Average Acceleration (g)	Projectile Design
HS1476	1	3.1/2/6.6	8.5	1271	1369	13,200	Fig. 2b (Al)
HS1492	1	3/2/7.5	10	1317	1554	34,700	Fig. 2b (Al)
HS1494	1	3/2/7.5	11	1310	1560	32,500	Fig. 2b (Al)
HS1499	1	3/2/7.5	10	1278	1483	23,000	Fig. 2d (Mg)
HS1500	1	3/2/7.5	12	1300	1532	29,800	Fig. 2d (Mg)
HS1504	1	2.5/2/10	12.5	1320	1491	21,800	Fig. 2d (Mg)
HS1505	1	2/2/9.5	12.5	1245	1478	29,800	Fig.2d (Mg)
HS1506-10	1	2.5-3.5/2/9.2-9.8	15	1286-1325	unstart	NA	Fig. 2d (Mg)
HS1511	1	3.5/2/9.8	15	1286	wave falloff	NA	Fig. 2e (Mg)
HS1512	1	3/2/9.5	15	1305	unstart	NA	Fig. 2e (Mg)
HS1513	1	3.3/2/9.7	15	1296	1501	26,000	Fig. 2e (Mg)

Appendix C

Summary of Experimental Results at 150 - 200 atm Fill Pressure

Presented at 36th AIAA/ASME/SAE/ASEE Joint Propulsion Conference, Huntsville, AL
July 16-19, 2000

Investigation of Ram Accelerator Operation at Fill Pressures up to 20 MPa

C. Bundy,* C. Knowlen,† and A.P. Bruckner‡
Aerospace and Energetics Research Program
University of Washington, Box 352250
Seattle, WA 98195-2250

Abstract

An experimental investigation of the starting and operational characteristics of the ram accelerator with propellant fill pressures of 15 MPa and greater is in progress at the University of Washington. Starting the 38-mm bore ram accelerator with magnesium and titanium projectiles of masses between 46 gm and 120 gm, has been achieved using methane/oxygen/nitrogen propellants at fill pressures of up to 20 MPa. At fill pressures of 15 MPa, it was found that magnesium projectiles with a throat diameter of 25 mm could be started in a relatively wide range of propellant compositions and at entrance speeds as low as 1200 m/s. Due to the rapid deterioration of magnesium projectiles in the severe high density aerothermal environment, they were shown to be useful only for experiments using accelerator tube lengths of less than 2 m. Titanium projectiles of similar design were shown to start and accelerate in propellants of more energetic chemistry and to withstand ram acceleration for at least 3 m in 15 MPa propellant. At fill pressures of 20 MPa, it was shown that reliable starting of magnesium and titanium projectiles could be achieved by reducing the throat diameter to 23 mm while maintaining an entrance speed of 1200 m/s. The average accelerations achieved across 20 MPa stages were in general somewhat less than predicted for thermally choked operation when using the Boltzmann virial expansion for the equation of state.

I. Introduction

Ram accelerator technology has the potential to launch massive projectiles at high velocity from relatively short length tubes.[1] Since the ram accelerator operates with a ramjet-like propulsive cycle,[2-3] the amount of thrust generated is directly proportional to the fill pressure and increases with increasing heat release of the propellant. Thus the highest acceleration performance for a given projectile mass will be achieved by operating at the highest fill pressure feasible, within the strength constraints of the accelerator tube, and with the most energetic propellant that will sustain ram acceleration. These operating conditions subject the projectile to a severe aerothermal environment and introduce significant logistical challenges to initiating the ram accelerator process itself. Addressing these issues is the primary focus of the high pressure research program in progress at the University of Washington (UW).

Several different ram accelerator propulsive cycles have been identified which are characterized by the manner in which the propellant heat release occurs and by the velocity of the projectile relative to the Chapman-Jouguet (CJ) detonation speed.[4] Only high pressure operation in the thermally choked propulsive mode is discussed in this paper; details of the other propulsive modes can be found in the cited references.[4-6] A brief overview of the ram accelerator starting process and possible results of that process are presented in Section II, and theoretical considerations of high pressure operation are discussed in Section III. The UW ram accelerator facility is described in Section IV and key results of prior high pressure experimental work are summarized in Section V. Results from the most recent investigations are presented and their implications discussed in Section VI.

II. Ram Accelerator Starting

The starting process encompasses the phenomena associated with launching the subcaliber projectile and tube-occluding obturator from rest to the entrance of the ram accelerator test section, and the establishment of the thermally choked ram accelerator flow field.[7-10] During

---

* Graduate Student, Student Member AIAA.

† Research Scientist, Senior Member AIAA.

‡ Professor and Director, Fellow AIAA.

this process, the occlusion provided by the obturator causes a normal shock wave to be driven onto the rear body of the projectile. The obturator then quickly recedes and ceases to influence the flow field after the projectile has traveled for about 1-m beyond the test section entrance.[8] Propellant ignition occurs as a result of the complex interactions of shock waves in the residual air in the launch tube (resulting from its imperfect evacuation) with the projectile, the obturator, and the diaphragm at the entrance to the test section.[9] The ram accelerator is successfully started once supersonic flow is established behind the projectile throat, and the normal shock wave is stabilized on the rear body by thermal choking of the flow behind the projectile, as shown in Fig. 1.[10]

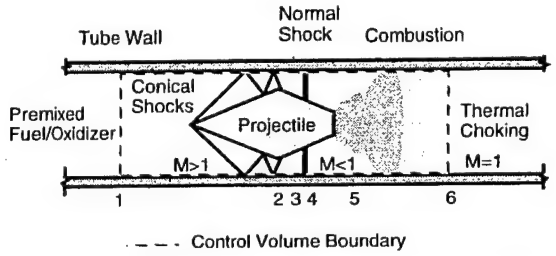

Fig. 1 Thermally choked ram accelerator propulsive mode.

Under certain conditions a prolonged delay in the combustion stabilization process occurs in which the flow remains supersonic relative to the projectile throat and the projectile is weakly accelerated. Ultimately, the flow becomes thermally choked and the acceleration increases dramatically. This delay in the starting process is referred to as a "delayed start". In experiments having a test section length of only 1 m, there may not be sufficient test section length for the projectile to travel beyond that required to establish thermal choking and achieve a "successful start"; however, the delayed start does indicate that the conditions necessary for a successful start other than thermal choking are met and that the particular permutation of propellant, obturator, and projectile used do not preclude successful ram accelerator operation.

When the necessary conditions for ram acceleration starting or delayed starting are not met, the projectile decelerates. A "wave fall-off" occurs when there is insufficient heat release to drive a normal shock up onto the rear body, in which case the projectile coasts supersonically through the propellant as the normal shock wave falls behind. If the entrance velocity to the test section is too low, or the projectile nose cone is significantly damaged as it penetrates the entrance diaphragm, or there is substantial heat release ahead of the projectile throat, then the flow chokes at the throat and a strong normal shock wave is driven ahead of the projectile. This result, when caused by these phenomena, is referred to as a "sonic diffuser unstart." If the normal shock wave overtakes the projectile throat at some point after which supersonic flow is established behind the throat, thrust ceases and the resulting failure is referred to as a "wave unstart". Some factors which produce wave unstarts include too much heat release from the propellant, too much flow occlusion by obturator, and excessive obturator mass. The outcome of a ram accelerator start attempt is readily determined from tube wall pressure data and the velocity-distance profile of the projectile.[10]

III. Theoretical Considerations

The net axial force (thrust) acting on a ram accelerator projectile is dependent on the propellant composition, fill pressure, equation of state, and the Mach number of the projectile relative to the quiescent propellant. The theoretical thrust of the thermally choked propulsive mode is readily determined in the reference frame of the projectile by applying the steady, one-dimensional gas dynamic conservation equations to the entrance (station 1) and exit (station 6) planes of an appropriately chosen control volume, as shown in Fig. 1, and assuming that the exit flow is at sonic velocity with respect to the projectile.[11] Since the flow properties at the exit of the control volume correspond to a thermally choked state, the theoretical thrust is independent of projectile geometry.[12] Real gas effects are incorporated with a compressibility term "σ" in the ideal gas equation of state as follows: $P = \sigma\rho RT$, where P is pressure, T is temperature, ρ is density, and R is the gas constant.[13] This modeling approach enables an analytical expression to be readily determined for ram accelerator thrust which incorporates the real gas correction term.[14]

A computer code has been developed which can accommodate several different equations of state to investigate real gas effects on the temperature, pressure, and chemical equilibria of the products at the choke point.[15,16] Fugacity coefficients are used to evaluate shifts in chemical equilibria due to molecular interactions and finite volumes. For the purposes of this paper, real gas effects are evaluated with the Boltzmann virial expansion of the equation of state.[13,14]

Compressibility corrections for the unreacted propellant are not very significant for the thermally choked ram accelerator thrust-Mach number predictions, and thus are not considered in the following calculations. More details of the numerical procedures can be found in Refs. 15-17. The calculated variation with Mach number of the non-dimensional thrust, non-dimensional heat release, the ratio of thermally choked pressure to fill pressure, and acoustic speed in the thermal choking plane as a result of incorporating real gas effects is discussed in Ref. 18.

The theoretical model has several limitations which must be considered when interpreting the results. First of all, this model does not account for the presence of an obturator and is thus not expected to provide much insight on the experimental conditions needed to effect a successful start of the ram accelerator. Secondly, the model is exact (in a one dimensional sense) only when the projectile is not accelerating. At high fill pressure the ratio of propellant density to projectile density becomes non-trivial,[3] resulting in a higher fraction of the chemical energy being used to accelerate the propellant within the control volume. Consequently the theoretical model is expected to overpredict projectile acceleration for thermally choked operation at high pressure. The model is still useful as a reference for experimental results and to estimate the effects on performance anticipated with changes in propellant composition, fill pressure, and Mach number. Experimentation is necessary to determine the regimes of Mach number and heat release in which a particular projectile geometry can be accelerated.

Previous experiments conducted in propellants at fill pressures of 7.5 MPa and greater indicated that the projectile entrance velocity to the ram accelerator test section must be increased with increasing fill pressure, and that the sonic diffuser unstart Mach number increases with the fill pressure-to-projectile mass ratio.[18] This observation may be partially attributable to the behavior of the acoustic speed of the propellant at high fill pressures. An analytical expression for the acoustic speed of a real gas indicates that with temperature held constant, the acoustic speed varies with pressure. For purposes of illustration, the acoustic speed of a typical propellant used in the experiments described in this paper is shown as a function of fill pressure in Fig. 2. The calculated acoustic speed uses the Redlich-Kwong equation of state, with empirically determined mixture values used for the two real gas constants in the equation to account for the interactions of dissimilar molecules.[19]

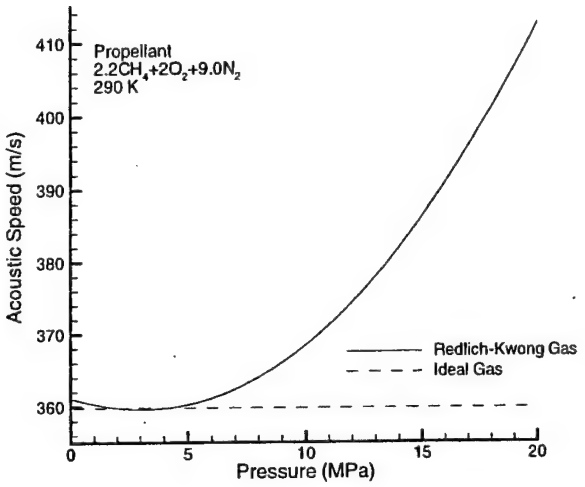

Fig. 2 Variation of acoustic speed of $2.2CH_4+2O_2+9.0N_2$ with pressure at constant temperature (290 K).

The ideal gas acoustic speed (which does not vary with pressure when temperature is a constant) is also shown in Fig. 2 for comparison. At 20 MPa, the real gas acoustic speed is 53 m/s greater than that of the ideal gas, i.e., a 15% increase. The trend toward higher acoustic speeds at higher pressure requires the projectile to have a higher entrance velocity to avoid flow choking at the projectile throat, causing a start failure.

As previously stated, the one-dimensional control volume approach to thermally choked ram accelerator performance prediction is not strictly correct unless the projectile (and thus the control volume surrounding it) is not accelerating. Analysis of the model indicates that at modest rates of acceleration (~10,000 g) and high velocities, the quasi-steady assumption is sufficiently accurate for predicting performance.[3] At high fill pressures, however, the expected accelerations are on the order of 100,000 g, thus requiring that the unsteady condition of the true flow field be taken into account. From consideration of the unsteady momentum equation, it can be readily shown that the acceleration of the projectile reference frame decreases the predicted thrust, and thus should be accounted for in the model.[3] Efforts to incorporate the effects of projectile acceleration in the performance model are currently in progress.

IV. Experimental Facility

The facility at the University of Washington (UW) enables ram accelerator experimentation at propellant

fill pressures up to 20 MPa. Brief descriptions of the facility test section and the various projectiles used in the experiments are provided in this section. Details of the light gas gun pre-launcher, propellant filling system, and other major system components can be found in Refs. 18, 20, and 21.

High Pressure Test Section

The first 4 m of the ram accelerator test section, shown in Fig. 3, consist of two 1-m-long and one 2-m-long high pressure tubes, with an outer diameter of 152 mm and an inner diameter of 38 mm,[20] connected together using bolted flange joints. The high pressure tubes are manufactured from AISI 4340 steel, and are designed for a maximum static load of 1000 MPa. The remaining 12 m of the test section is comprised of six low pressure tubes manufactured from AISI 4140 steel, each 2 m in length, with outer diameters of 102 mm. These tubes are connected with threaded collars and are designed to withstand a static load of up to 550 MPa. The two parts of the test section are connected using a bolted flange joint containing an insert piece to properly join the two different tube designs.

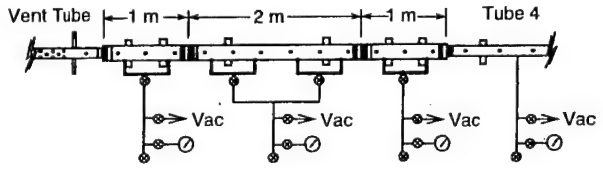

Fig. 3 High pressure test section of the 38-mm bore ram accelerator facility.

Each 1-m-long tube (Fig. 3) has three instrument stations with diametrically opposed ports; the 2-m-long tube has six pairs of ports. These stations are spaced along the tubes at 333 mm intervals. The first instrument station in the high pressure test section is 167 mm from the entrance diaphragm. The last station in the high pressure tubes is spaced 167 mm from their exit and 396 mm from the first instrument port in the low pressure part of the test section. The instrument stations are spaced 400 mm apart throughout the low pressure part of the test section. The instrument ports can accommodate electromagnetic (EM) probes and PCB model A119A11 or A119A12 piezoelectric pressure transducers (550 or 800 MPa maximum pressure range, respectively).

All of the tubes in the high pressure test section have two fill ports per meter of length, as shown in Fig. 3. These fill ports are isolated from the fill lines by air-actuated Snotrik valves (300 MPa rated), which separate the gas handling system from the extreme pressure pulses generated in the experiments. The low pressure part of test section has fill ports placed every 2 m. In between any pair of adjacent tubes, Mylar diaphragms can be inserted to separate the propellants, enabling multiple stages of different propellants, and hence acoustic speeds, to be used. Any tubes not filled with a propellant are evacuated for the experiments.

Experimental Projectiles

Several different projectile geometries and materials were used in this investigation. Four- and five-finned one-piece projectiles were manufactured from magnesium ZK60A-T5 alloy and from titanium 6Al-6V-2Sn alloy in similar basic geometries, with adjustments to the geometry machined post-fabrication as necessary for individual experiments. The basic designs are shown in Fig. 4, with nose cone angle, body length, fin rake angle, fin thickness, and throat diameter varying for individual projectiles, determined as required for each experiment, and fully detailed in the experiment descriptions in Section VI. All the projectiles feature fin diameters of 38 mm, and a hole in the base of 14 mm diameter, into which a ceramic or neodymium magnet was inserted and held at the projectile throat by a threaded Mg plug. The remainder of the clearance hole was left open to reduce the overall mass of the projectiles. In most of the experiments, the fin leading edges were knife-edged at a 15° angle to their centerlines, in order to reduce the strength of the shock waves attached to the fins near the projectile throat; this modification is also shown in Fig. 4. The masses of the projectiles varied considerably, depending on the characteristic design parameters; the masses are noted for each experimental series or design configuration where appropriate.

The obturator, shown in Fig. 5a, is placed behind the projectile base to prevent gas blow-by from the light gas gun initial launcher and to drive a normal shock onto the projectile rear body upon entrance to the test section. The perforated two-piece obturators are fabricated from polycarbonate as a cylinder perforated with 7 holes of 6.4 mm diameter and 12 holes of 3.2 mm diameter (giving an open area ratio of 23%). A solid backplate covers the open holes at launch. The obturator and backplate have a combined mass of 16 gm when the obturator length is 13 mm and 19 gm when the length is 15 mm. The solid obturator, shown in Fig. 5b, is a single piece manufactured from polycarbonate and uses a Bridgeman seal to occlude the tube and prevent gun gas blow-by. This obturator was used in experiments in

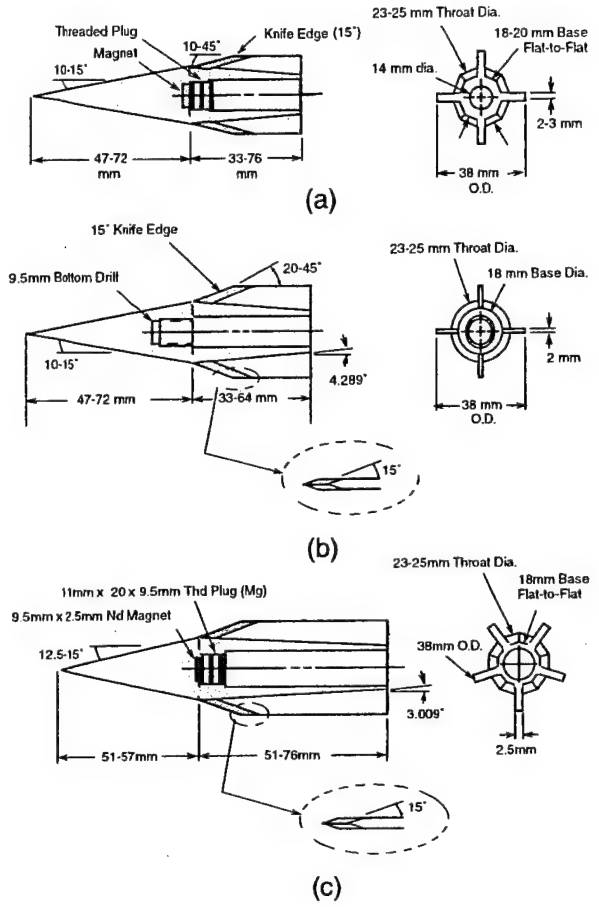

Fig. 4 Generalized projectile designs: a) four-finned Mg alloy, b) four-finned Ti alloy, c) five-finned Mg alloy.

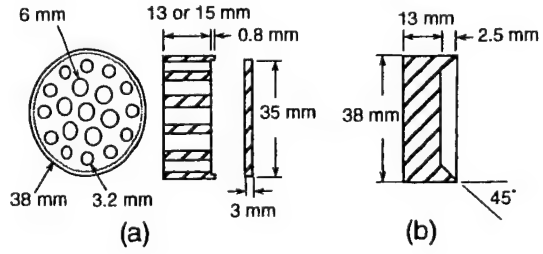

Fig. 5 Perforated and solid obturator configurations.

which the required gas gun breech pressure exceeded 35 MPa. The solid obturator has a mass of 18 gm. Both types of obturator are glued to the projectile with cyanoacrylate adhesive for the process of loading them into the light gas gun.

V. Prior High Pressure Results

A brief summation of the results of prior experiments conducted in the UW ram accelerator facility at 15 MPa fill pressures is provided in this section. Experiments were carried out to investigate starting in propellants at 15 MPa using 25 mm throat, 10^{o} solid nosed, one-piece magnesium projectiles. Due to concerns of possible projectile instability, the length of the fin in contact with the wall was increased by increasing the rake angle of the fins from 10^{o} to 20^{o}. In addition, the fins were knife-edged to reduce the influence of shock waves off the fins. These projectiles entered the test section in the velocity range of 1270-1305 m/s. Velocity-distance data from three experiments are shown in Fig. 6.

The projectile was able to successfully enter the $3.3CH_4+2O_2+9.7N_2$ propellant and to accelerate throughout the 1-m long stage. Also in this figure are results from two of the "bounding" experiments. The less energetic propellant ($3.5CH_4+2O_2+9.8N_2$) was not able to be ignited, resulting in the occurrence of a wave fall-off, typical of an unacceptably "cold" mixture. The more energetic propellant ($3CH_4+2O_2+9.5N_2$) produced a wave unstart, which is typical of excessively "hot" propellants. A theoretical velocity-distance curve is also shown in Fig. 6 for the conditions of the successful 15 MPa start, using the Boltzmann equation of state. The predicted average acceleration through the stage is 80,000 g, while the average acceleration achieved was only 26,000 g. The relatively low level of thrust achieved in this experiment indicates that the ram accelerator had experienced a delayed start.

Tube wall pressure data for the delayed start at 15 MPa are shown in Fig. 7. The first strong shock observed behind the throat is due to the intersection of shocks attached to the leading edges of the fins on the aft body of the projectile.[22] The combustion-driven shock wave system seems to be just behind the base of the projectile. These waveforms do not provide conclusive evidence that a thermally choked flow field was fully established within the 1 m stage,[23] thus supporting the hypothesis that the weak thrust is caused by a delay in establishment of thermal choking in the stage.

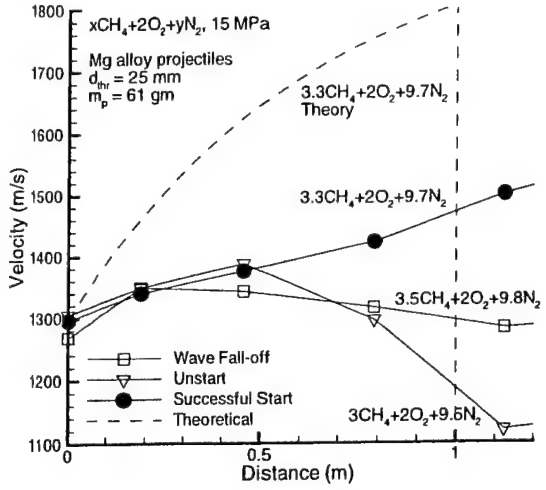

Fig. 6 Results from first 15 MPa starting experiments.

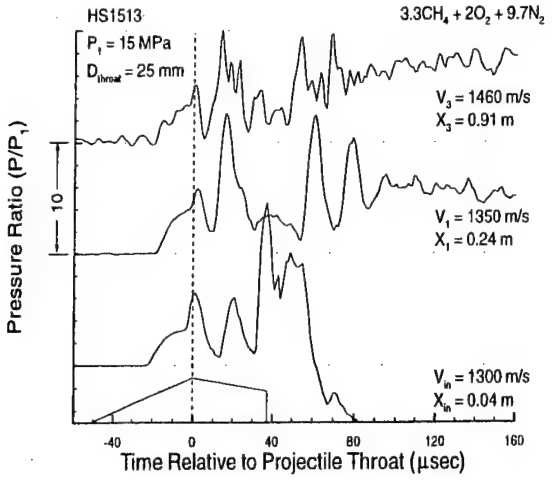

Fig. 7 Tube wall pressure data for 25 mm throat projectile at 15 MPa.

VI. Recent High Pressure Experiments

Using Mg alloy projectiles, the range of propellant variations which enable ram accelerator starting at 15 MPa was investigated. Attempts were then made to explore alternate projectile geometries which could start at 15 MPa and would not exceed the mass which the initial launcher could accelerate to the minimum entrance velocity when duplicated in Ti alloy. The operational envelope of the Mg alloy projectile design at 15 MPa was explored. A similar study was performed for Ti alloy projectiles of the same design. The role of the aft body length on projectile stability was briefly investigated. Experiments at 20 MPa were also performed, using Ti and Mg alloy projectiles with throat diameters reduced from 25 to 23 mm. The results of these investigations are presented in the following subsections.

Propellant Chemistry Variations

A sequence of experiments was conducted to determine whether the range of propellant variations at 15 MPa which enable starting of the ram accelerator was as limited as the first set of experiments at 15 MPa had indicated.[18] Also to be determined was whether the entrance velocity could be reduced from the 1300 m/s with which the first delayed start at 15 MPa had been achieved. Each of the experiments used Mg alloy projectiles of the original 15 MPa design (Fig. 4a), having a 10^0 nose cone, 25 mm throat diameter, 51 mm aft body, 18 mm base diameter, fins with knife-edging and 20^0 rake angle, and a mass of 55 - 61 gm. These experiments also used the 23% open obturator with 13 mm thickness, as shown in Fig. 5a.

A two-stage experiment was conducted to determine the minimum entrance speed required for the projectile design. The test section configuration consisted of a 1-m-long stage of the propellant that had previously enabled starting at 15 MPa ($3.3CH_4+2O_2+9.7N_2$), followed by a 2-m-long stage of N_2 to act as a combustion stripper and to decelerate the projectile in order to induce a sonic diffuser unstart. The projectile entered the first stage at 1290 m/s, experienced a wave fall-off, and entered the second stage at 1310 m/s. The projectile then decelerated through the second stage, undergoing a sonic diffuser unstart at a velocity of ~1150 m/s. This sonic diffuser unstart velocity is considerably less than the entrance velocity used in the first set of 15 MPa experiments, which indicated that a lower entrance velocity could possibly be used.

Further experiments were conducted with entrance velocities of 1160 - 1240 m/s in a 1-m-long stage of propellant at 15 MPa with various compositions. Since one experiment had shown a wave fall-off occurs in the $3.3CH_4+2O_2+9.7N_2$ propellant, the experiments that followed used more energetic propellants. The composition of the propellant was varied from $3.15CH_4+2O_2+9.6N_2$ as the least energetic to $1.4CH_4+2O_2+8.5N_2$ as the most energetic; the corresponding values of the non-dimensional heat release Q_{CJ} (the ratio of the propellant heat release to

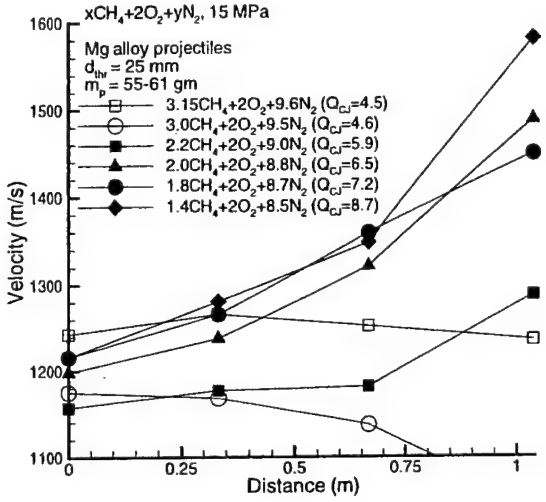

Fig. 8 Results of propellant composition variation using 25 mm throat Mg projectiles.

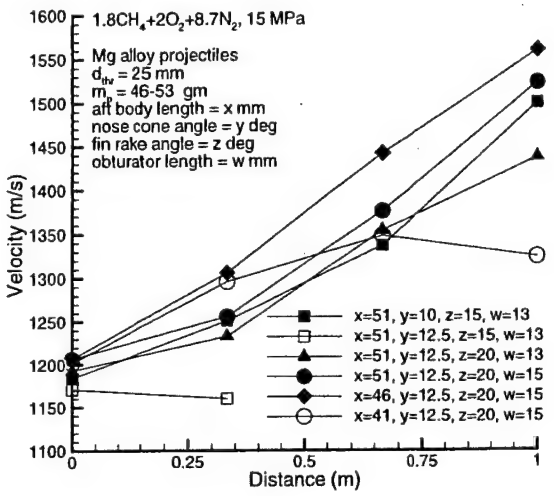

Fig. 9 Results from geometry variation experiments using Mg projectiles.

the product of the heat capacity and temperature of the quiescent propellant) varied from 4.5 to 8.7, respectively. The velocity-distance data from this set of experiments are shown in Fig. 8. In this figure, closed symbols denote experiments in which the projectile was gasdynamically started and continuously accelerated for at least 1 m, while open symbols denote experiments which failed to accelerate the projectile. Experiments using propellants with Q_{CJ} values equal to or greater than that of $2.2CH_4+2O_2+9.0N_2$ (Q_{CJ}=5.9) all resulted in successful ram accelerator operation and acceleration through the test section; those using less energetic propellants resulted in wave fall-offs.

Geometry Variations

An experimental series using Mg alloy projectiles with various geometries was conducted in order to determine a viable design for Ti alloy projectiles of sufficiently low mass for the light gas gun to be able to accelerate them to the entrance velocity required at 15 MPa. Using the 10° nose cone, 25 mm throat diameter, 51 mm aft body, 18 mm base diameter, knife-edged 20°-rake-angle four-fin Mg alloy projectiles and 13 mm-thick obturators from the previous series as a baseline, the nose cone angle, fin rake angle and leading edge quality, obturator thickness, and aft body length (and as a result, base diameter) were varied over several experiments while holding the propellant composition constant. The velocity-distance data for this series are shown in Fig. 9.

The experimental setup in each case used a 1-m-long stage of $1.8CH_4+2O_2+8.7N_2$ at 15 MPa. The projectiles entered the test section at velocities ranging from 1170 - 1210 m/s. The first variation (denoted by filled squares in Fig. 9) in which the fins were left blunt and the rake angle changed to 15°, (m_p = 58 gm), resulted in a successful entry and positive acceleration throughout the test section. The second variation (open squares) retained the 15°-rake blunt fins and changed the nose cone angle to 12.5°, resulting in a mass of 53 gm; this experiment resulted in a wave unstart. Wall pressure data indicate that the confluence of shock waves from the nose and the fins may have contributed to this unstart, thus the use of blunt fin leading edges was abandoned.

The third variation (solid triangles) retained the 12.5° nose cone angle and returned to the baseline 20°-rake knife-edged fins (m_p = 53 gm); in this case, the projectile successfully entered and accelerated throughout the test section. The fourth variation (solid circles) used the same projectile geometry but increased the thickness of the 23% open obturator to 15 mm in order to increase its strength; the thicker obturator would be more likely to be used with a Ti alloy projectile of the chosen design, in order to withstand the stress loading from the high breech pressure in the light gas gun necessary to launch the more massive projectile. This experiment, too, resulted in a successful entry and positive acceleration throughout the stage.

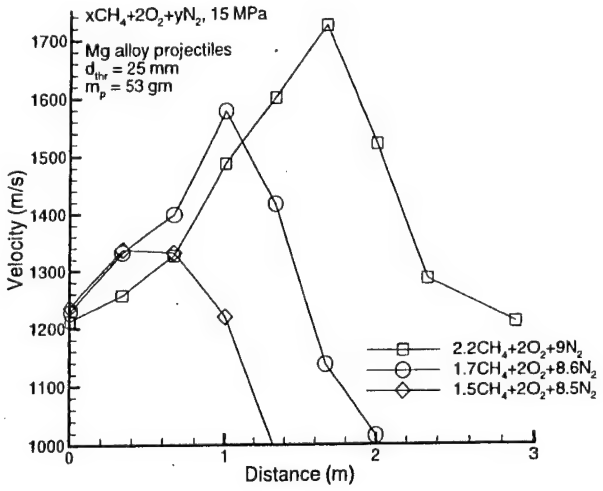

Fig. 10 Velocity-distance data from Mg projectile operation limit experiments.

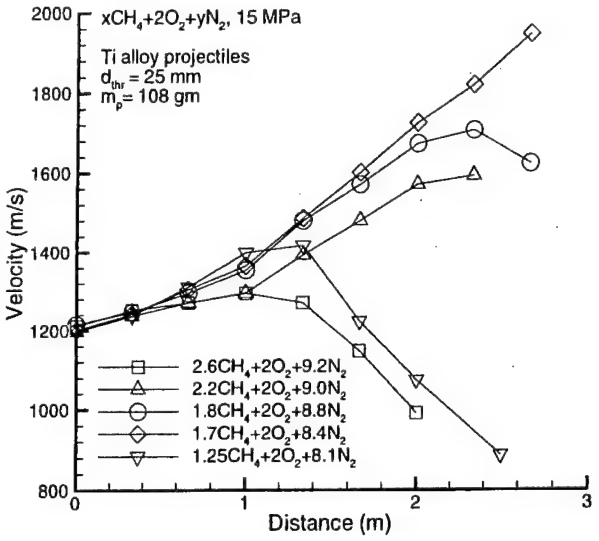

Fig. 11 Velocity-distance data from Ti projectile operation limit experiments.

The next experiments retained the 12.5° nose cone angle and 20°-rake knife-edged fins, as well as the thicker perforated obturator, while varying the aft body length of the projectile. The 51 mm aft bodies were simply cut short normal to the projectile axis; this necessarily resulted in a corresponding increase in base diameter. The fifth variation (solid diamonds) shortened the aft body to 46 mm (increasing the base diameter from 18 to 18.5 mm and decreasing the mass to 48 gm); the projectile successfully entered and accelerated through the stage, but wall pressure data indicated projectile canting in the test section.[23] The sixth variation (open circles) shortened the aft body to 41 mm (increasing the base diameter to 19 mm and decreasing the mass to 46 gm); this projectile unstarted almost immediately, with the wall pressure data showing signs of severe projectile canting. The data obtained from the experiments suggests that to assure projectile stability the aft body must be kept as long as possible.

High Pressure Operational Limits

The chemistry and geometry variation experiments provided data about which combinations of propellant and projectile design would enable the ram accelerator to operate for at least 1 m at 15 MPa; however, the operational limits of the successful propellants and designs were not quantified. A series of experiments was conducted with both Mg and Ti alloy projectiles to determine the limits of ram acceleration at 15 MPa.

A set of experiments was conducted using Mg alloy projectiles (Fig. 4a) of similar design (12.5° nose cone, 25 mm throat diameter, 51 mm aft body, 18 mm base diameter, knife-edged 20°-rake-angle fins, m_p ~53 gm). The experimental setup used a 3-m-long test stage having propellant variations ranging from $2.2CH_4+2O_2+9.0N_2$ (Q_{CJ}=5.9) to $1.5CH_4+2O_2+8.5N_2$ (Q_{CJ}=8.3), and the projectile entered the test section at 1200 - 1240 m/s. The velocity-distance data for the Mg series of experiments are shown in Fig. 10. The 15 mm-thick 23% open obturator was used for these and all subsequent Mg projectile experiments. In each of the experiments that followed, the ram accelerator was successfully started and the projectile accelerated for some distance (0.5 - 2 m) before undergoing a wave unstart. The longest run and highest velocity before unstart (~1740 m/s) was attained using $2.2CH_4+2O_2+9.0N_2$ propellant.

A series of Ti projectile experiments used the projectile geometry of Fig. 4b, with the following design parameters: 12.5° nose cone, 25 mm throat diameter, 51 mm aft body, 18 mm base diameter, knife-edged 20°-rake-angle fins. The resulting mass of the projectile was ~108 gm. Each experiment used a 3-m-long stage of propellant of various compositions [$2.6CH_4+2O_2+9.2N_2$ (Q_{CJ}=5.0) to $1.25CH_4+2O_2+8.1N_2$ (Q_{CJ}=9.5)], with the projectile entering the test

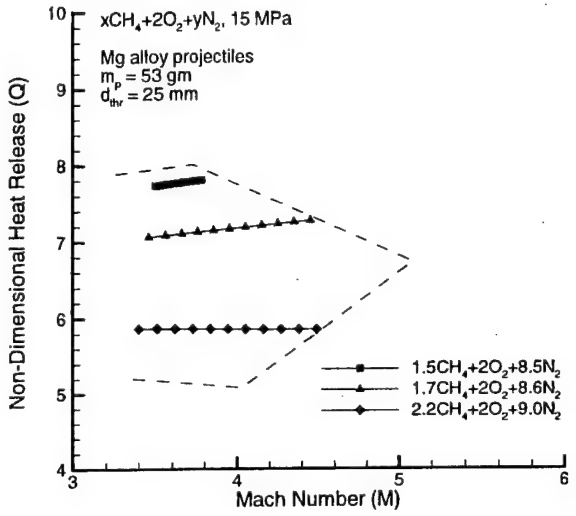

Fig. 12 Q-M data from Mg projectile operation limit experiments.

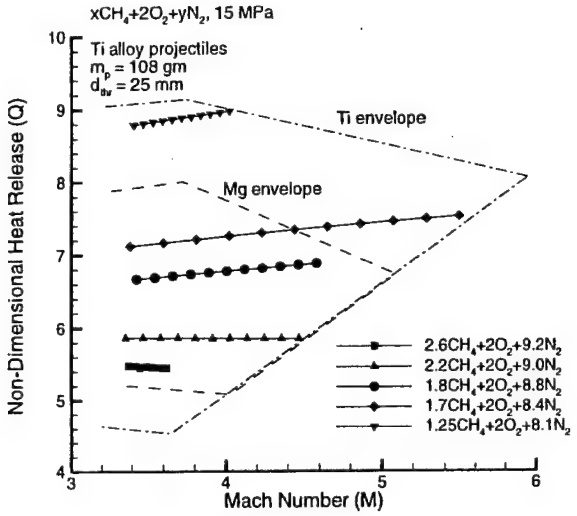

Fig. 13 Q-M data from Ti projectile operation limit experiments.

section at a velocity of 1200 - 1210 m/s. The velocity-distance data for this series is shown in Fig. 11. The initial experiment, not shown in Fig. 11, used a 15 mm-thick 23% open obturator (Fig. 5a) but resulted in an immediate unstart; fragments collected from the final dump tank indicated that the obturator had failed upon launch initiation. Because of this failure, each of the experiments that followed used the solid obturator shown in Fig. 5b. In all cases the projectiles were gasdynamically started and accelerated for at least 1 m. The velocity the projectiles achieved before unstart increased with increasing values of the propellant Q_{CJ}, with the exception of the $1.25CH_4+2O_2+8.1N_2$ propellant.

Previous investigations have shown that the operational envelope for a set of experimental conditions can be mapped in the heat release - Mach number (Q-M) plane as shown in Figs. 12 and 13.[24] Each of the boundaries represents a different condition which causes ram acceleration to cease: the uppermost boundary of each envelope is the upper limit of heat release, above which a wave unstart will occur immediately; the bottom-most boundary is the lower limit of heat release, below which a wave fall-off will always occur; the upper right limit indicates failures due to gas dynamic mechanisms; the lower right limit indicates failures likely due to structural or material failure.[25] While more experiments are necessary to map the boundaries accurately, the data obtained from these investigations suggest the approximate boundaries shown. The upper heat release limit for both envelopes was not reached in these experiments, but the data obtained indicate the limit is being approached as the propellant is made more energetic; the lower limit was not reached in this particular series, but the limit is indicated by wave fall-off results from earlier experiments.

None of the Mg projectiles remained started after 2 m, or attained a Mach number as large as that attained with Ti projectiles in the same propellant. Wall pressure data from the Mg experiments indicate serious projectile canting near the location of the wave unstarts; it is believed that fin erosion and body ablation are contributing factors to the severe canting and resulting unstarts. The Ti alloy, which is a more refractory material, does not exhibit signs of canting until considerably later than the Mg alloy under the same experimental conditions.

Stability Enhancements

A series of experiments was conducted with Mg and Ti projectiles modified to increase fin length and to place the center of gravity closer to the projectile base. These modifications were made to increase the acceleration distance and Mach number limit (expanding the Q-M envelope) the projectiles could achieve in 15 MPa propellants.

The first part of the series used 5-finned Mg alloy projectiles (Fig. 4c), with the following parameters: 12.5° nose cone, 25 mm throat diameter, 76 mm aft

body, 18 mm base diameter. The fins were knife-edged, with the rake angle varied between experiments. These projectiles had masses of 73 - 78 gm. The test section in each case consisted of a 3-m-long stage of $2.0CH_4+2O_2+8.8N_2$ at a fill pressure of 15 MPa, and the projectiles entered the stage at a velocity of 1200 - 1250 m/s. In the experiment in which the fin rake angle was 45°, the projectile unstarted immediately; in the 30° fin rake angle experiment, the ram accelerator started but a wave unstart occurred within the first meter of the test section. The pressure transducer data from these experiments suggested that the shock wave activity in the throat induced by the fins caused the projectiles to unstart earlier than the *Q-M* envelope (Fig. 12) would predict. Another experiment conducted with a rake angle of 20° resulted in a successful start with the projectile accelerating over 1 m before undergoing a wave unstart. In this case, the projectile traveled farther and reached a higher Mach number (4.34) than one of similar design with a 51 mm aft body (3.83) in the same propellant, demonstrating that the extension of fin length by extending the aft body, rather than increasing the fin rake angle, does improve the Mach number limit of the Mg projectile design, effectively expanding the boundaries of the *Q-M* envelope of Fig. 12.

Another means of improving the stability of the projectile is to move the center of gravity back from inside the nose toward the projectile base. The second part of the series moved the center of gravity (and altered the diffuser efficiency) by using 15° rather than 12.5° nose cone angles. The first experiment used the 5-fin Mg projectile (Fig. 4c) with a 15° nose cone, 25 mm throat diameter, 76 mm aft body, 18 mm base diameter, and knife-edged fins with a 20° rake angle. This projectile successfully accelerated through a 1-m-long stage of $2.0CH_4+2O_2+8.8N_2$ at 15 MPa. This experiment did not provide information about a *Q-M* limit, but by accelerating to the same Mach number (M~4.40) that was achieved with a projectile of similar design with a 12.5° nose cone, it did show that the steeper nose cone does not adversely affect the operating limits.

Two additional experiments were conducted with Ti alloy projectiles (Fig. 4b) with the following design parameters: 15° nose cone, 25 mm throat diameter, 51 mm aft body, 18 mm base diameter, knife-edged 20°-rake-angle fins, masses of ~110 gm. These projectiles were launched into 3-m-long stages of $2.2CH_4+2O_2+9.0N_2$ and $2.6CH_4+2O_2+9.2N_2$, each at a fill pressure of 15 MPa, at velocities of 1210 m/s and 1230 m/s, respectively. In each case the ram accelerator was gasdynamically started and the projectile accelerated for a distance of 1.5 - 2.5 m before undergoing a wave unstart. In both cases, the final Mach number slightly exceeded that reached by similar projectiles with 12.5° nose cones in the same propellants. These experiments demonstrated that a 15° nose cone did not reduce the Mach number limits of the Mg and Ti projectile designs.

Extended 15 MPa Experiment

Using the data collected from the previous 15 MPa experiments and the design improvements suggested by them, an attempt was made to design a projectile which would successfully start at 15 MPa and accelerate continuously throughout the entire available length of high pressure test section. The projectile was manufactured from Ti alloy as shown in Fig. 4b, with the following design parameters: 12.5° nose cone, 23 mm throat diameter, 76 mm aft body, 18 mm base diameter, knife-edged 20°-rake-angle fins, mass of 118 gm. The solid obturator (Fig. 5b) was used for the launch. The test section consisted of the entire 4 m length of high pressure ram accelerator tube, with $2.6CH_4+2O_2+9.2N_2$ as the propellant. The velocity-distance data from this experiment, along with the theoretical data calculated by the one-dimensional control volume method with the Boltzmann equation of state, are shown in Fig. 14. The projectile entered the test section at 1190 m/s; the ram accelerator was successfully started and the projectile accelerated continuously throughout the stage.

The experimental data show the projectile experienced very weak acceleration over the first meter of the stage. If the theoretical data are considered starting from the beginning of the second meter of the stage (translated to the right as shown in Fig. 14), the velocity-distance profiles of the theoretical and experimental data are in better agreement. While the velocity-distance data do not match the theory as well as the lower pressure experiments, the one-dimensional theory does not take into account the effects of unsteady flow. The velocity-distance and wall pressure data from the experiment, as in the earliest 15 MPa experiments (Fig. 7), suggest that the ram accelerator is not thermally choked over the first meter; however, the velocity-distance data do indicate that full thermal choking, along with the performance expected, begins farther down the tube.

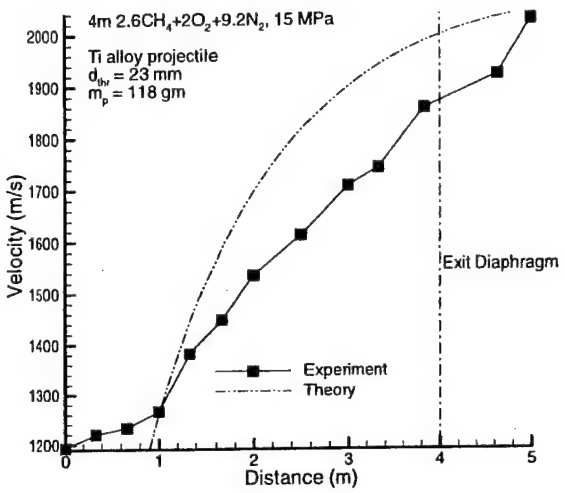

Fig. 14 Results from 15 MPa experiment with 4-m stage.

Just as a fluid flow entering a pipe from a stagnant condition requires a characteristic "entry length" before it attains the fully developed velocity profile, the ram accelerator appears to require a particular length during a delayed start before thermally choked performance is fully realized. This effect has been observed at other ram accelerator facilities at fill pressures of 3 - 4.5 MPa.[26,27] This effect appears to be magnified by propellant fill pressure. The delayed start hypothesis suggests an answer for the apparently poor performance of the ram accelerator during 1-m stage starting experiments at high pressure; the projectiles exited the test section before the thermal choking had been established. At present, it is not known whether the weak acceleration during a delayed start is due to the effects of the unsteady flow field, rapid deceleration of the obturator, the rate of mixing of unburned propellant with hot expended propellant, the induction time of the propellant at high pressure, or a combination of these and other causes. This subject is still under investigation.

Experiments at 20 MPa

A series of experiments at 20 MPa was conducted to explore the combinations of projectile design and propellant composition that would enable successful ram accelerator operation at that pressure. Two experiments used Ti alloy projectiles (Fig. 4b) with the following design parameters: 12.5° nose cone, 23 mm throat diameter, 34 mm aft body, 18 mm base diameter, knife-edged 20°-rake-angle fins, mass of ~86 gm. A reduction in throat diameter from 29 to 25 mm had proved necessary to enable starting at 12.5 - 15 MPa; however, a preliminary experiment using a 25 mm throat projectile had failed to start at 20 MPa, suggesting that further throat reduction was necessary to enable starting. Thus a constant area throat section 17 mm in length and 23 mm in diameter extending from the base of the nose cone to the leading edge of the fins was added. The constant area section was introduced to maintain minimum nose cone wall thickness at the magnet cavity after modification of the pre-fabricated projectiles to the required specifications.

These Ti projectile experiments used of a 1-m-long stage of propellant at 20 MPa and a solid obturator (Fig. 5b) for the launch process. The velocity-distance data from these experiments at the entrance and exit are shown in Table 1. With no data to suggest what entrance speed might be necessary to effect a successful start, the first projectile was injected into the test section containing $2.6CH_4+2O_2+9.2N_2$ at the maximum velocity the initial launcher could provide (~1300 m/s). The projectile was gasdynamically started and ram accelerated continuously throughout the test section. The second experiment used $2.2CH_4+2O_2+9.0N_2$ as the propellant, and the projectile was launched into the stage at the lower velocity of 1220 m/s. This projectile also gasdynamically started and accelerated continuously throughout the test section. The modest average accelerations in the stage shown in Table 1 are due to the lack of thermal choking within the 1 m stage; i.e., the projectile undergoes a delayed start.

Table 1 20MPa experiment results with Ti projectiles

Experiment	Entrance Velocity (m/s)	Exit Velocity (m/s)	Average Acceleration (g)
$2.6CH_4+2O_2$ $+9.2N_2$	1300	1370	9,400
$2.2CH_4+2O_2$ $+9.0N_2$	1220	1270	7,200

Additional experiments were conducted using Mg alloy projectiles. The first used a 5-finned projectile (Fig. 4c) with the following design parameters: 12.5° nose cone, 23 mm throat diameter, 51 mm aft body, 18 mm base diameter, knife-edged 20°-rake-angle fins, 17 mm long constant area section, mass of ~56 gm. This experiment was intended to determine whether the Mach number limit of Mg projectiles at 20 MPa was sufficiently high to allow for continued ram accelerator

starting tests using Mg projectiles. The second projectile used the same design but without the constant area section; this experiment was meant to determine whether the leading edges of the fins could be brought back to the throat without the shock waves attached to them interfering with the starting process.

These Mg projectile experiments used a test section consisting of a 1-m-long stage of $2.2CH_4+2O_2+9.0N_2$ propellant at 20 MPa, and used a 15 mm-thick 23% open obturator (Fig. 5a) in the launch process. The velocity-distance data for the Mg projectile experiments at 20 MPa at the entrance and exit of the stage are shown in Table 2. In the first experiment, the projectile entered the stage at 1180 m/s; the ram accelerator was gasdynamically started and the projectile accelerated throughout the stage. It was thus confirmed that Mg projectiles could still prove useful for geometry variation and starting studies at this pressure. The second experiment was conducted, with the projectile entering the stage at 1230 m/s; this projectile, too, was gasdynamically started and accelerated through the stage. This experiment demonstrated that the knife-edged 20°-rake-angle fins could remain at the throat without jeopardizing starting of the ram accelerator at 20 MPa.

The average acceleration of the Mg projectile in the second experiment was 56,300 g, while the theory, as calculated using the one-dimensional control volume approach with the Boltzmann virial equation of state, predicts an average acceleration of 201,000 g. The disparity in the two results is due to the lack of thermal choking in the 1 m stage, believed to be due to transient effects in the starting process which are magnified at high pressure, and is still under investigation.

Table 2 20MPa experiment results with Mg projectiles

Experiment	Entrance Velocity (m/s)	Exit Velocity (m/s)	Average Acceleration (g)
w/ constant area section	1180	1570	54,300
w/o constant area section	1230	1620	56,300

VII. Conclusions

High pressure experiments conducted in the 38 mm bore ram accelerator facility have demonstrated that the range of propellant compositions which will enable gasdynamic starting at 15 MPa is considerably wider than earlier experiments had indicated. The shock waves attached to the leading edges of the projectile fins can be prevented from interfering with the ram accelerator starting process by maintaining the fin rake angle at 20° or less. Projectile canting due to fin erosion and projectile instability contribute to limiting the Mach number at which operation is possible. Improvements to projectile stability, effected by lengthening the aft body and shortening the nose cone to move the center of gravity toward the projectile base, increase the operational Mach number limit above that determined for otherwise similar designs in the same propellants. Experiments in extended stages of 15 MPa propellant indicate that the ram accelerator requires a length of 0.5 - 1 m before thermally choked performance can be realized; this effect appears to be increased by higher fill pressure. The average acceleration after thermal choking has been established is 25% less than predicted using a real gas equation of state. Delayed starts of the ram accelerator in 20 MPa propellants have been demonstrated using projectiles with throat diameters reduced to 23 mm from the 25 mm that successfully operates in 15 MPa propellants; the reduction of the throat is necessary in part due to the variation of acoustic speed with stage fill pressure.

Acknowledgments

These experiments were performed under U.S. Army Research Office grant number DAAG55-97-1-0131. The assistance of Dr. Liu Sen and Prof. Yung-Hwan Byun with the experiments is greatly appreciated. Consultations with Prof. Pascal Bauer on acoustic speed calculations were also very helpful.

References

1. Kruczynski, D., Liberatore, F., and Nusca, M., "NAVRAM5 - An Analysis of Ram Acceleration for Specific Naval Applications," ARL-TR-1073, April 1996.

2. Hertzberg, A., Bruckner, A.P., and Bogdanoff, D.W., "Ram Accelerator: A New Chemical Method for Accelerating Projectiles to Ultrahigh Velocities", *AIAA Journal*, Vol. 26, 1988, pp. 195-203.

3. Bruckner, A.P., Knowlen, C., Hertzberg, A., and Bogdanoff, D.W., "Operational Characteristics of the Thermally Choked Ram Accelerator", *AIAA Journal of Propulsion and Power*, Vol. 7, 1991, pp. 828-836.

4. Hertzberg, A., Bruckner, A.P., and Knowlen, C., "Experimental Investigation of Ram Accelerator

Propulsion Modes," *Shock Waves*, Vol. 1, 1991, pp. 17-25.

5. Burnham, E.A., Kull, A.E., Knowlen, C., Bruckner, A.P., and Hertzberg, A., "Operation of Ram Accelerator in Transdetonative Velocity Regime," AIAA Paper 90-1985, July 1990.

6. Knowlen, C., Higgins, A.J., Bruckner, A.P., and Bauer, P., "Ram Accelerator Operation in the Superdetonative Velocity Regime," AIAA Paper 96-0098, July 1996.

7. Bruckner A.P., Burnham E.A., Knowlen C., Hertzberg A., Bogdanoff D.W. (1992) "Initiation of Combustion in the Thermally Choked Ram Accelerator." *Shock Waves*, Takayama, K. (ed), Springer-Verlag, Berlin, 1992, pp. 623-630.

8. Schultz, E., Knowlen, C., and Bruckner, A.P., "Obturator and Detonation Experiments in the Subdetonative Ram Accelerator," *Shock Waves*, in press.

9. Stewart, J.F., Knowlen, C., and Bruckner, A.P., "Effects of Launch Tube Gases on Starting of the Ram Accelerator", AIAA Paper 97-3175, July 1997.

10. Schultz, E., Knowlen, C., and Bruckner, A.P., "Overview of the Subdetonative Ram Accelerator Starting Process", *Ram Accelerators*, Takayama K., Sasoh A. (eds), Springer-Verlag, Heidelberg, 1998, pp. 189-203.

11. Knowlen, C., and Sasoh, A., "Ram Accelerator Performance Modeling", *Ram Accelerators*, Takayama K., Sasoh A. (eds), Springer-Verlag, Heidelberg, 1998, pp. 25-37.

12. Knowlen, C. and Bruckner, A.P., "A Hugoniot Analysis of the Ram Accelerator," *Shock Waves*, Takayama, K. (ed), Springer-Verlag, Berlin, 1992, pp. 617-622.

13. Bauer, P. Legendre, J.F., Henner, M., and Giraud, M., "Real Gas Effects in Ram Accelerator Propellant Mixtures: Theoretical Concepts and Applied Thermochemical codes," *Ram Accelerators*, Takayama K., Sasoh A. (eds), Springer-Verlag, Heidelberg, 1998, pp. 39-52.

14. Bauer, P., Knowlen, C., and Bruckner, A.P., "Real Gas Effects on the Prediction of Ram Accelerator Performance," *Shock Waves*, Vol. 8, 1998, pp. 113-118.

15. Buckwalter, D.L., Knowlen, C., and Bruckner, A.P., "Ram Accelerator Performance Analysis Code Incorporating Real Gas Effects", AIAA Paper 96-2945, July 1996.

16. Buckwalter, D.L., Knowlen, C., and Bruckner, A.P., "Real Gas Effects on Ram Accelerator Analysis," AIAA Paper 97-2894, July 1997.

17. Buckwalter D.L., Knowlen C., and Bruckner A.P. (1998), "Real Gas Effects on Thermally Choked Ram Accelerator Performance." *Ram Accelerators*, Takayama K, Sasoh A (eds), Springer-Verlag, Heidelberg, pp. 125-134.

18. Bundy, C., Knowlen, C., and Bruckner, A.P., "Ram Accelerator Operating Characteristics at Fill Pressures Greater Than 10 MPa", AIAA Paper 99-2261, June 1999.

19. Moran, M.J., and Shapiro, H.N., *Fundamentals of Engineering Thermodynamics*, John Wiley and Sons, New York, 1988, pp. 482-538.

20. Knowlen, C., Li, J.G., Hinkey, J., and Dunmire, B., "University of Washington Ram Accelerator Facility", 42nd Meeting of the Aeroballistic Range Association, Adelaide, Australia, October 22-25, 1991.

21. Stewart J.F., Bruckner A.P., Knowlen C. (1998), "Effects of Launch Tube Shock Dynamics on Initiation of Ram Accelerator Operation," *Ram Accelerators*, Takayama K, Sasoh A (eds), Springer-Verlag, Heidelberg, pp. 181-189.

22. Hinkey, J.B., Burnham, E.A., and Bruckner, A.P., "Investigation of Ram Accelerator Flow Fields Induced by Canted Projectiles", AIAA Paper 93-2186, June 1993.

23. Bundy, C., Knowlen, C., and Bruckner, A.P., "Experiments in a 38-mm Bore Ram Accelerator at Pressures up to 12.5 MPa", 49th Meeting of the Aeroballistic Range Association, Scheveningen, Netherlands, October 5-9, 1998.

24. Higgins, A.J., Knowlen, C., and Bruckner, A.P., "Ram Accelerator Operating Limits, Part 1: Identification of Limits", *AIAA Journal of Propulsion and Power*, Vol. 14, 1998, pp. 951-958.

25. Higgins, A.J., Knowlen, C., and Bruckner, A.P., "Ram Accelerator Operating Limits, Part 2: Nature of Observed Limits", *AIAA Journal of Propulsion and Power*, Vol. 14, 1998, pp. 959-966.

26. Giraud, M., Legendre, J.F., and Henner, M., "RAMAC in Subdetonative Propulsion Mode: State of the ISL Studies" *Ram Accelerators*, Takayama K., Sasoh A. (eds), Springer-Verlag, Heidelberg, 1998, pp. 65-78.

27. Sasoh, A., Hamate, Y., and Takayama, K., "Significance of Unsteadiness in Operation of the Small Bore Ram Accelerator", AIAA Paper 98-3446, July 1998.

Appendix D

Summary of Experimental Results at 200 atm Fill Pressure

Submitted to 18th ICDERS, July 29 - August 3, 2000, Seattle, WA, USA

Ram Accelerator Operation at 15 to 20 MPa Fill Pressure

C. Bundy, C. Knowlen, and A.P. Bruckner
Aerospace and Energetics Research Program
University of Washington
Seattle, WA 98125

Abstract

An investigation of the experimental conditions which permit ram accelerator operation at fill pressures up to 20 MPa is reported. Titanium alloy projectiles at entrance velocities as low as 1200 m/s were successfully started in propellants at fill pressures of 15 MPa, and continuous acceleration was achieved in one- and two-stage experiments at fill pressures up to 20 MPa, the highest operating pressure achieved to date in any ram accelerator. Due to real gas effects on the acoustic speed of the propellant, the throat-to-bore diameter ratio of the projectiles needed to be reduced from the nominal value of 0.760 to 0.600 in order to enable operation at pressures greater than 15 MPa. The average acceleration achieved in these experiments was lower than that predicted by the real-gas calculations of the one-dimensional quasi-steady control volume model. The data analyzed indicate several factors that may account for the discrepancies between theory and experiment.

Introduction

The ram accelerator is a hypervelocity launcher that uses a ramjet-like propulsive cycle to generate thrust for projectiles. The thrust is proportional to the fill pressure and increases with increasing heat release from propellant combustion.[1] The highest possible performance for a given projectile mass will thus be obtained by using the maximum fill pressure the facility can accommodate, and with the most energetic propellant that will sustain ram acceleration. The primary focus of the high pressure ram accelerator research is to address the logistical challenges presented by the extreme aerothermal environment to which the projectiles are subjected under conditions of high pressure operation.

The thermally choked ram accelerator propulsive mode[2] is initiated by launching a subcaliber projectile into a tube containing a premixed gaseous propellant and establishing the self-sustaining combusting flow field, as shown in Fig. 1. This propulsive mode is characterized by subsonic combustion and a projectile velocity less than the Chapman-Jouguet detonation speed of the propellant. During the starting process, the occlusion provided by a full-bore obturator drives a normal shock wave onto the rear body of the projectile. Propellant ignition occurs as a result of the complex interactions of shock waves in the residual air in the launch tube (resulting from imperfect evacuation) with the projectile, obturator, and diaphragm at the entrance to the test section.[3] The ram accelerator is successfully started once supersonic flow is established behind the projectile throat (the cross-section of minimum flow area) and the normal shock wave produced by the obturator is stabilized on the rear body of the projectile by thermal choking of the reacting flow behind the projectile.

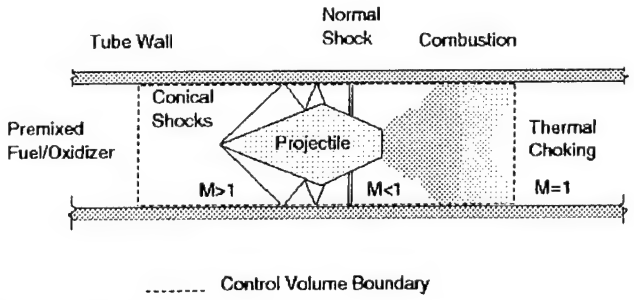

Fig. 1. Thermally choked ram accelerator propulsive mode.

If supersonic flow is not established behind the throat due to factors such as insufficient entrance velocity, nose cone damage, or substantial heat release ahead of the throat, the flow chokes at the throat and the normal shock wave is driven ahead of the projectile. This result is referred to as a "sonic diffuser unstart" (SDU). If the normal shock wave overtakes the throat at some time after supersonic flow is established behind the throat, the resulting failure is referred to as a "wave unstart". A wave unstart can be caused by excessive heat release from the propellant, excessive obturator mass, or other factors. In either case, thrust ceases and the projectile decelerates.

Experimental Facility

The 38 mm facility at the University of Washington enables ram accelerator experimentation at propellant fill pressures of up to 20 MPa. The first 4 m of the ram accelerator test section, shown in Fig. 2, consists of two 1-m-long and one 2-m-long high pressure tubes, with a bore diameter of 38 mm and an outer diameter of 152 mm.[4] The high pressure tubes are manufactured from AISI 4340 steel and are designed for a maximum static load of 1000 MPa. The remaining 12 m of the test section is comprised of six low pressure tubes manufactured from AISI 4140 steel, each 2 m in length, with outer diameters of 102 mm, and are designed to withstand a static load of up to 550 MPa.[5]

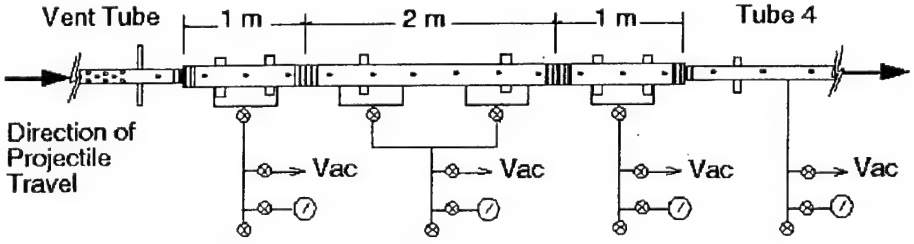

Fig. 2. High pressure test section schematic.

Each 1-m-long tube (Fig. 2) has three instrument stations with diametrically opposed ports; the 2-m-long tube has six pairs of ports. These stations are spaced along the tubes at 333 mm intervals. The first instrument station in the high pressure section is 167 mm from the entrance diaphragm. The last station in the high pressure tubes is spaced 167 mm from the exit and 396 mm from the first instrument port in the low pressure part of the test section. The instrument ports can accommodate electromagnetic (EM) probes and PCB model A119A11 or

A119A12 piezoelectric pressure transducers (550 or 800 MPa maximum pressure range, respectively).[5]

All of the tubes in the high pressure test section have two fill ports isolated from the fill lines by air-actuated Snotrik valves (300 MPa rated), which separate the gas handling system from the extreme pressure pulses generated in the experiments. The low pressure part of the test section has a fill port in each 2 m tube section. Mylar diaphragms can be inserted between any pair of adjacent tubes, enabling multiple stages of different propellants, and hence acoustic speeds, to be used. Any tubes not filled with a propellant are evacuated. Details of the light gas gun pre-launcher, propellant filling system, and other major system components can be found in Refs. 4, 6, and 7.

Several different projectile geometries were used in this investigation. Four-finned one-piece projectiles were manufactured from titanium 6Al-6V-2Sn alloy in a single basic design, with adjustments to the geometry machined post-fabrication, as necessary for individual experiments. The basic design is shown in Fig. 3a, with body length determined as required for each particular experiment. The projectiles feature fin spans of 38 mm, throat diameters of 23 mm, nose cone angles of 12.5°, and fin rake angles of 20°. The interior of the projectile body is hollow to minimize the projectile's overall mass. A neodymium magnet is inserted and held at the projectile throat by a threaded magnesium plug. The fin leading edges are knife-edged at 15° in order to reduce the strength of the attached shock waves near the projectile throat. The total masses of the projectiles ranged from 106 to 135 gm, depending on their characteristic design parameters.

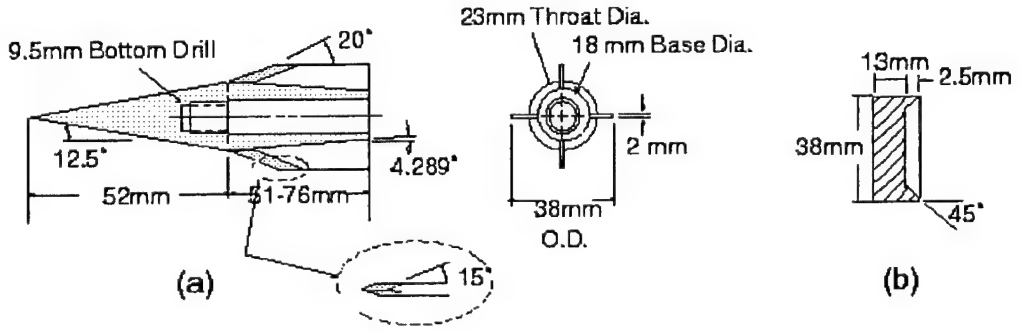

Fig. 3. a) Generalized Ti alloy projectile design. b) Obturator design.

The obturator, shown in Fig. 3b, is placed behind the projectile base to prevent gas blow-by from the light gas gun pre-launcher and to drive a normal shock onto the projectile rear body upon entrance to the test section, as required by the starting process.[8] The obturator is manufactured from polycarbonate and has a mass of approximately 18 gm. It is glued to the projectile with cyanoacrylate adhesive for the process of loading the two into the light gas gun.

Results and Discussion

The dimension of the projectile throat is a critical parameter in high pressure ram accelerator experiments. In order to effect a successful start, supersonic flow must be achieved

behind the projectile throat. The minimum Mach number required to fulfill this condition is that which causes the supersonic flow to become choked at the projectile throat (SDU). While a steady ideal gas flow model has been useful in determining the minimum required SDU velocity when the fill pressure is 5 MPa or less, experiments conducted at 7.5 MPa indicated that the minimum |SDU velocity is greater than the model predicts.[6,9]

At fill pressures greater than 5 MPa, it becomes necessary to use a real gas equation of state to accurately model ram accelerator performance.[5,6,9,10] When real gas effects are accounted for by a non-ideal equation of state, the acoustic speed of the propellant varies with fill pressure, and thus affects the minimum Mach number required for starting the ram accelerator. The variation of acoustic speed with fill pressure for a typical propellant modeled with the Redlich-Kwong equation of state is shown in Fig. 4.[5] The ideal gas acoustic speed is shown in the figure for comparison.

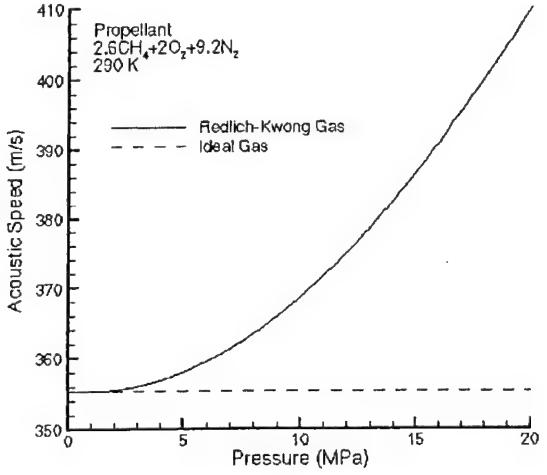

Fig. 4. Variation of $2.6CH_4+2O_2+9.2N_2$ acoustic speed with pressure at 290 K.

The model accounts for both the enthalpy deviation from non-ideal gas behavior and the variation of the specific heat capacity with pressure and temperature.[11] Since the acoustic speed of the quiescent propellant increases with fill pressure, the projectile is required to have a higher entrance velocity to avoid flow choking at the projectile throat and thus a start failure. To reduce the entrance velocity requirement, the projectile throat diameter must be reduced, thus decreasing the Mach number necessary for successful starting. Previous experiments at high pressure have demonstrated that reducing the throat-to-bore diameter ratio from 0.760 to 0.667 was necessary to enable starting at fill pressures greater than 11 MPa with entrance velocities of ~1200 m/s, while at fill pressures greater than 15 MPa, a further reduction to 0.600 was needed.[5,6]

Data collected from earlier experiments[5] using only the first 1-m tube suggested a projectile design that would successfully start at 15 MPa. The projectile geometry used in the experiment described here is as shown in Fig. 3a, with a 76 mm aft body, 18 mm base diameter, and a mass of 118 gm. The test section for the experiment was a 4-m stage of $2.6CH_4+2O_2+9.2N_2$ propellant at 15 MPa. The velocity-distance data from this experiment are shown in Fig. 5, along with the theoretical performance predicted for these conditions by the

one-dimensional control volume method[12] using the Boltzmann equation of state. The use of a real gas equation of state helps to account for the pressure-dependent variation of the heat release derived from combustion of the propellant and the acoustic speed of the gas at the thermally choked state,[6] which affect the expected thrust performance.

The experimental data indicate the projectile experienced very weak thrust over the first meter of the stage. If the theoretical data are considered starting from the beginning of the second meter (translated to the right as shown in Fig. 5), the velocity-distance profiles are in better agreement. This weak acceleration during the starting process has been observed in other ram accelerator facilities at pressures as low as 3 to 4.5 MPa.[13] The late development of the thermally choked velocity profile may be caused by highly unsteady flow effects, rapid deceleration of the obturator, the induction time of the propellant at high pressure, or a combination of these and other causes; the subject is under investigation. The average acceleration over the final 3m was 31,400 g.

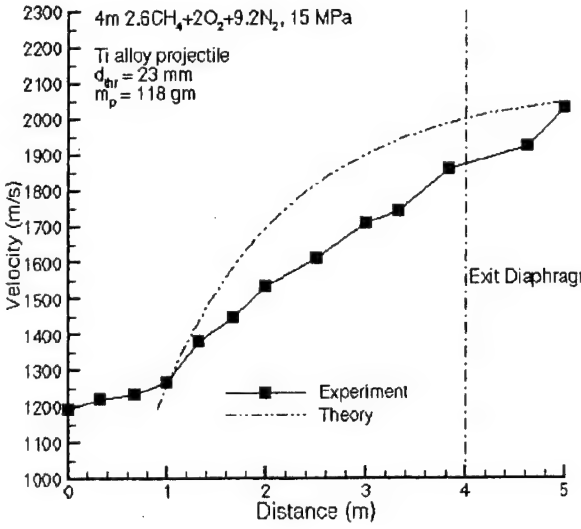

Fig. 5. Results from 4-m 15 MPa experiment.

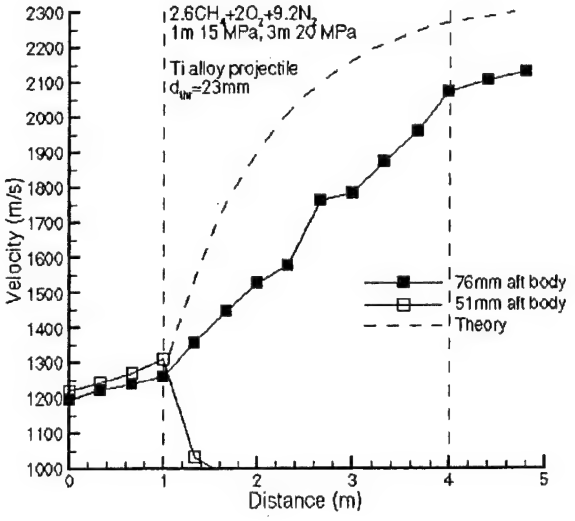

Fig. 6. Results from two-stage 15/20 MPa experiments.

Additional experiments were conducted using Ti projectiles in test sections consisting of a 1-m stage at 15 MPa followed by a 3-m stage at 20 MPa. Both stages used $2.6CH_4+2O_2+9.2N_2$ as the propellant. The projectile aft body ranged in length from 51 to 76 mm; the projectile masses varied from 105 to 118 gm. The velocity-distance data from these experiments are shown in Fig. 6, along with theoretical data for the conditions of the 76 mm body experiment in the 20 MPa stage. The 76 mm aft body projectile starts and continuously accelerates throughout the test section, for an average 46,000 g acceleration in the 20 MPa stage, while the 51mm aft body unstarts early in the second stage. Wall pressure data from these experiments indicate that in the case of the 51 mm aft body, the projectile was severely canted just before the wave unstart occurred. The severe aerothermal environment produced by the thermally choked ram accelerator flow field at these fill pressures may be such that the projectile fins are degraded to a degree that makes the projectile unstable; ground-down fins on projectiles recovered after these experiments corroborate this hypothesis.

An additional experiment was conducted using a Ti projectile in a 4-m test section, with $2.6CH_4+2O_2+9.2N_2$ at 20 MPa as the propellant. The projectile aft body was 64 mm in length; the overall mass of the projectile was 106 gm. The projectile was launched ino the test section at 1250 m/s and successfully started and continuously accelerated throughout the length of the test section. The velocity-distance data and the corresponding theory, translated to the right to discount the region of weak thrust which occurs in the first meter of the test section, are shown in Fig. 7. The agreement between the theoretical and experimental results is similar to that achieved in the 4-m 15 MPa experiment (see Fig. 5), though the discrepancy between the two is slightly greater in the 20 MPa case; the average acceleration over the last 3 m was 38,600 g. This may be partially attributed to unsteady flow effects unaccounted for by the theoretical model, which become greater in magnitude as the fill pressure of the stage increases.

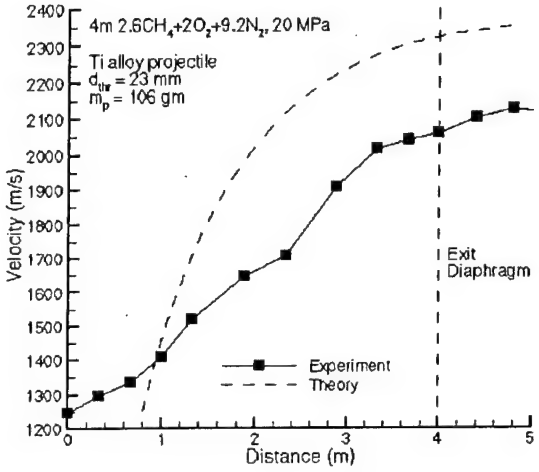

Fig. 7. Results from 4-m 20 MPa experiment.

Summary

Experiments in the 38-mm-bore ram accelerator have demonstrated starting of Ti alloy projectiles with throat-to-bore diameter ratios of 0.600 and continuous acceleration in 15 and 20 MPa propellants. The decrease in throat diameter from previous projectile designs is necessary in part due to the increased acoustic speed of the propellant at high fill pressures. The projectiles experience a period of relatively weak acceleration over the first meter of test section before nominal ram accelerator operation is achieved. The average accelerations over the last 3 m of the test sections were 31,400 g for a 118 gm projectile in 15 MPa propellant, 46,000 g for 118 gm in 20 MPa, and 38,600 g for 106 gm in 20 MPa. The peak velocities were 1860, 2070, and 2060 m/s which correspond to velocity increases over the final 3m of 590, 810, and 660 m/s, respectively. The acceleration for identical projectiles did increase about as expected with increasing fill pressure, however, the projectile with a shorter afterbody length did not accelerate as hard as a more massive, longer-bodied projectile. These experimental results are some of the first demonstrations that 4 m of ram accelerator operation can be realized at 20 MPa fill pressure and many aspects of the operating characteristics are still under investigation.

References

1. Hertzberg, A., Bruckner, A.P., and Bogdanoff, D.W., "Ram Accelerator: A New Chemical Method for Accelerating Projectiles to Ultrahigh Velocities," *AIAA J.*, Vol. 26, 1988, pp. 195-203.

2. Hertzberg, A., Bruckner, A.P., and Knowlen, C., "Experimental Investigation of Ram Accelerator Propulsion Modes," *Shock Waves*, Vol. 1, 1991, pp. 17-25.

3. Stewart, J.F., Knowlen, C., and Bruckner, A.P., "Effects of Launch Tube Gases on Starting of the Ram Accelerator," AIAA Paper 97-3175, July 1997.

4. Knowlen, C., Bundy, C., Schwab, R, and Bruckner, A.P., "University of Washington Ram Accelerator Facility," 50th Meeting of the Aeroballistic Range Association, Pleasanton, CA, October 1999.

5. Bundy, C., Knowlen, C., and Bruckner, A.P., "Investigation of Ram Accelerator Operation at Fill Pressures up to 20 MPa," AIAA Paper 2000-3231, July 2000.

6. Bundy, C., Knowlen, C., and Bruckner, A.P., "Ram Accelerator Operating Characteristics at Fill Pressures Greater than 10 MPa," AIAA Paper 99-2261, June 1999.

7. Stewart, J.F., Bruckner, A.P., and Knowlen, C., "Effects of Launch Tube Shock Dynamics on Initiation of Ram Accelerator Operation," in *Ram Accelerators*, Takayama K., and Sasoh, A. (eds), Springer-Verlag, Heidelberg, 1998, pp.181-189.

8. Schultz, E., Knowlen, C., and Bruckner, A.P., "Starting Envelope of the Ram Accelerator," *J. Propulsion and Power*, Vol. 16, No. 6, 2000, pp. 1040-1052.

9. Bundy, C., Knowlen, C., and Bruckner, A.P., "Ram Accelerator Operating Characteristics at Elevated Fill Pressures," *J. Physique IV*, Vol. 10, 2000, pp. Pr11-11 to Pr11-21.

10. Bundy, C., Knowlen, C., and Bruckner, A.P., "Elevated Pressure Experiments in a 38mm Bore Ram Accelerator," AIAA Paper 98-3144, July 1998.

11. Cengel, Y., and Boles, M., *Thermodynamics: An Engineering Approach, 2nd Edition,* McGraw-Hill, New York, 1994, pp. 629-690.

12. Bruckner, A.P., Knowlen, C., Hertzberg, A., and Bogdanoff, D.W., "Operational Characteristics of the Thermally Choked Ram Accelerator," *J. Propulsion and Power*, Vol. 7, No. 5, 1991, pp. 828-836.

13. Giraud, M., Legendre, J.F., and Henner, M., "RAMAC in Subdetonative Propulsion Mode: State of the ISL Studies," in *Ram Accelerators*, Takayama, K., and Sasoh, A. (eds), Springer-Verlag, Heidelberg, 1998, pp. 65-78.

Appendix E

Drawings of Projectiles Used in High Pressure Research Program

Ram Accelerator
10° Aluminum Nose Cone
11 October 1995

ALL DIMENSIONS IN INCHES
UNLESS OTHERWISE NOTED

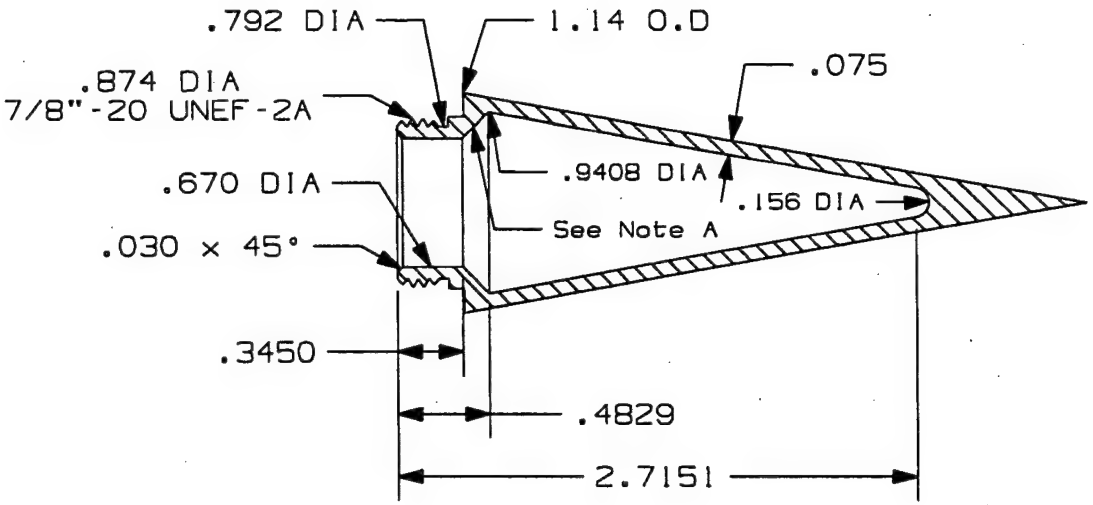

Note A: Make interior angle as steep as possible while maintaining .075 inch minimum wall thickness

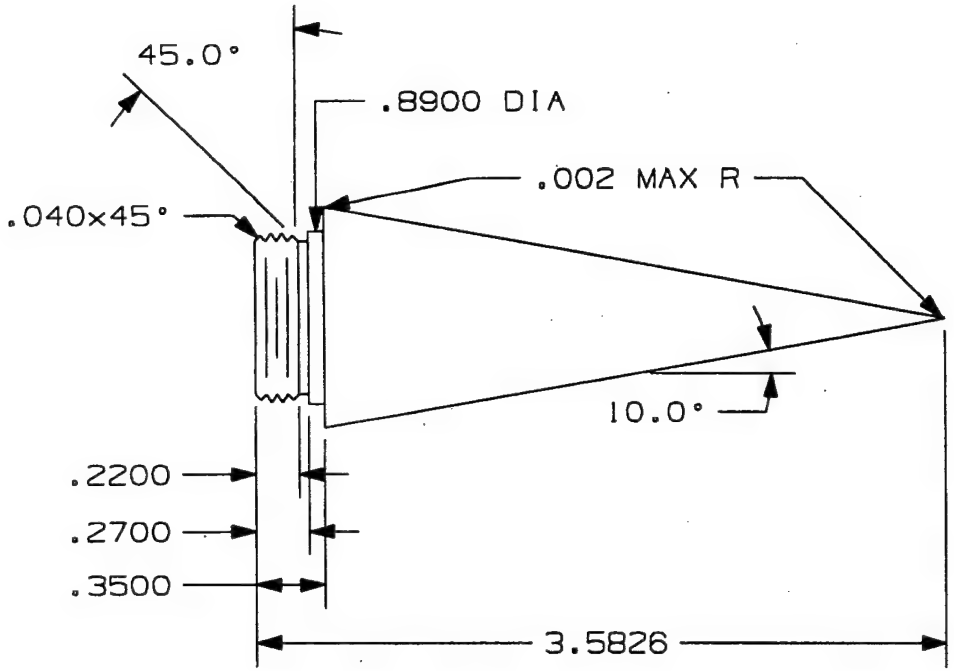

Material; 7075-T651 Aluminum
NOTES; Wall Thickness: .075
Unless otherwise specified;
External Fillets and Edge Breaks .005 max
Internal Fillets and Edge Breaks .010 max
Concentricity is .001 T.I.R. about the .890 Dia.
Tolerance: .XXX±.001
.XXXX±.0005

Ram Accelerator
Five Fin Aluminum Body
18 October 1995

ALL DIMENSIONS IN INCHES
UNLESS OTHERWISE NOTED

Material; 7075-T651 Aluminum
NOTES; Wall Thickness: .075
Unless otherwise specified;
External Fillets and Edge Breaks .005 max
Internal Fillets and Edge Breaks .010 max
Concentricity is .001 T.I.R. about the .890 Dia.
Tolerance: .XXX±.001
.XXXX±.0005

SECTION A-A

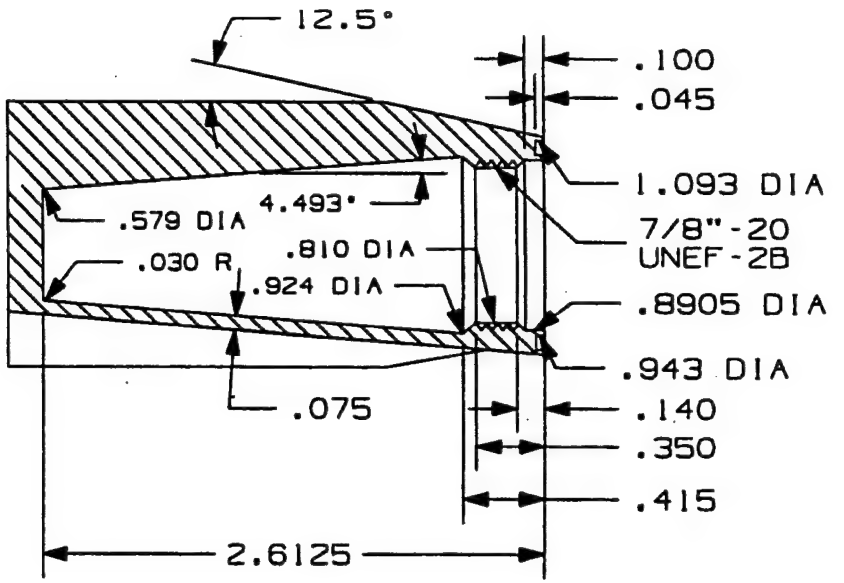

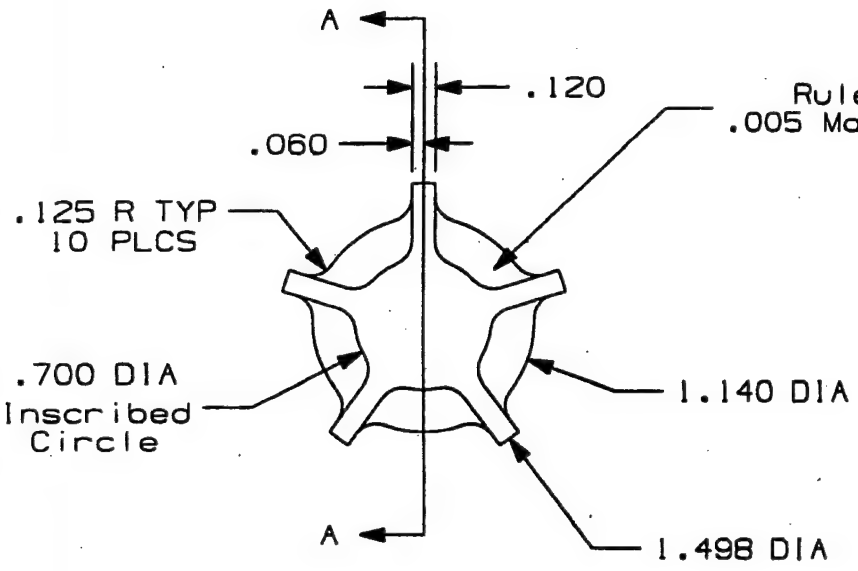

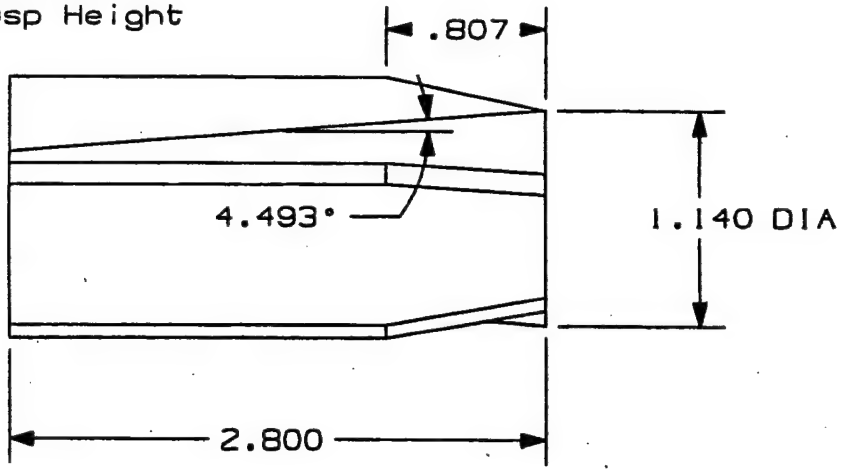

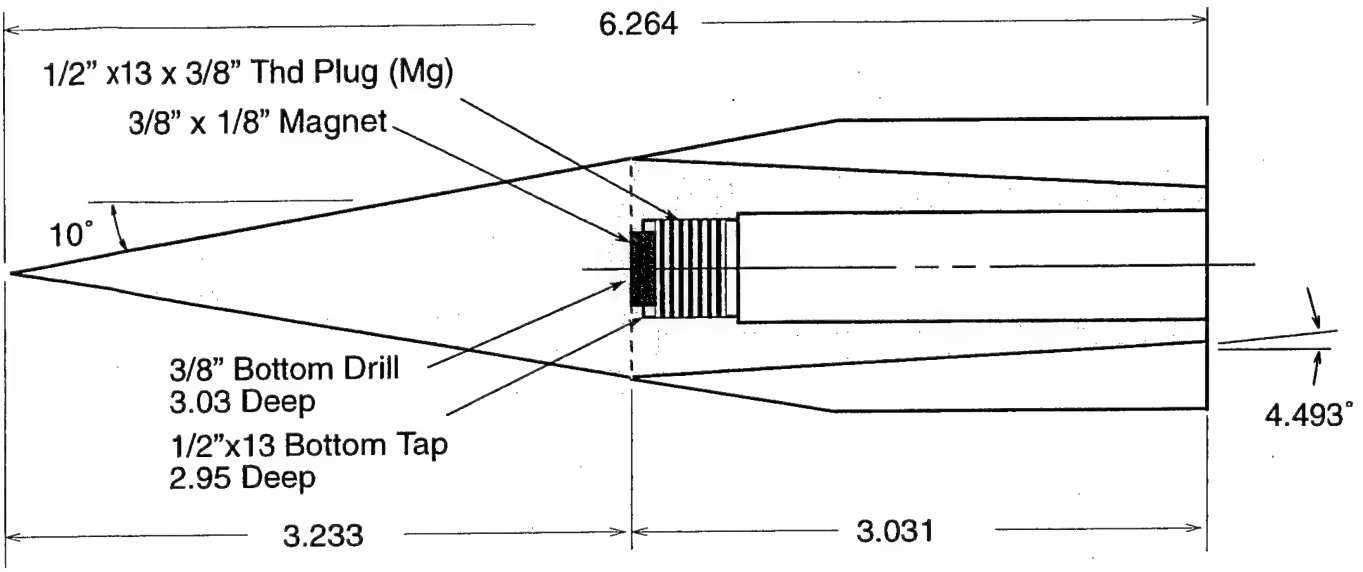

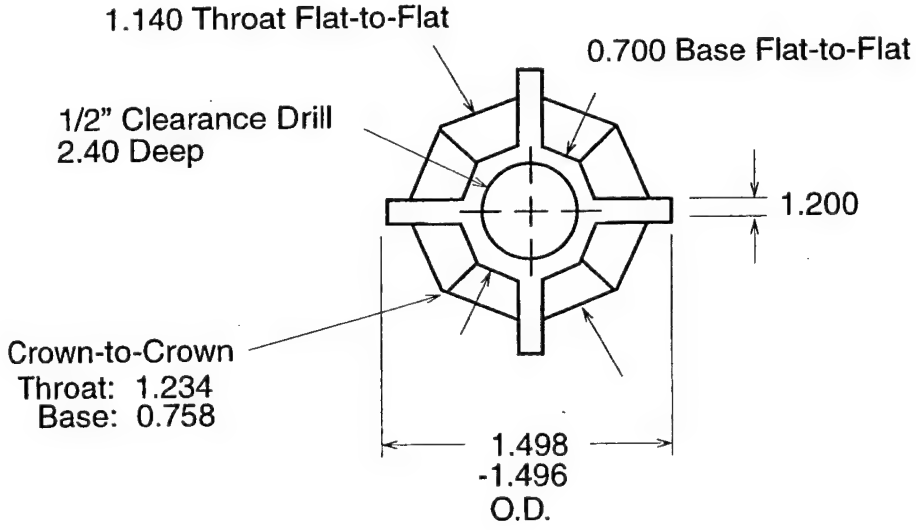

Dimensions: Inches Tolererances: .x = +/- 0.1 .xx = +/- 0.03 .xxx = +/- 0.005 Unless otherwise specified	Ram Accelerator Project Title: Solid Projectile (Standard) Material: Mg ZK60-AT5 Date: 12-24-98 Drawn By: CK Scale: 1" = 1" Drawing No. 1016-1

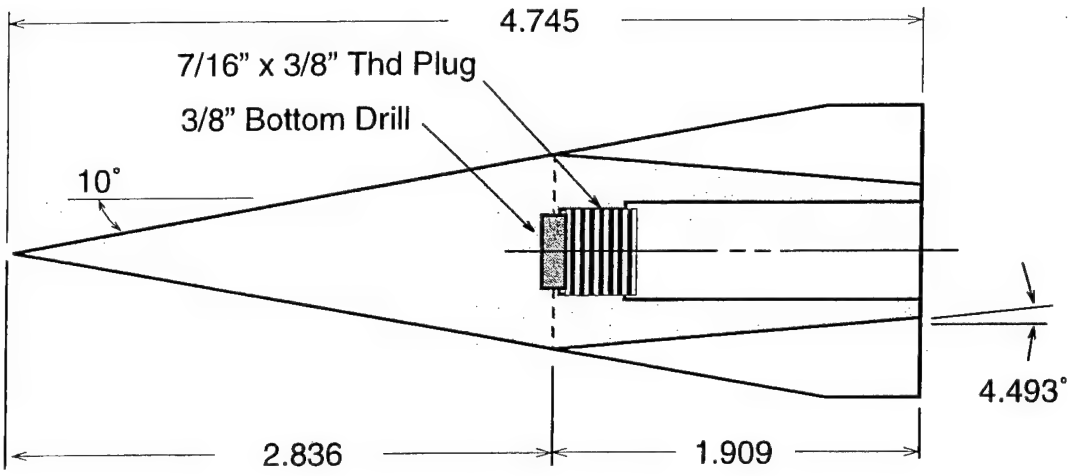

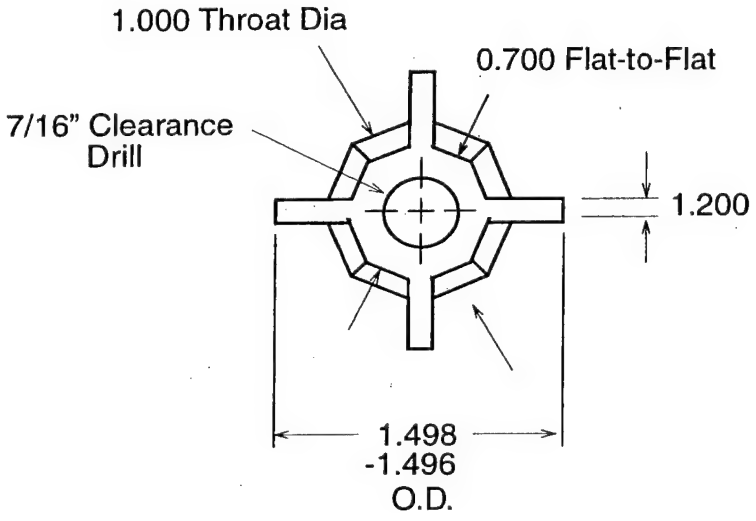

Dimensions: Inches Tolererances: .x = +/- 0.1 .xx = +/- 0.03 .xxx = +/- 0.005 Unless otherwise specified	Ram Accelerator Project Title: Solid Projectile (Reduced Throat) Material: Mg ZK60-AT5 Date: 11-30-98 Drawn By: CK Scale: 1" = 1" Drawing No. 1017

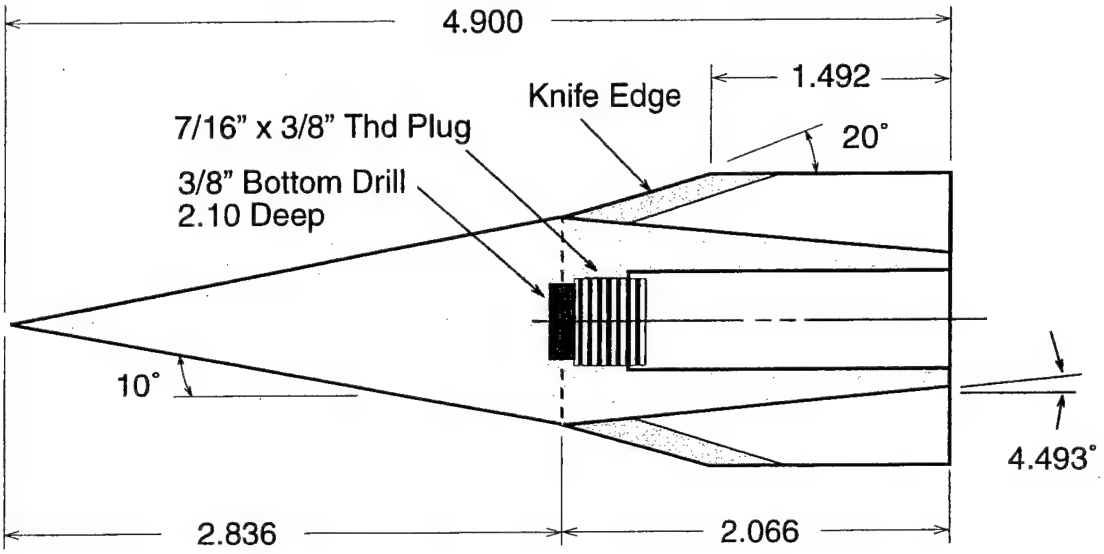

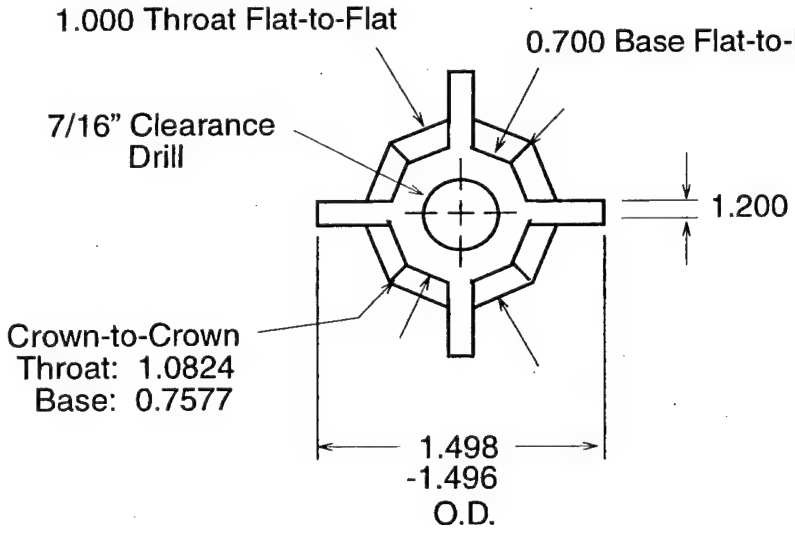

Dimensions: Inches Tolererances: .x = +/- 0.1 .xx = +/- 0.03 .xxx = +/- 0.005 Unless otherwise specified	Ram Accelerator Project	
	Title: Solid Projectile w/ 20° Fin Rake Material: Mg ZK60-AT5 Date: 12-11-98 Drawn By: CK Scale: 1" = 1"	Drawing No. 1020

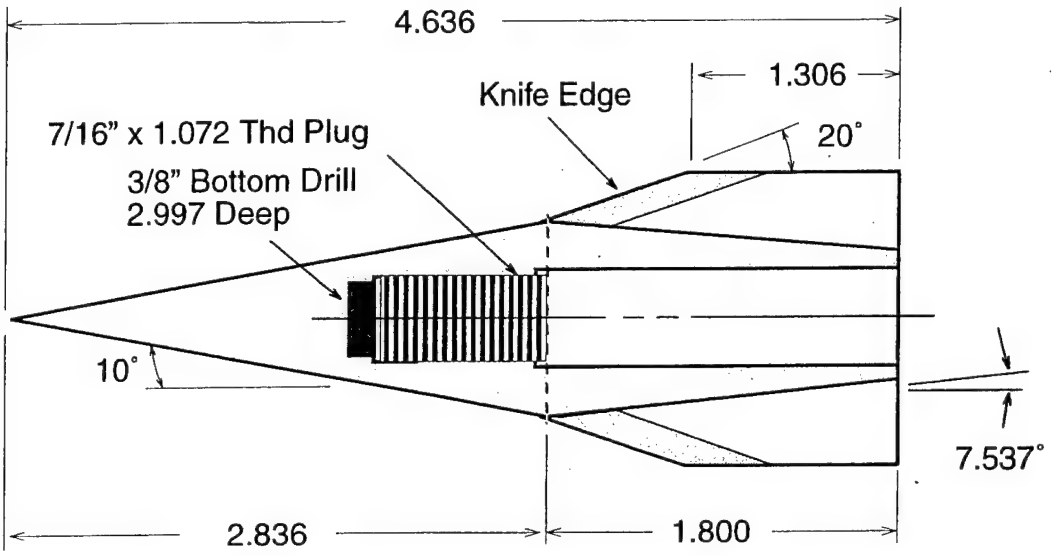

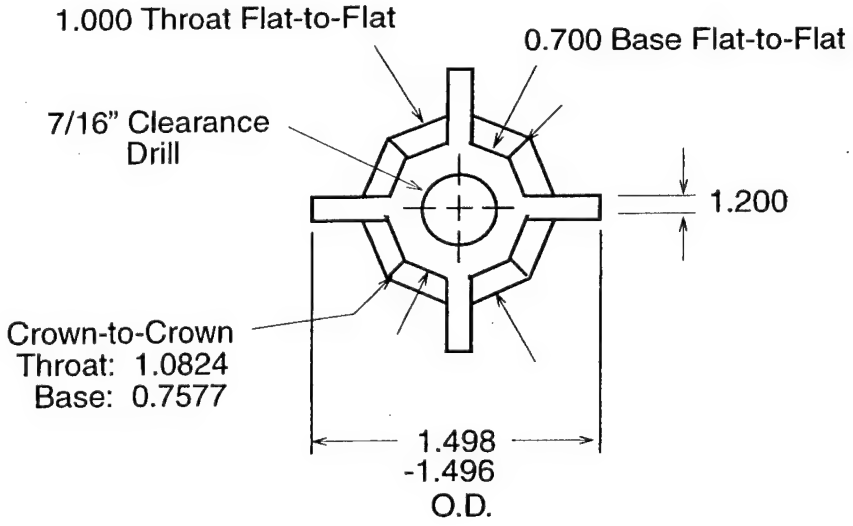

Dimensions: Inches Tolererances: .x = +/- 0.1 .xx = +/- 0.03 .xxx = +/- 0.005 Unless otherwise specified	Ram Accelerator Project Title: Solid, 20° Fin Rake, 1.00" throat Material: Mg ZK60-AT5 Date: 8-24-99 Drawn By: CK Scale: 1" = 1" Drawing No. 1024

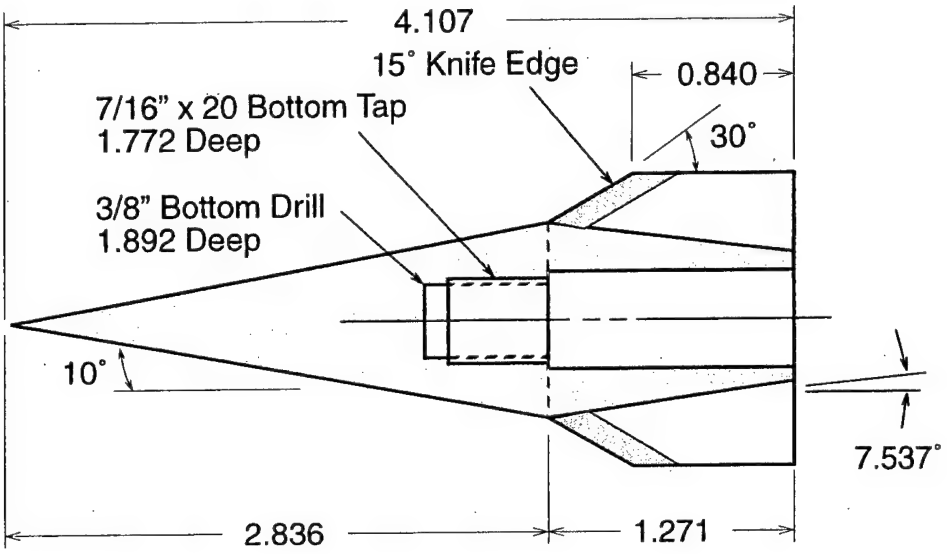

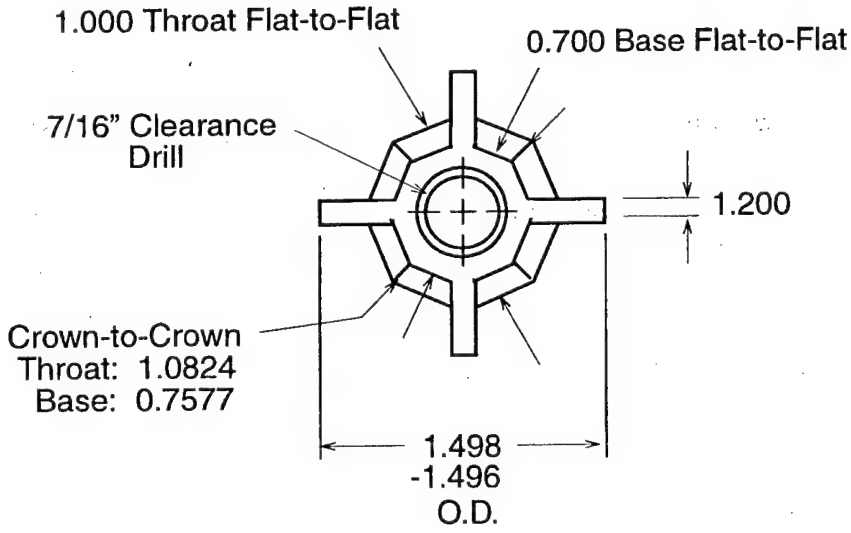

Dimensions: Inches Tolererances: .x = +/- 0.1 .xx = +/- 0.03 .xxx = +/- 0.005 Unless otherwise specified	Ram Accelerator Project Title: Solid, 30° Fin Rake, 1.00" throat Material: Mg ZK60-AT5 Date: 9-10-99 Drawn By: CK Scale: 1" = 1" Drawing No. 1025

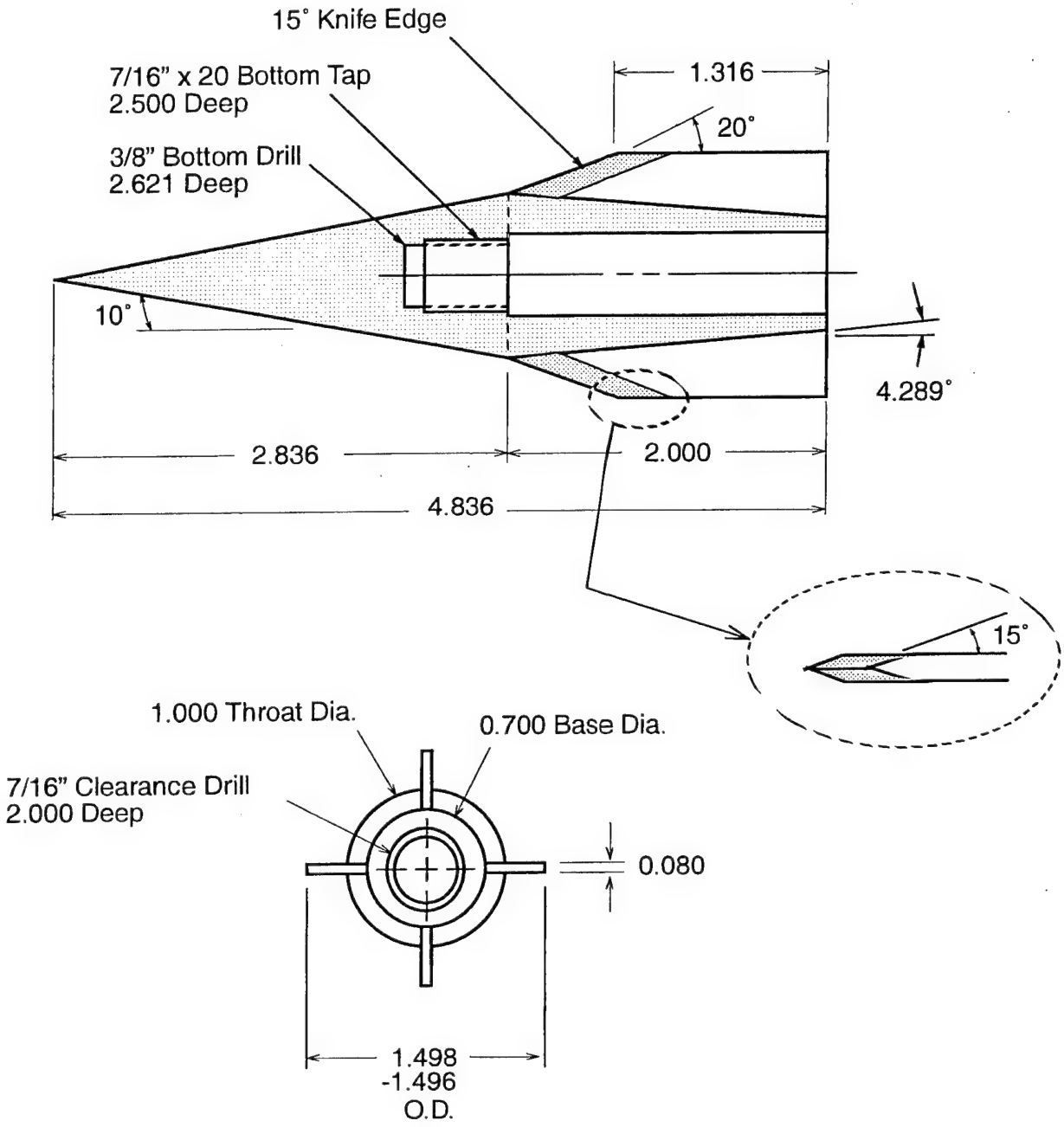

Dimensions: Inches Tolererances: .x = +/- 0.1 .xx = +/- 0.03 .xxx = +/- 0.005 Unless otherwise specified	Ram Accelerator Project Title: Solid, 20° Fin Rake, 1.00" throat Material: Ti 6Al-6V-2Sn Date: 9-10-99 Drawn By: CK Scale: 1" = 1" Drawing No. 1026

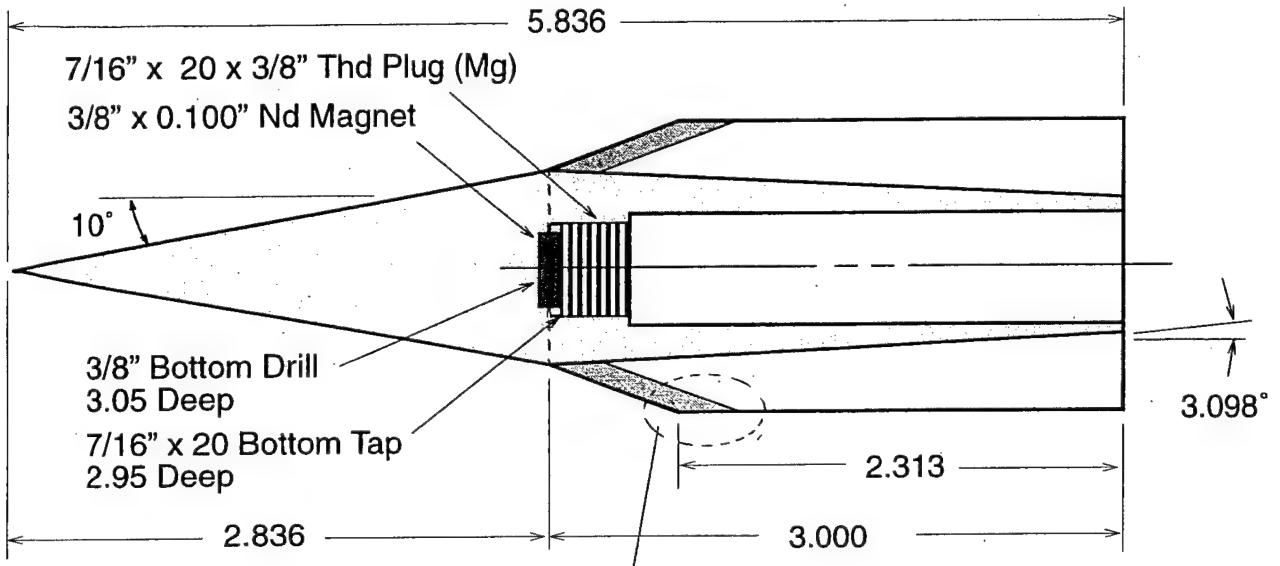

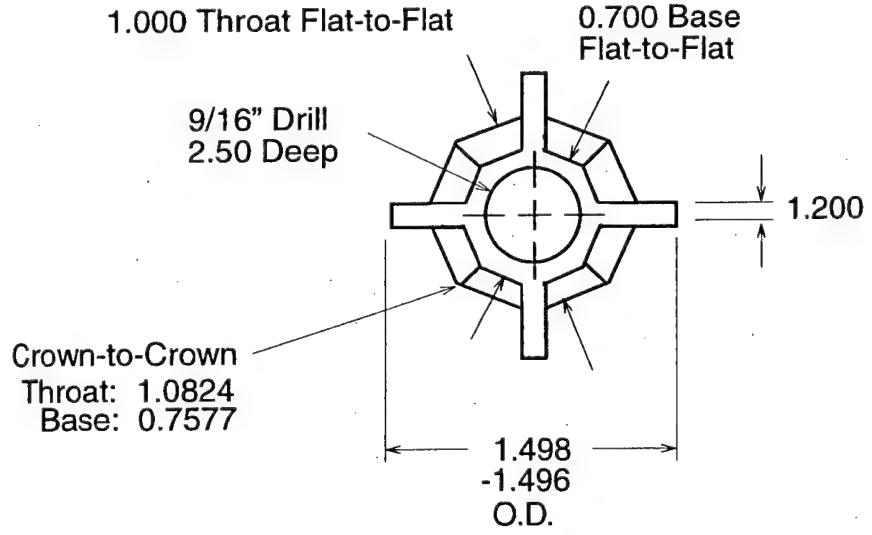

Dimensions: Inches Tolererances: .x = +/- 0.1 .xx = +/- 0.03 .xxx = +/- 0.005 Unless otherwise specified	Ram Accelerator Project Title: Solid Projectile (1" throat) Material: Mg ZK60-AT5 Date: 01-31-00 Drawn By: CK Scale: 1" = 1"	Drawing No. 1027

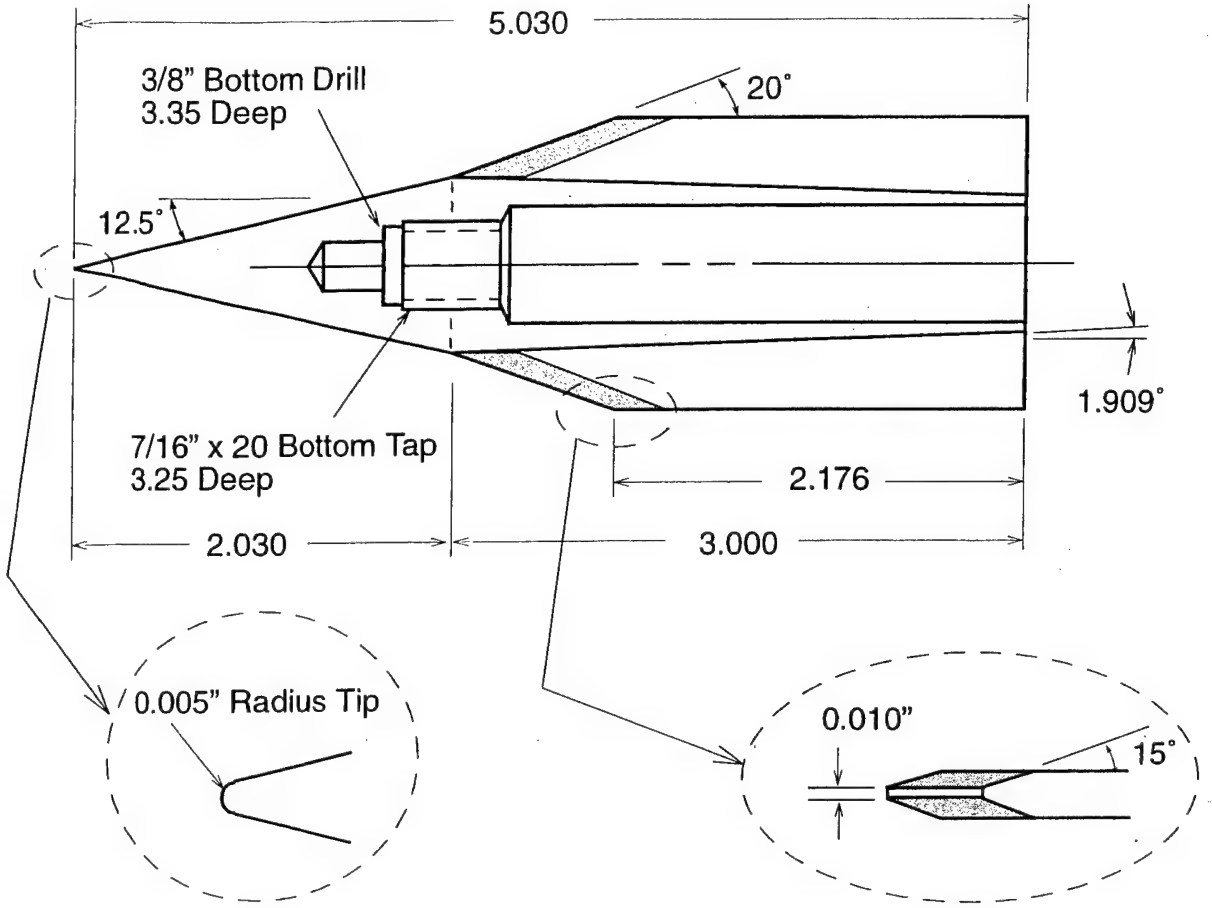

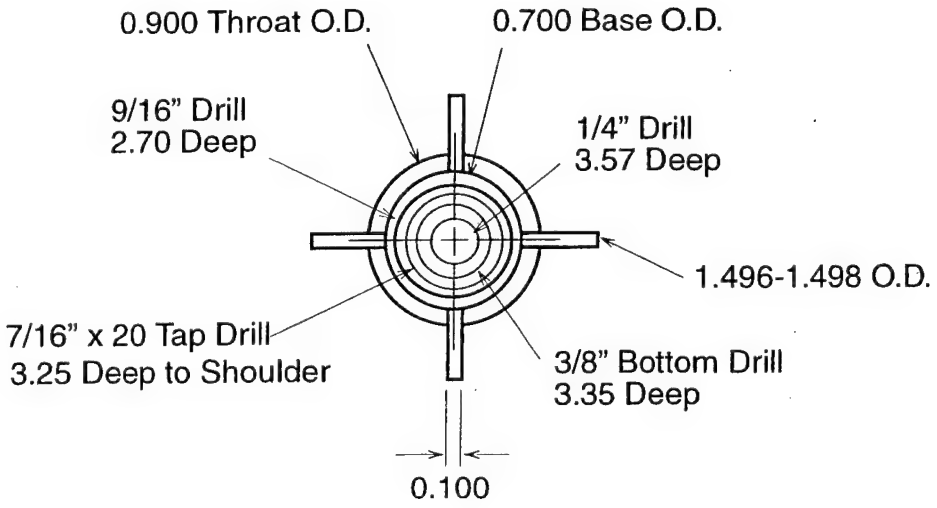

Dimensions: Inches Tolererances: .x = +/- 0.1 .xx = +/- 0.03 .xxx = +/- 0.005 Unless otherwise specified	Ram Accelerator Project	
	Title: 4 Fin Solid Projectile (0.9" throat) Material: Ti 6Al-6V-2Sn Date: 05-17-00 Drawn By: CK Scale: 1" = 1"	Drawing No. 1034

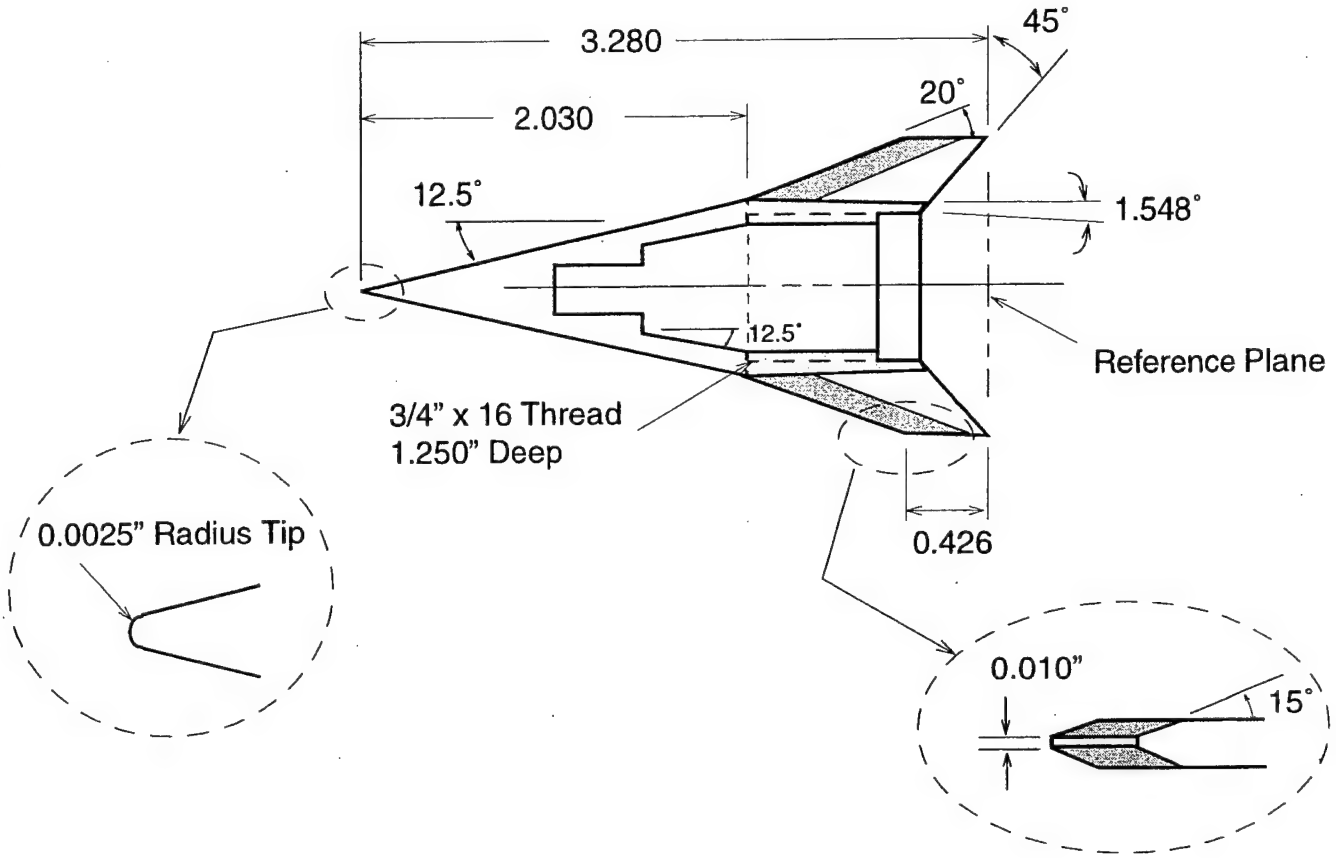

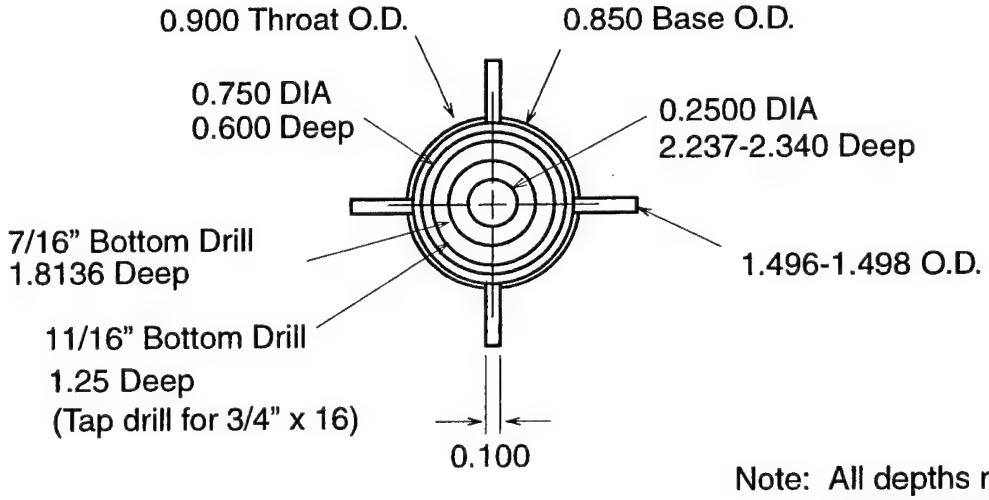

Note: All depths relative to Reference Plane

Dimensions: Inches Tolererances: .x = +/- 0.1 .xx = +/- 0.03 .xxx = +/- 0.005 Unless otherwise specified	Ram Accelerator Project Title: 2 Piece: Front Half (0.90" Throat) Material: Ti 6Al-6V-2Sn Date: 06-16-00 Drawn By: CK Scale: 1" = 1" Drawing No. 1035-1

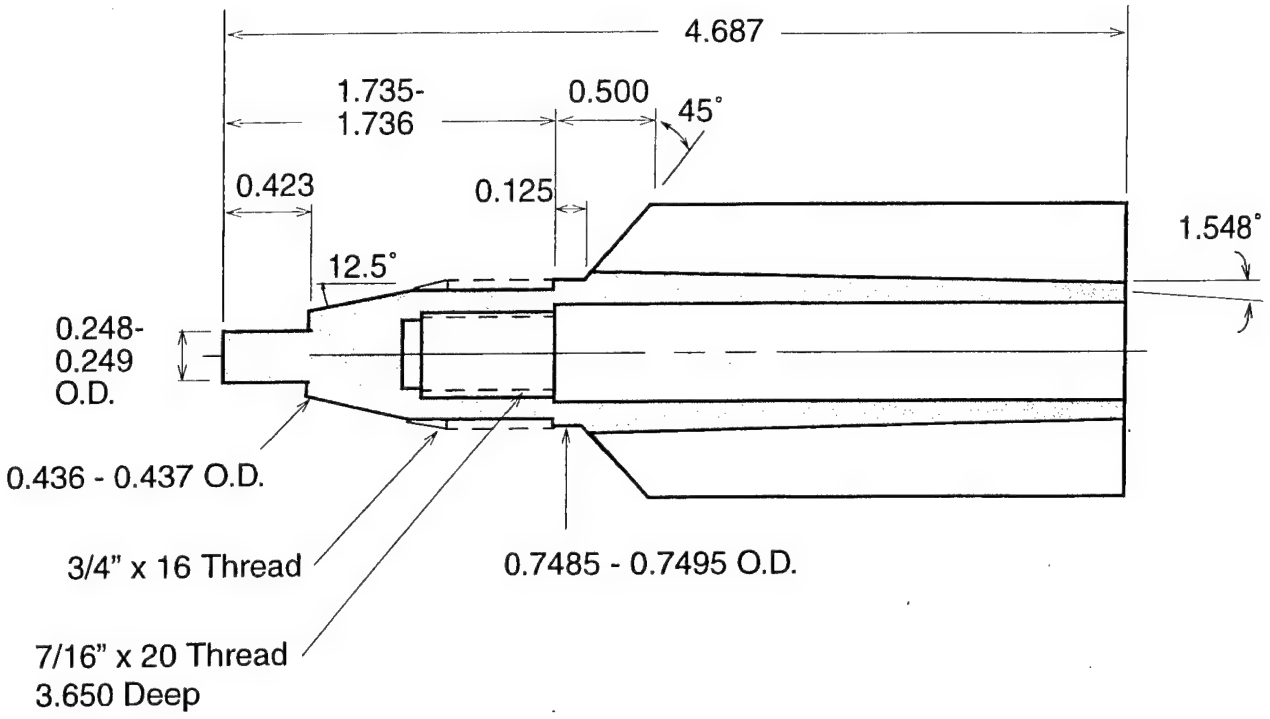

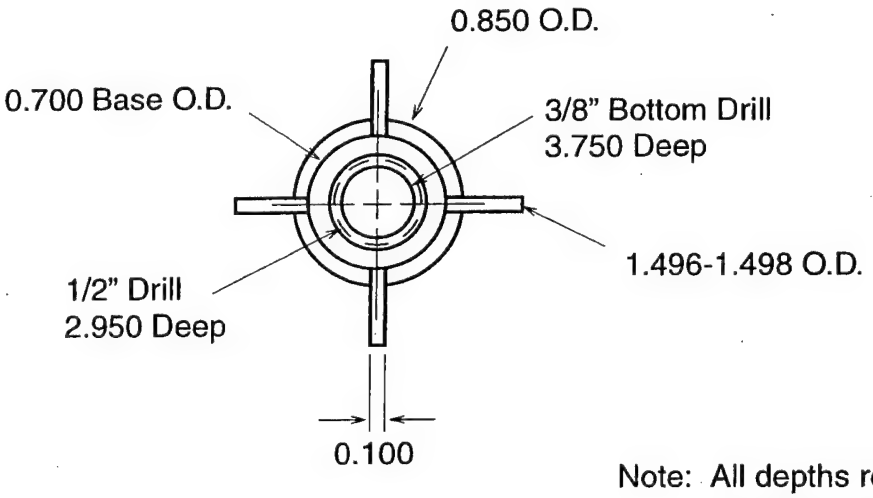

Note: All depths relative to Projectile Base

Dimensions: Inches Tolererances: .x = +/- 0.1 .xx = +/- 0.03 .xxx = +/- 0.005 Unless otherwise specified	Ram Accelerator Project Title: 2 Piece: Rear Half (0.90" Throat) Material: Al 7075-T6 Date: 06-16-00 Drawn By: CK Scale: 1" = 1" Drawing No. 1036-1

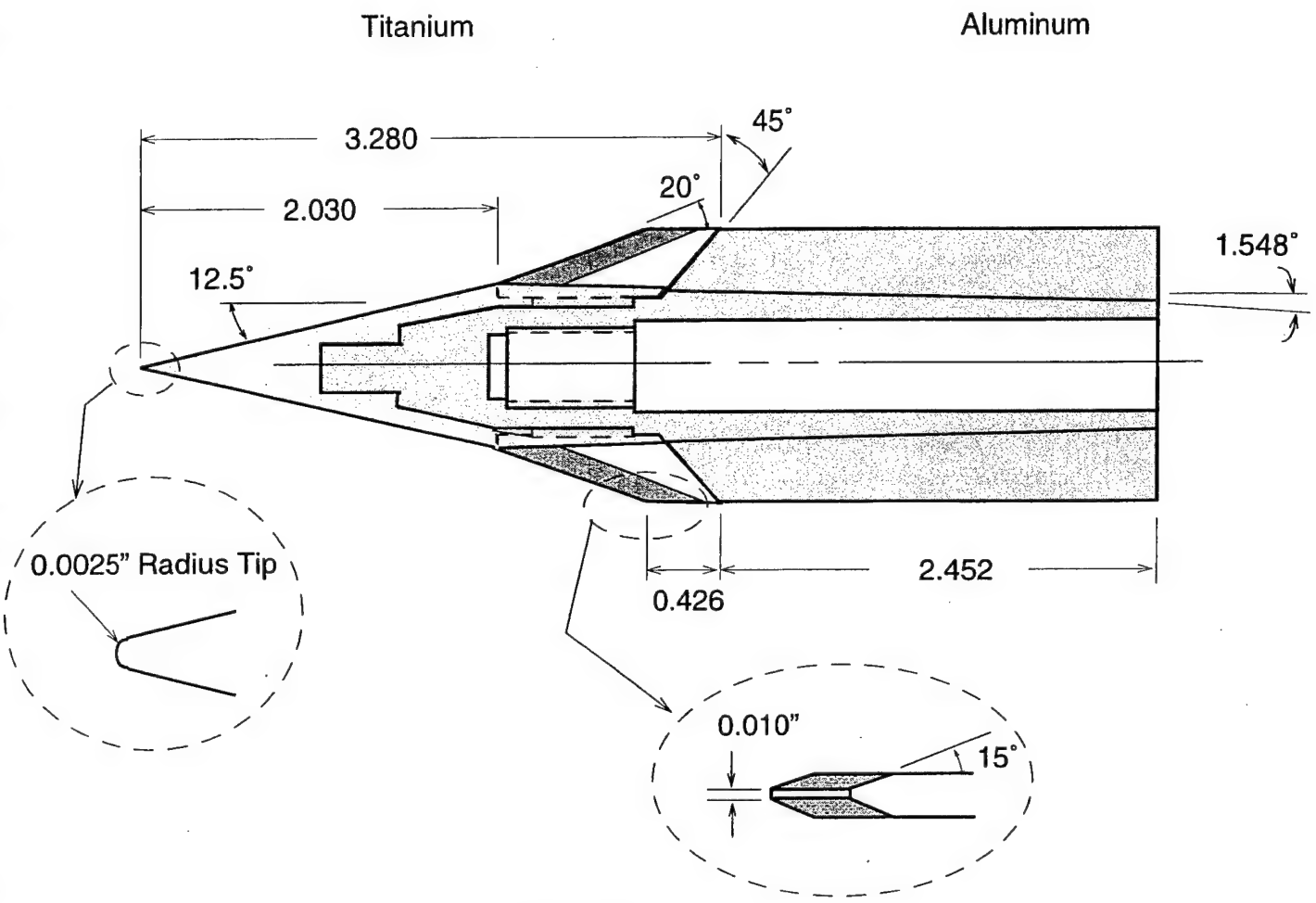

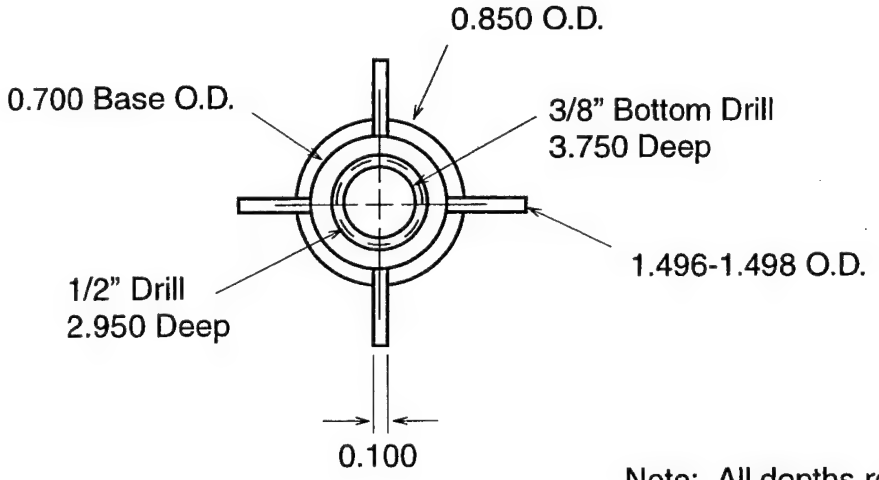

Note: All depths relative to Projectile Base

Dimensions: Inches Tolererances: .x = +/- 0.1 .xx = +/- 0.03 .xxx = +/- 0.005 Unless otherwise specified	Ram Accelerator Project Title: 2 Piece Assembled Material: Ti 6Al-6V-2Sn / Al 7075-T6 Date: 08-07-00 Drawn By: CK Scale: 1" = 1" Drawing No. 1037

Appendix F

Experiment Shot Log for High Pressure Research Program

	Projectile									Sabot		Propellant					Result				
	Nose	Throat	Body	Base	Number Fins /	Fin	Nose	Body				Moles	Moles	Moles	Fill Pres	Stage	Vin	Vmax	Run ΔX	Average	
HS #	Angle (deg)	Dia (mm)	Length (mm)	Dia (mm)	Lead Edge	Thick (mm)	Mtrl	Mtrl	Mass (g)	Mass (g)	Type	CH4	Ox	N2	(atm)	(m)	(m/s)	(m/s)	(m)	Accel (g)	Comments
1636	12.5	22.9	76.2	17.8	4KE	2.54	Ti	Al	101.7	28.4	Solid	2.6	2	9.2	200.1	4	1263	2397	4	52885	Ran out
1635	12.5	22.9	63.5	18.6	4KE	2.54	Ti	Ti	106.5	27.8	Solid	2.6	2	9.2	196.3	4	1247	2060	4	34258	Ran out
1634	12.5	22.9	57.2	19.1	4KE	2.54	Ti	Ti	99.9	28.2	Solid	2.6	2	9.2	200.5	4	1242	2297	3.66	51994	Unst by Sta. 11
1633	12.5	22.9	63.5	18.6	4KE	2.54	Ti	Al	92.4	38.1	Solid	2.6	2	9.2	200.4	3	1163	1233	0.5	17097	Unst by Sta. 3
1632	12.5	22.9	63.5	18.6	4KE	2.54	Ti	Al	92.1	27.6	Solid	2.6	2	9.2	200.7	4	1242	2250	3.5	51259	Unst by Sta. 11
1631	12.5	22.9	63.5	18.6	4KE	2.54	Ti	Al	92.2	30.5	Solid	2.6	2	9.2	200.3	3	1199	1376	1	23230	Unst by Sta. 4
1630	12.5	22.9	63.5	18.6	4KE	2.54	Ti	Al	92.3	27.8	Solid	2.6	2	9.2	200.3	3	1257	2186	3	54342	Ran out
1629	12.5	22.9	63.5	18.6	4KE	2.54	Ti	Al	92.3	28.8	Solid	2.6	2	9.2	201.0	3	?	?	?	?	Trigger Failure
1628	12.5	22.9	76.2	17.8	4KE	2.54	Ti	Al	94.1	28.7	Solid	2.6	2	9.2	198.4	3	1252	1947	2.5	45327	Unst by Sta. 8
1627	12.5	22.9	63.5	18.6	4KE	2.54	Ti	Al	92.6	23.2	Solid	2.6	2	9.2	197.5	3	1279	1388	1.5	9878	Unst by Sta. 5
1626	12.5	22.9	63.5	18.6	4KE	2.54	Ti	Al	92.1	17.7	Solid	2.6	2	9.2	200.0	3	1298	1332	1	4558	Unst by Sta. 4
1625	12.5	22.9	63.5	18.6	4 KE	2.54	Ti	Ti	106.4	17.8	Solid	2.2	2	9.0	197.0	1	1236	1345	1	14339	SS
"												2.6	2	9.2	197.0	3	1345	1448.	0.5	29325	Unst by Sta. 6
1624	12.5	22.9	50.8	19.5	4 KE	2.54	Ti	Ti	93.3	17.8	Solid	2.6	2	9.2	200.4	3	1298	1301.	0.2	1987	Unst by Sta. 2
1623	12.5	22.9	76.2	17.8	4 KE	2.54	Ti	Ti	117.7	17.9	Solid	2.2	2	9.0	150.2	1	1212	1347	1	17608	SS
"												2.2	2	9.0	201.5	3	1347	1442	0.2	67522	Unst by Sta. 5
1622	12.5	22.9	76.2	17.8	4 KE	2.54	Ti	Ti	117.5	17.8	Solid	2.6	2	9.2	150.9	1	1222	1311	1	11490	SS
"												2.6	2	9.2	201.5	3	1311	2100	3	45723	Ran out
1621	12.5	22.9	76.2	18.7	4 KE	2.54	Ti	Al	101.7	17.8	Solid	2.6	2	9.2	151.9	1	1267	1376	1	14683	SS
"												2.6	2	9.2	191.1	3	1376	2012	2.2	49920	Unst by Sta. 11
1620	12.5	22.9	94.0	17.8	4 KE	2.54	Ti	Al	114.0	17.7	Solid	2.6	2	9.2	154.5	1	1203	1295	1	11713	SS
"												2.6	2	9.2	197.4	3	1295	1767	2	36831	Unst by Sta. 10
1619	12.5	22.9	76.2	18.7	4 KE	2.54	Ti	Al	101.4	17.7	Solid	2.6	2	9.2	192.6	4	1247	1327	1.2	8746	Unst by Sta. 5
1618	12.5	22.9	76.2	18.7	4 KE	2.54	Ti	Al	101.7	17.8	Solid	2.6	2	9.2	151.4	1	1246	1342	1	12663	SS
"												2.6	2	9.2	197.4	3	1342	2342	3	62589	Ran out
1617	12.5	22.9	76.2	17.8	4 KE	2.54	Ti	Ti	117.9	17.7	Solid	2.6	2	9.2	151.7	1	1198	1261	1	7896	SS
"												2.6	2	9.2	198.8	3	1261	2074	3	46064	Ran out
1616	12.5	22.9	76.2	17.8	4 KE	2.54	Ti	Ti	118.5	17.8	Solid	2.6	2	9.2	152.0	1	1207	1296	1	11354	SS
"												2.6	2	9.2	200.3	2	1296	1857	2	45077	Ran out
1615	12.5	22.9	61.0	18.8	4 KE	2.54	Ti	Ti	104.6	17.7	Solid	2.2	2	9.0	199.6	3	1236	1343	1.1	12786	Unst by Sta. 4
1614	12.5	22.9	63.5	18.6	4 KE	2.54	Ti	Ti	106.9	17.6	Solid	2.6	2	9.2	199.1	3	1231	1281	1	6402	Unst by Sta. 4
1613	12.5	22.9	76.2	17.8	4 KE	2.54	Ti	Ti	118.4	18.0	Solid	2.2	2	9.0	198.6	4	1173	1198	0.33	9155	Unst by Sta. 2
1612	12.5	22.9	76.2	17.8	4 KE	2.54	Ti	Ti	118.4	17.2	Solid	2.6	2	9.2	198.6	4	1196	1207	0.33	4083	Unst by Sta. 2
1611	12.5	22.9	76.2	17.8	4 KE	2.54	Ti	Ti	118.2	17.8	Solid	2.6	2	9.2	149.2	4	1193	1858	4	25853	Ran out
1610	12.5	22.9	50.8	?	5 KE	?	Mg	Mg	47.4	15.9	23%	2.2	2	9.0	198.1	1	1229	1617	1	56282	Ran out
1609	12.5	22.9	48.3	?	5 KE	?	Mg	Mg	59.2	15.8	23%	2.2	2	9.0	197.9	1	1182	1569	1	54263	Ran out
1608	12.5	22.9	38.1	?	5 KE	?	Mg	Mg	46.7	16.0	23%	2.2	2	9.0	198.0	1	977	824	0.33	-42559	Launch failure
1607	12.5	22.9	33.8	?	4 KE	2.29	Ti	Ti	86.3	17.5	Solid	2.2	2	9.0	197.7	1	1215	1272	1	7225	Ran out
1606	12.5	22.9	33.8	?	4 KE	2.29	Ti	Ti	84.4	17.5	Solid	2.6	2	9.2	198.3	?	1254	1276	0.33	8597	Unst by Sta. 2
1605	12.5	22.9	33.0	?	4 KE	2.29	Ti	Ti	86.1	17.7	Solid	2.6	2	9.2	197.9	1	1302	1371	1	9400	Ran out
1604	12.5	25.4	50.8	17.8	4 KE	2.29	Ti	Ti	109.3	17.2	Solid	2.6	2	9.2	151.7	1	1212	1295	1	10606	SS
"												2.6	2	9.2	198.3	2	1295	1271	0.33	-9512	Unst by Sta. 4
1603	12.5	25.4	45.7	18.5	4 KE	2.29	Ti	Ti	102.5	17.6	Solid	1.8	2	8.7	197.8	1	1244	1140	0.33	-38294	Unst by Sta. 1
1602	12.5	25.4	50.8	17.8	4 KE	2.29	Ti	Ti	111.5	17.5	Solid	2.6	2	9.2	195.4	1	1225	1133	0.33	-33506	Unst by Sta. 1
1601	15.0	25.4	50.8	17.8	4 KE	2.29	Ti	Ti	109.7	17.4	Solid	2.6	2	9.2	146.0	1	1225	1133	0.33	-33506	Unst by Sta. 1
1600	10.0 : 15.0	25.4	50.8	17.8	4 KE	2.29	Ti	Ti	103.1	17.5	Solid	2.2	2	9.0	149.8	3	1227	1435	1.33	21219	Unst by Sta. 5
1599	15.0	25.4	50.8	17.8	4 KE	2.29	Ti	Ti	103.0	17.8	Solid	2.2	2	9.0	149.6	3	1227	1593	2.5	21042	Unst by Sta. 8
1598	15.0	25.4	76.2	18.0	4 KE	2.29	Mg	Mg	70.8	16.0	23%	2.	2	8.8	147.5	1	1257	1563	1	43982	Ran out
1597	12.5	25.4	76.2	18.0	4 KE	2.29	Mg	Mg	73.9	15.8	23%	2	2	8.8	148.2	1	?	?	?	?	Unst by Sta. 3
1596	12.5	25.4	50.8	19.0	4 KE	2.29	Ti	Mg	99.7	17.6	Solid	2	2	8.8	149.5	3	?	?	?	?	Unst by Sta. 7
1595	12.5	25.4	76.2	18.0	4 KE	2.29	Ti/Mg	Mg	76.9	15.9	23%	2	2	8.8	150.1	3	?	?	?	?	Unst by Sta. 5
1594	12.5	25.4	50.8	17.8	4 KE	2.29	Mg/Ti	Ti	104.2	17.5	Solid	2	2	8.8	149.6	3	1231	1393	1.5	14444	Unst by Sta. 5
1593	12.5	25.4	50.8	17.8	4 KE	2.29	Ti	Ti	112.0	17.6	Solid	2	2	8.8	150.1	3	1212	1616	2.33	24992	Unst by sta. 8
1592	12.5	25.4	76.2	18.0	4 KE	2.29	Mg	Mg	78.5	16.0	23%	2.2	2	9.0	149.9	3	1304	?	0.33	?	Unst by Sta. 1

1591	12.5	25.4	76.2	18.0	4 KE	2.29	Mg	Mg	73.0	15.9	23%	2.2	2	9.0	149.8	3	1262	1640	1.5	37273	Unst by Sta. 5
1590	12.5	25.4	50.8	17.8	4 KE	2.29	Ti	Ti	110.8	17.6	Solid	2.2	2	9.0	149.7	3	1198	1593	2.33	24116	Unst by Sta. 8
1589	12.5	25.4	50.8	17.8	4KE	2.29	Ti	Ti	119.3	17.7	Solid	2.2	2	9.0	149.6	3	1158	1189	0.33	11237	Unst by Sta. 1
1588	12.5	25.4	50.8	19.0	4KE	2.29	Mg	Mg	75.4	15.9	23%	2.2	2	9.0	149.8	3	1212	1725	1.83	41963	Unst by Sta. 6
1587	12.5	25.4	50.8	19.0	4KE	2.29	Mg	Mg	52.1	15.9	23%	2	2	8.8	150.1	3	1241	1365	0.5	32940	Unst by Sta. 3
1586	12.5	25.4	76.2	18.0	5 KE	2.5	Mg	Mg	72.8	15.9	23%	1.7	2	8.6	149.1	3	1231	1593	1.33	39176	Unst by Sta 4
1585	12.5	25.4	50.8	19.0	4KE	2.29	Al	Al	72.8	15.9	23%	1.7	2	8.6	149.5	3	1216	1447	1.50	20902	Unst by Sta 5
1584	12.5	25.4	50.8	19.0	4KE	2.29	Mg	Mg	51.9	15.9	23%	1.5	2	8.5	150.0	3	1236	1337	0.5	26491	Unst by Sta 2
1583	12.5	25.4	50.8	19.0	4KE	2.29	Mg	Mg	53.2	?	23%	1.7	2	8.6	150.1	3	1227	1578	1.33	37730	Unst by sta 4
1582	12.5	25.4	50.8	19.0	4KE	2.29	Mg	Mg	54.4	17.6	Solid	1.7	2	8.6	149.8	3	1193	?	0.33	?	Unst by Sta 1
1581	12.5	25.4	50.8	19.0	4KE	2.29	Ti	Ti	107.3	17.1	Solid	1.4	2	8.4	148.1	3	1202	1417	1.5	19133	Unst by Sta. 5
"												0	0	1 CO2	50.7	3					
1580	12.5	25.4	50.8	19.0	4KE	2.29	Ti	Ti	108.1	17.3	Solid	1.5	2	8.5	149.6	3	1202	2050	3	46852	Ran out
"												0	0	1 CO2	48.2	3	2050		3		Ran out
1579	12.5	25.4	50.8	19.0	4KE	2.29	Ti	Ti	108.1	17.8	Solid	1.7	2	8.6	146.1	3	1216	1707	2.5	29260	Unst by Sta. 8
1578	12.5	25.4	50.8	19.0	4KE	2.29	Ti	Ti	108.9	15.6	Solid	1.8	2	8.7	149.9	3	1207	1207	0.33	0	Unst by Sta. 1
"												0	0	1 CO2	52.3	3					
1577	10.0	25.4	45.7	19.5	4KE	2.29	Ti	Ti	113.4	15.8	Solid	1.8	2	8.7	150.2	3	1207	1542	1.5	31292	Unst by Sta 5
"												0	0	1 CO2	53.5	3					
1576	10.0	25.4	45.7	19.5	4KE	2.29	Ti	Ti	114.3	15.7	Solid	1.8	2	8.7	150.1	3	1024	555	3	-12582	SDU by Sta. 1
1575	12.5	25.4	45.7	19.5	4KE	2.29	Ti	Ti	104.5	15.0	Solid	1.8	2	8.7	148.3	1	1261	1350	1	11844	SS
"												3.25	2	9.7	149.3	2	1350	1507	1.66	13772	Unst by Sta. 6
"												0	0	1.0	84.4	3					
1574	12.5	25.4	45.7	19.5	4KE	2.29	Ti	Ti	104.6	13.8	Solid	1.8	2	8.7	147.9	3	1231	1632	2.33	25114	Unst by Sta. 7
"												0	0	1.0	49.5	3					
1573	12.5	25.4	45.7	19.5	4KE	2.29	Ti	Ti	103.8	15.9	23%	1.8	2	8.7	149.1	3	1189	?	0.33	?	Unst by Sta. 1
"												0	0	1.0	49.6	3					Sabot failure
1572	12.5	25.4	40.6	20.0	4KE	3	Mg	Mg	46.0	15.9	23%	1.8	2	8.7	147.9	1	1202	1324	0.83	18924	Unst by Sta. 3
1571	12.5	25.4	45.7	19.5	4KE	3	Mg	Mg	47.6	15.9	23%	1.8	2	8.7	147.9	1	1207	1560	1	49783	Ran out
1570	12.5	25.4	50.8	19.0	4KE	3	Mg	Mg	49.2	15.7	23%	1.8	2	8.7	146.9	1	1189	1487	0.83	48969	Unst by Sta. 3
1569	12.5	25.4	50.8	19.0	4KE	3	Mg	Mg	52.5	15.9	23%	1.8	2	8.7	147.7	1	1207	1523	1	43969	Ran out
1568	12.5	25.4	50.8	19.0	4KE	3	Mg	Mg	53.6	13.6	23%	1.8	2	8.7	146.2	1	1193	1514	1	44289	Ran out
1567	10..12.5	25.4	50.8	19.0	4KE	3	Mg	Mg	56.5	13.5	23%	1.8	2	8.7	147.9	1	1198	1337	0.33	54423	Unst by Sta. 1
1566	12.5	25.4	50.8	19.0	4Sq	3	Mg	Mg	52.9	12.3	23%	1.8	2	8.7	147.9	1	1171	1171	0.5	0	Unst by Sta. 2
1565	10.0	25.4	50.8	19.0	4Sq	3	Mg	Mg	58.3	12.6	23%	1.8	2	8.7	147.7	1	1184	1500	1	43229	Ran out
1564	10.0	25.4	50.8	19.0	4Sq	3	Mg	Mg	58.3	14.1	23%	1.8	2	8.7	148.3	1.076	?	?	0.33	?	Unst by Sta. 1
1563	10.0	25.4	50.8	19.0	4KE	3	Mg	Mg	58.3	14.0	23%	1.4	2	8.4	147.8	1.076	1216	1581	1.076	48359	Ran out
1562	10.0	25.4	50.8	19.0	4KE	3	Mg	Mg	57.6	13.5	23%	1.8	2	8.7	148.4	1	1216	1449	1	31649	Ran out
1561	10.0	25.4	50.8	19.0	4KE	3	Mg	Mg	57.2	13.3	23%	2	2	8.8	148.1	1.076	1198	1488	1.076	36897	Ran out
1560	10.0	25.4	50.8	19.0	4KE	3	Mg	Mg	54.5	13.9	23%	2.2	2	9.0	148.4	1.076	1226	1295	0.66	13433	Unst by Sta. 3
1559	10.0	25.4	30.5	20.8	4KE	3	Mg	Mg	43.6	13.4	23%	3.25	2	9.7	147.9	1	1226	1226	0.5	0	Unst by Sta. 2
1558	10.0	25.4	30.5	20.8	4KE	3	Mg	Mg	42.6	13.2	23%	3.25	2	9.7	148.1	1	1256	1311	0.5	14392	Unst by Sta. 2
1557	10.0	25.4	30.5	20.8	4KE	3	Mg	Mg	43.5	13.1	23%	2.2	2	9.0	147.9	1	1287	1296	0.5	2370	Unst by Sta. 2
1556	10.0	25.4	30.5	20.8	4KE	3	Mg	Mg	43.7	13.1	23%	2.2	2	9.0	147.5	1	1116	1121	0.33	1728	Unst by Sta. 2
1555	12.5	29.0	45.7	18.0	4KE	3	Mg	Mg	60.9	15.7	23%	3.25	2	9.7	147.4	1	1293	1293	0.33	0	Unst by Sta. 1
1554	10.0	25.4	45.7	18.0	4KE	3	Mg	Mg	54.3	13.3	23%	2.2	2	9.0	147.5	1	1184	1184	0.5	0	Unst by Sta. 2
1553	10.0	25.4	45.7	18.0	4KE	3	Mg	Mg	54.3	13.0	23%	2.2	2	9.0	146.7	1.076	1193	1193	0.33	0	Unst by Sta. 1
1552	10.0	25.4	45.7	18.0	4KE	3	Mg	Mg	53.0	15.9	23%	2.2	2	9.0	147.7	1.076	1193	1229	0.33	13467	Unst by Sta. 1
1551	10.0	25.4	45.7	18.0	4KE	3	Mg	Mg	53.3	15.8	23%	2	2	9.0	147.9	1.076	1149	1149	0.33	0	Unst by Sta. 1
1550	10.0	25.4	45.7	18.0	4KE	3	Mg	Mg	57.6	13.3	23%	2	2	8.8	148.3	1	1162	1337	1	22290	SS
												3.15	2	9.6	144.3	2.076	1337	1496	0.33	69571	Unst by Sta. 4
1549	10.0	25.4	45.7	18.0	4KE	3	Mg	Mg	57.6	13.3	23%	2.3	2	9.1	147.9	1	1153	1153	0.5	0	Unst by Sta. 2
												3.15	2	9.6	149.1	2.076					
1548	10.0	25.4	45.7	18.0	4KE	3	Mg	Mg	57.5	13.2	23%	2.2	2	9.0	148.2	1.076	1149	1222	0.83	10629	Unst by Sta. 3

1547	10.0	25.4	45.7	18.0	4KE	3	Mg	Mg	57.2	13.2	23%	3.15	2	9.6	149.2	2				
1546	10.0	25.4	45.7	18.0	4KE	3	Mg	Mg	57.8	13.3	23%	2.2	2	9.0	149.4	3.076	1157	1582	1.66	35742	Unst by Sta. 6
1545	10.0	25.4	45.7	18.0	4KE	3	Mg	Mg	58.0	13.3	23%	2.2	2	9.0	148.2	1.076	1157	1288	1.076	15172	Ran out
1544	10.0	25.4	45.7	18.0	4KE	3	Mg	Mg	54.1	13.3	23%	2.6	2	9.2	147.7	1.076	1162	1162	0.66	0	Unst by Sta. 3
1543	10.0	25.4	45.7	18.0	4KE	3	Mg	Mg	54.3	13.3	23%	2.7	2	9.3	151.1	1.076	1153	1153	0.5	0	Unst by Sta. 2
1542	10.0	25.4	45.7	18.0	4KE	3	Mg	Mg	53.9	13.4	23%	3	2	9.5	148.3	1.076	1175	1046	1.076	-13571	WFO
1541	10.0	25.4	45.7	18.0	4KE	3	Mg	Mg	60.0	13.3	23%	3.15	2	9.6	147.9	1.076	1179	1133	0.66	-8213	Unst by Sta. 3
1540	10.0	25.4	45.7	18.0	4KE	3	Mg	Mg	60.3	13.3	23%	3.15	2	9.6	149.4	1.076	1243	1266	0.33	8913	WFO
1539	10.0	25.4	45.7	18.0	4KE	3	Mg	Mg	60.8	13.4	23%	3.15	2	9.6	148.3	3	1309	1493	2	13139	Unst by Sta. 7
"												3.25	2	9.7	147.8	1.076	1286	1321	0.66	7046	WFO by Sta. 3
CS70	10.0	25.4	45.7	18.0	4KE	3	Mg	Mg	67.2	13.4	23%	0	0	1.0	136.6	2	1313	1313			SDU by Sta. 8
CS69	10.0	25.4	45.7	18.0	4KE	3	Mg	Mg	58.8	13.3	23%	0	0	1.0	151.9	1.076	1266	1271	0.66	980	Unst by Sta. 3
CS68	10.0	25.4	45.7	18.0	4KE	3	Mg	Mg	57.7	13.4	23%	0	0	1.0	150.9	1	1281	1282	0.5	261	Unst by Sta. 2
1518	10.0	25.4	45.7	18.0	4KE	3	Mg	Mg	62.1	15.9	23%	0	0	1.0	148.6	3	1355	1355	0.66	0	Unst by Sta. 3
1517	10.0	25.4	45.7	18.0	4KE	3	Mg	Mg	61.8	15.9	23%	3.25	2	9.7	172.1	1	1318	1370	0.33	21588	Unst by Sta. 1
CS66	10.0	25.4	45.7	18.0	4KE	3	Mg	Mg	62.0	16.0	23%	3.25	2	9.7	160.7	1	1317	1358	0.33	16939	Unst by Sta. 1
1516	10.0	22.9			4KE	3	Mg	Mg	40.3	15.9	23%	0	0	1.0	197.0	1					Unst
1515	10.0	25.4	45.7	18.0	4KE	3	Mg	Mg	60.8	16.0	23%	4	2	10.2	189.9	1	1396	1454	0.33	25531	Unst by Sta. 1
1514	10.0	25.4	45.7	18.0	4KE	3	Mg	Mg	60.9	16.0	23%	4	2	10.2	190.1	1	1323	1349	0.33	10730	Unst by Sta. 1
1513	10.0	25.4	45.7	18.0	4KE	3	Mg	Mg	60.3	16.0	23%	3.5	2	9.8	195.3	1	1328	1344	0.33	6603	Unst by Sta. 1
1512	10.0	25.4	45.7	18.0	4KE	3	Mg	Mg	61.4	16.0	23%	3.25	2	9.7	149.4	1	1296	1501	1	29225	Ran out
1511	10.0	25.4	45.7	18.0	4KE	3	Mg	Mg	60.7	16.0	23%	3	2	9.5	148.8	1	1305	1388	0.5	22785	Unst by Sta. 2
1510	10.0	25.4	45.7	18.0	4KE	3	Mg	Mg	60.7	16.0	23%	3.5	2	9.8	148.9	1	1268	1349	0.5	21608	WFO by Sta. 2
1509	10.0	25.4	45.7	18.0	4Sq	3	Mg/St	Mg	68.0	16.0	23%	2.5	2	9.2	149.1	1	1325	1435	0.5	30948	Unst by Sta. 2
1508	10.0	25.4	45.7	18.0	4Sq	3	Mg	Mg	60.0	16.0	23%	2.5	2	9.2	148.1	1	1315	1417	0.5	28406	Unst by Sta. 2
1507	10.0	25.4	45.7	18.0	4Sq	3	Mg	Mg	60.6	16.0	23%	2.5	2	9.2	149.2	1	1286	1349	0.5	16922	Unst by Sta. 2
1506	10.0	25.4	45.7	18.0	4Sq	3	Mg	Mg	61.3	16.0	23%	3.5	2	9.8	149.2	1	1315	1343	0.5	7587	Unst by Sta. 2
1505	10.0	25.4	45.7	18.0	4Sq	3	Mg	Mg	60.3	16.0	23%	3	2	9.5	148.4	1	1286	1404	0.5	32357	Unst by Sta. 2
1504	10.0	25.4	45.7	18.0	4Sq	3	Mg	Mg	60.9	16.0	23%	2	2	9.5	124.9	1	1245	1478	1	32337	Ran out
1503	10.0	25.4	46.0	18.0	4Sq	3.8	Mg	Al	66.5	16.0	23%	2.5	2	10.0	124.6	1	1320	1491	1	24500	Ran out
1502	10.0	25.4	46.0	18.0	4Sq	3.8	Mg	Al	66.9	16.0	23%	3	2	7.5	119.4	1	1349	1349	0.33	0	Unst by Sta. 1
1501	10.0	25.4	46.0	18.0	4Sq	3.8	Mg	Al	66.5	16.0	23%	3	2	7.5	119.4	1	1281	1306	0.33	9989	Unst by Sta. 1
1500	10.0	25.4	45.7	17.8	4Sq	3	Mg	Mg	61.7	16.1	23%	3	2	7.5	119.5	1	1236	1268	0.33	12376	Unst by Sta. 1
1499	10.0	25.4	45.7	18.0	4KE	3	Mg	Mg	68.6	16.0	23%	3	2	7.5	119.6	1	1300	1532	1	33487	Ran out
1498	10.0	29.0	46.0	18.0	4Sq	3.8	Ti	Ti	73.6	16.0	23%	3	2	7.5	99.8	1	1278	1483	1	28848	Ran out
"												3	2	7.5	87.9	0.076	1281	1323	0.076	73346	Ran out
1497	10.0	29.0	45.7	18.0	4Sq	3	Mg	Mg	85.0	16.1	23%	3	2	7.5	101.3	1	1323	1330	0.33	2868	Unst by Sta. 1
1496	10.0	29.0	75.8	18.0	4Sq	3	Mg	Mg	98.1	16.1	23%	3	2	7.5	110.3	1	1253	1306	0.33	20948	Unst by Sta. 1
1495	10.0	29.0	46.0	18.0	4Sq	3.8	Al	Al	66.0	16.0	23%	3	2	7.5	110.5	1	1236	1260	0.33	9252	Unst by Sta. 1
1494	10.0	29.0	46.0	18.0	4Sq	3.8	Al	Al	66.0	16.0	23%	3	2	7.5	119.2	1	1300	1349	0.33	20048	Unst by Sta. 1
1493	10.0	29.0	46.0	18.0	4Sq	3.8	Al	Al	66.1	16.0	23%	3	2	7.5	109.7	1	1310	1560	1	36570	Ran out
1492	10.0	29.0	46.0	18.0	4Sq	3.8	Al	Al	65.9	16.0	23%	3	2	7.5	108.5	1	1178	1206	0.33	10310	Start Failure
1491	10.0	29.0	46.0	18.0	4Sq	3.8	Al	Ti	70.0	16.0	23%	3	2	7.5	97.5	1	1317	1581	1	38994	Ran out
1490	10.0	29.0	71.0	18.8	5Sq	3	Al	Al	110.7	16.0	23%	3	2	7.5	93.8	1	1269	1322	0.5	13998	Unst by Sta. 2
1489	15.0	29.0	46.0	18.0	4Sq	3.8	Mg	Mg	79.3	15.9	23%	3	2	7.5	96.6	1	1168	1168	0.33	0	Unst by Sta. 1
1488	10.0	29.0	46.0	18.0	4Sq	3.8	Ti	Ti	73.3	16.0	23%	3	2	7.5	97.1	1	1260	1340	0.33	32126	Unst by Sta. 1
1487	10.0	29.0	46.0	18.0	4Sq	3.8	Al	Ti	69.7	16.0	23%	3	2	7.5	97.9	1	1298	1306	0.5	2124	Unst by Sta. 2
1486	10.0	29.0	46.0	18.0	4Sq	3.8	Ti	Ti	73.5	16.0	23%	3	2	7.5	96.6	1	1288	1578	0.83	51038	Unst by Sta. 3
1485	10.0	29.0	46.0	18.0	4Sq	3.8	Al	Ti	69.3	16.0	23%	3	2	7.5	97.9	1	1288	1348	0.5	16122	Unst by Sta. 2
1484	10.0	29.0	71.0	18.8	5Sq	3	Al	Ti	115.4	15.1	23%	3	2	7.5	98.3	1	1270	1473	0.83	34194	Unst by Sta. 3
"												3	2	6.5	73.2	1	1151	1286	1	16768	SS
"												3	2	7.5	86.0	2	1286	1354	0.5	18300	Unst by Sta. 5
												3	2	7.5	124.1	1					
1483	10.0	29.0	71.0	18.8	5Sq	3	Ti	Ti	116.2	15.2	23%	3	2	6.5	72.8	1	1134	1262	1	15631	SS

"												3	2	7.5	85.6	2	1262	1580	2	23031	Ran out
"												8	2	0.0	123.9	1	1580	1580	0.33	0	Unst by Sta.10
1482	10.0	29.0	71.0	18.8	5Sq	3	Ti	Ti	115.3	16.0	23%	3	2	6.5	73.7	1	1142	1283	1	17427	SS
"												3	2	7.5	85.8	2	1283	1561	2	20149	Ran out
"												3	2	7.5	124.5	1	1561	1561	0.5	0	Unst by Sta. 11
1481	10.0	29.0	75.8	18.0	4Sq	3	Mg	Mg	101.5	16.0	23%	3	2	6.3	74.7	1	1159	1343	1	23464	Ran out
1480	10.0	29.0	75.8	18.0	4Sq	3	Mg	Mg	95.8	16.0	23%	3.1	2	6.6	74.1	1	1173	1348	1	22486	Ran out
1479	10.0	29.0	75.8	18.0	4Sq	3	Mg	Mg	98.1	18.2	13%	3.1	2	6.6	74.4	1	1205	1257	0.66	9887	Unst by Sta. 3
1478	10.0	29.0	46.0	18.0	4Sq	3.8	Ti	Ti	59.2	12.4	42%	3.1	2	6.6	83.6	1	1297	1413	1	16022	SS
"												0	0	1.0	85.4	3	1413	1528			Coast out
1477	10.0	29.0	46.0	18.0	4Sq	3.8	Ti	Ti	59.5	12.5	42%	3	2	7.5	96.6	1	1332	1332	0.5	0	Unst by Sta. 2
"												0	0	1.0	99.2	3					
1476	10.0	29.0	71.0	18.8	5Sq	3	Ti	Al	72.6	12.4	42%	3.1	2	6.5	85.1	1	1271	1369	1	13187	SS
"												0	0	1.0	84.4	5	1369	1417			SDU by Sta. 10
1475	10.0	29.0	71.0	18.8	5Sq	3	Ti	Ti	111.6	12.5	42%	3.05	2	6.5	76.0	3	1151	1257	1.33	9782	Unst by Sta. 5
"												3	2	7.5	119.6	1					
1474	10.0	29.0	71.0	18.8	5Sq	3	Ti	Ti	111.2	12.4	42%	3	2	6.4	75.7	3	1155	1229	1.2	7493	Unst by Sta. 4
"												3	2	7.5	118.8	1					
1473	10.0	29.0	71.0	18.8	5Sq	3	Ti	Ti	111.2	12.5	42%	3	2	6.4	72.7	3	1155	1604	3	21046	SS
"												3	2	7.5	111.1	1	1604	1687	1	13922	Ran out
1472	10.0	29.0	71.0	18.8	5Sq	3	Ti	Ti	111.2	12.4	42%	3.1	2	6.6	75.7	3	1168	1185			WFO, SDU by 7
"												3	2	7.5	109.2	1					
1471	10.0	29.0	71.0	18.8	5Sq	3	Al	Ti	111.9	12.4	42%	3.1	2	6.6	74.7	3	1164	1623	3	21733	SS
"												3	2	7.5	118.0	1	1623	1649	0.5	8672	Unst by Sta. 11
1470	10.0	29.0	71.0	18.8	5Sq	3	Al	Ti	111.5	12.1	42%	3.1	2	6.6	74.7	3	1147	1623	3	22401	SS
"												3	2	7.5	108.8	1	1623	1657	0.66	8612	Unst by Sta. 12
1469	10.0	29.0	71.0	18.8	5Sq	3	Ti	Ti	112.6	12.5	42%	3.1	2	6.6	75.1	3	1151	1623	3	22245	SS
"												3	2	7.5	109.2	1	1623	1699	0.5	25736	Unst by Sta. 11
1468	10.0	29.0	71.0	18.8	5Sq	3	Al	Al	113.4	12.6	42%	3.1	2	6.6	74.7	3	1151	1624	3	22300	SS
"												3	2	7.5	109.6	1	1624	1682	0.5	19546	Unst by Sta. 11
1467	10.0	29.0	71.0	18.8	5Sq	3	Al	Al	113.4	12.6	42%	0	0	0.0	0.0	1	1129	1144	1	1738	
"												3	2	6.4	76.6	2	1144	1204	1	7180	Unst by Sta. 7
"												3	2	7.5	109.6	1					
1466	10.0	29.0	71.0	18.8	5Sq	3	Ti	Ti	111.9	12.5	42%	0	0	0.0	0.0	1	1137	1161	1	2811	
"												3.1	2	6.6	76.5	2	1161	1301	1.33	13209	Unst by Sta. 8
"												3	2	7.5	109.4	1					
1465	10.0	29.0	71.0	18.8	5Sq	3	Ti	Ti	112.1	12.5	42%	0	0	0.0	0.0	1	1137	1153	1	1867	
"												3.1	2	6.6	76.5	2	1153	1454	2	19998	SS
"												3	2	7.5	109.6	1	1454	1461	0.33	3152	Unst by Sta. 10
1464	10.0	29.0	71.0	18.8	5Sq	3	Ti	Ti	112.3	12.6	42%	0	0	0.0	0.0	1	1125	1141	1	1848	
"												3.1	2	6.6	76.6	2	1141	1337	1.5	16503	Unst by Sta. 8
"												3	2	7.5	109.8	1					
1463	10.0	29.0	71.0	18.8	5Sq	3	Al	Al	113.5	12.5	42%	0	0	0.0	0.0	1	1141	1165	1	2821	
"												3.1	2	6.6	76.6	2	1165	1506	2	23211	SS
"												3	2	7.5	109.9	1	1506	1590	1	13255	Ran out
1462	10.0	29.0	71.0	18.8	5Sq	3	Al	Al	113.6	12.4	42%	0	0	0.0	0.0	1	1108	1126	1	2050	
"												3.1	2	6.6	77.2	2	1126	1126	0.33	0	Unst by Sta. 4
"												3	2	7.5	109.6	1					
1461	10.0	29.0	71.0	18.8	5Sq	3	Al	Al	113.5	12.5	42%	0	0	0.0	0.0	1	1133	1134	1	116	
"												3.1	2	6.6	76.6	2	1134	1134	0.33	0	Unst by Sta. 4
"												3	2	7.5	109.0	1					
1460	10.0	29.0	75.8	18.0	4Sq	3	Mg	Mg	103.0	12.6	42%	3.1	2	6.6	72.8	1.076	1112	1289	1	21660	SS
"												0	0	1.0	74.9	5	1289	1327			SDU by Sta. 8
1459	10.0	29.0	71.0	18.8	5Sq	3	Al	Al	113.6	12.5	42%	3.1	2	6.6	72.9	1.076	1112	1301	1	23244	SS

"												0	0	1.0	74.6	5	1301	1348			SDU by Sta. 14
CS65	10.0	29.0	75.8	18.0	4Sq	3	Mg	Mg	102.1	12.5	42%	0	0	1.0	74.8	3.076	1120	1152	0.33	11229	Unst by Sta. 1
CS64	10.0	29.0	75.8	18.0	4Sq	3	Mg	Mg	103.8	12.4	42%	0	0	1.0	51.1	3.076	1097	1118	0.33	7184	Unst by Sta. 1
CS63	10.0	29.0	71.0	18.8	5Sq	3	Al	Al	73.0	12.5	42%	0	0	1.0	84.5	3.076	1104	?	0.33	?	Unst by Sta. 1
CS62	10.0	28.8	69.6	18.2	4Sq	4.3	Al	Al	65.9	12.5	42%	0	0	1.0	49.8	3.076	1097	1148	1	5836	SS
CS61	10.0	29.0	71.0	18.8	5Sq	3	Al	Al	113.4	12.5	42%	0	0	1.0	75.3	3	1082	1118	0.5	8073	Unst by Sta. 2
CS60	10.0	29.0	71.0	18.8	5Sq	3	Al	Ti	110.9	12.6	42%	0	0	1.0	76.8	3	1082	1086	0.33	1339	Unst by Sta. 1
CS59	10.0	29.0	75.8	18.0	4Sq	3	Mg	Mg	?	12.4	42%	0	0	1.0	76.2	1	1050	?	0.33	?	Unst by Sta. 1
1458	10.0	29.0	71.0	18.8	5Sq	3	Al	Al	113.7	12.5	42%	0	0	0.0	0.0	1	1108	1118	1	1135	
"												3.1	2	6.6	85.3	2	1118	1118	0.33	0	Unst by Sta. 4
1457	10.0	29.0	71.0	18.8	5Sq	3	Al	Al	113.7	12.5	42%	0	0	0.0	0.0	1	1133	1150	1	1978	
"												3.1	2	6.6	76.2	2	1150	1154			WFO, SDU by 7
"												3	2	7.5	99.1	1					
1456	10.0	29.0	71.0	18.8	5Sq	3	Al	Al	113.6	12.3	42%	0	0	0.0	0.0	1	1129	1147	1	2088	
"												3	2	7.5	85.0	2	1147	1147	0.33	0	Unst by Sta. 4
1455	10.0	29.0	71.0	18.8	5Sq	3	Ti	Ti	117.0	12.5	42%	0	0	0.0	0.0	1	1129	1149	1	2322	
"												3.1	2	6.6	76.4	2	1149	1470	2	21425	SS
"												3	2	8.5	119.6	1	1470	1470	0.5	0	Unst by Sta. 11
1454	15.0	29.0	72.7	29.0	no fins	NA	Mg	Mg	107.0	12.3	42%	0	0	0.0	0.0	1	1167	1182	1	1796	
"												3.1	2	6.6	76.1	2	1182	1182	0.33	0	Unst by Sta. 4
1453	10.0	29.0	71.0	18.8	5Sq	3	Al	Al	113.5	12.6	42%	0	0	0.0	0.0	1	1120	1141	1	2420	
"												3.1	2	6.6	76.4	2	1141	1480	2	22643	SS
"												3	0	9.5	119.8	1	1480	1487	0.5	2117	Unst by Sta. 11
1452	10.0	29.0	71.0	18.8	5Sq	3	Al	Al	113.6	12.5	42%	0	0	0.0	0.0	1	1168	1186	1	2160	
"												3.1	2	6.7	76.4	2	1186	1359	0.83	27037	Unst by Sta. 9
"												3	0	9.5	120.3	1					
1451	10.0	29.0	71.0	18.8	5Sq	3	Al	Al	113.6	12.5	42%	0	0	0.0	0.0	1	1158	1178	1	2381	
"												3.1	2	6.6	76.4	2	1178	1233	1.5	4506	Unst by Sta. 8
"												3	0	9.5	120.3	1					
1450	10.0	29.0	71.0	18.8	5Sq	3	Al	Al	113.7	12.4	42%	0	0	0.0	0.0	1	1163	1182	1	2271	
"												3.1	2	6.6	76.3	2	1182	1493	2	21201	SS
"												3	0	9.5	109.6	1	1493	?	1	?	Ran out
1449	10.0	29.0	71.0	18.8	5Sq	3	Al	Al	113.5	12.5	42%	0	0	0.0	0.0	1	1152	1169	1	2011	
"												3.1	2	6.6	76.4	2	1169	1480	2	20995	SS
"												3	2	7.5	119.7	1	1480	1480	0.33	0	Unst by Sta. 10
1448	10.0	29.0	71.0	18.8	5Sq	3	Al	Al	113.5	12.3	42%	0	0	0.0	0.0	1	1156	1177	1	2497	
"												3.1	2	6.6	76.4	2	1177	1500	2	22035	SS
"												3	2	7.5	110.0	1	1500	1689	1	30720	Ran out
1447	10.0	29.0	71.1	17.8	4Sq	3	Mg	Mg	102.8	12.5	42%	0	0	0.0	0.0	1	1150	1180	1	3563	
"												3.1	2	6.6	76.9	2	1180	1180	0.2	0	Unst by Sta. 4
CS58	10.0	29.0	71.0	18.8	5Sq	3	Al	Al	113.6	12.5	42%	0	0	0.0	0.0	1	1150	1180	1	3563	
"												3	0	9.5	84.8	2	1180	?	0.33	?	Unst by Sta. 4
1446	10.0	29.0	71.0	18.8	5Sq	3	Al	Al	113.4	12.6	42%	0	0	0.0	0.0	1	1158	1173	1	1782	
"												3	2	7.5	85.1	2	1173	1173	0.33	0	Unst by Sta. 4
"												3	2	7.5	109.8	1					
1445	10.0	29.0	71.0	18.8	5Sq	3	Al	Al	113.5	12.6	42%	0	0	0.0	0.0	1	975	975	0	?	Sabot Failure
"												3	2	7.5	85.4	2					
"												3	2	7.5	98.6	1					
1444	10.0	29.0	71.0	18.8	5Sq	3	Al	Al	113.3	12.5	42%	0	0	0.0	0.0	1	1158	1173	1	1782	SS
"												3.1	2	6.6	75.6	2	1173	1487	2	21285	Ran out
"												3	2	7.5	98.7	1	1487	1692	1	33216	Ran out
1443	10.0	29.0	71.0	18.8	5Sq	3	Al	Al	113.8	?	42%	3.1	2	6.6	74.9	1	1185	1306	1	15362	SS
"												3	2	7.5	101.3	2	1306	1306	0.33	0	Unst by Sta. 4
"												3	2	7.5	109.8	1					

"												0	0	1.0	74.6	5	1301	1348			SDU by Sta. 14
CS65	10.0	29.0	75.8	18.0	4Sq	3	Mg	Mg	102.1	12.5	42%	0	0	1.0	74.8	3.076	1120	1152	0.33	11229	Unst by Sta. 1
CS64	10.0	29.0	75.8	18.0	4Sq	3	Mg	Mg	103.8	12.4	42%	0	0	1.0	51.1	3.076	1097	1118	0.33	7184	Unst by Sta. 1
CS63	10.0	29.0	71.0	18.8	5Sq	3	Al	Al	73.0	12.5	42%	0	0	1.0	84.5	3.076	1104	?	0.33	?	Unst by Sta. 1
CS62	10.0	28.8	69.6	18.2	4Sq	4.3	Al	Al	65.9	12.5	42%	0	0	1.0	49.8	3.076	1097	1148	1	5836	SS
CS61	10.0	29.0	71.0	18.8	5Sq	3	Al	Al	113.4	12.5	42%	0	0	1.0	75.3	3	1082	1118	0.5	8073	Unst by Sta. 2
CS60	10.0	29.0	71.0	18.8	5Sq	3	Al	Ti	110.9	12.6	42%	0	0	1.0	76.8	3	1082	1086	0.33	1339	Unst by Sta. 1
CS59	10.0	29.0	75.8	18.0	4Sq	3	Mg	Mg	?	12.4	42%	0	0	1.0	76.2	1	1050	?	0.33	?	Unst by Sta. 1
1458	10.0	29.0	71.0	18.8	5Sq	3	Al	Al	113.7	12.5	42%	0	0	0.0	0.0	1	1108	1118	1	1135	
"												3.1	2	6.6	85.3	2	1118	1118	0.33	0	Unst by Sta. 4
1457	10.0	29.0	71.0	18.8	5Sq	3	Al	Al	113.7	12.5	42%	0	0	0.0	0.0	1	1133	1150	1	1978	
"												3.1	2	6.6	76.2	2	1150	1154			WFO, SDU by 7
"												3	2	7.5	99.1	1					
1456	10.0	29.0	71.0	18.8	5Sq	3	Al	Al	113.6	12.3	42%	0	0	0.0	0.0	1	1129	1147	1	2088	
"												3	2	7.5	85.0	2	1147	1147	0.33	0	Unst by Sta. 4
1455	10.0	29.0	71.0	18.8	5Sq	3	Ti	Ti	117.0	12.5	42%	0	0	0.0	0.0	1	1129	1149	1	2322	
"												3.1	2	6.6	76.4	2	1149	1470	2	21425	SS
"												3	2	8.5	119.6	1	1470	1470	0.5	0	Unst by Sta. 11
1454	15.0	29.0	72.7	29.0	no fins	NA	Mg	Mg	107.0	12.3	42%	0	0	0.0	0.0	1	1167	1182	1	1796	
"												3.1	2	6.6	76.1	2	1182	1182	0.33	0	Unst by Sta. 4
1453	10.0	29.0	71.0	18.8	5Sq	3	Al	Al	113.5	12.6	42%	0	0	0.0	0.0	1	1120	1141	1	2420	
"												3.1	2	6.6	76.4	2	1141	1480	2	22643	SS
"												3	0	9.5	119.8	1	1480	1487	0.5	2117	Unst by Sta. 11
1452	10.0	29.0	71.0	18.8	5Sq	3	Al	Al	113.6	12.5	42%	0	0	0.0	0.0	1	1168	1186	1	2160	
"												3.1	2	6.7	76.4	2	1186	1359	0.83	27037	Unst by Sta. 9
"												3	0	9.5	120.3	1					
1451	10.0	29.0	71.0	18.8	5Sq	3	Al	Al	113.6	12.5	42%	0	0	0.0	0.0	1	1158	1178	1	2381	
"												3.1	2	6.6	76.4	2	1178	1233	1.5	4506	Unst by Sta. 8
"												3	0	9.5	120.3	1					
1450	10.0	29.0	71.0	18.8	5Sq	3	Al	Al	113.7	12.4	42%	0	0	0.0	0.0	1	1163	1182	1	2271	
"												3.1	2	6.6	76.3	2	1182	1493	2	21201	SS
"												3	0	9.5	109.6	1	1493	?	1	?	Ran out
1449	10.0	29.0	71.0	18.8	5Sq	3	Al	Al	113.5	12.5	42%	0	0	0.0	0.0	1	1152	1169	1	2011	
"												3.1	2	6.6	76.4	2	1169	1480	2	20995	SS
"												3	2	7.5	119.7	1	1480	1480	0.33	0	Unst by Sta. 10
1448	10.0	29.0	71.0	18.8	5Sq	3	Al	Al	113.5	12.3	42%	0	0	0.0	0.0	1	1156	1177	1	2497	
"												3.1	2	6.6	76.4	2	1177	1500	2	22035	SS
"												3	2	7.5	110.0	1	1500	1689	1	30720	Ran out
1447	10.0	29.0	71.1	17.8	4Sq	3	Mg	Mg	102.8	12.5	42%	0	0	0.0	0.0	1	1150	1180	1	3563	
"												3.1	2	6.6	76.9	2	1180	1180	0.2	0	Unst by Sta. 4
CS58	10.0	29.0	71.0	18.8	5Sq	3	Al	Al	113.6	12.5	42%	0	0	0.0	0.0	1	1150	1180	1	3563	
"												3	0	9.5	84.8	2	1180	?	0.33	?	Unst by Sta. 4
1446	10.0	29.0	71.0	18.8	5Sq	3	Al	Al	113.4	12.6	42%	0	0	0.0	0.0	1	1158	1173	1	1782	
"												3	2	7.5	85.1	2	1173	1173	0.33	0	Unst by Sta. 4
"												3	2	7.5	109.8	1					
1445	10.0	29.0	71.0	18.8	5Sq	3	Al	Al	113.5	12.6	42%	0	0	0.0	0.0	1	975	975	0	?	Sabot Failure
"												3	2	7.5	85.4	2					
"												3	2	7.5	98.6	1					
1444	10.0	29.0	71.0	18.8	5Sq	3	Al	Al	113.3	12.5	42%	0	0	0.0	0.0	1	1158	1173	1	1782	SS
"												3.1	2	6.6	75.6	2	1173	1487	2	21285	Ran out
"												3	2	7.5	98.7	1	1487	1692	1	33216	Ran out
1443	10.0	29.0	71.0	18.8	5Sq	3	Al	Al	113.8	?	42%	3.1	2	6.6	74.9	1	1185	1306	1	15362	SS
"												3	2	7.5	101.3	2	1306	1306	0.33	0	Unst by Sta. 4
"												3	2	7.5	109.8	1					

1442	10.0	29.0	71.0	18.8	5Sq	3	Al	Al	113.4	12.6	42%	3.1	2	6.6	75.3	1	1131	1252	1	14696	SS
"												3	2	7.5	100.3	2	1252	1311	0.5	15415	Unst by Sta. 5
"												3	2	7.5	109.8	1					
1441	10.0	29.0	71.0	18.8	5Sq	3	Al	Al	113.5	12.6	42%	3.2	2	6.9	71.2	1	1150	1185	0.66	6311	WFO by 3
"												3	2	6.5	100.3	2					
"												3	2	6.5	108.7	1					
1440	10.0	29.0	71.0	18.8	5Sq	3	Ti	Ti	112.4	12.6	42%	3	2	6.5	75.8	1	1154	1154	0.33	0	Unst by Sta. 1
"												3	2	6.5	96.5	2					
"												3	2	6.5	109.4	1					
1439	10.0	29.0	71.0	18.8	5Sq	3	Al	Al	113.6	12.6	42%	3	2	6.5	76.0	1	1163	1300	1	17198	SS
"												3	2	6.5	100.7	2	1300	?	0.83	?	Unst by Sta. 6
"												3	2	6.5	109.4	1					
1438	10.0	29.0	71.0	18.8	5Sq	3	Al	Al	113.7	12.6	42%	3	2	6.5	74.7	1	1112	1144	0.33	11150	Start Failure
"												3	2	6.5	100.1	2					
"												3	2	6.5	109.8	1					
1437	10.0	29.0	71.0	18.8	5Sq	3	Al	Al	113.4	12.6	42%	3	2	6.5	75.1	1	1096	1099	0.33	1017	Start Failure
"												3	2	6.5	100.5	2					
"												3	2	6.5	109.2	1					
1436	10.0	29.0	71.0	18.8	5Sq	3	Ti	Ti	112.4	12.5	42%	3	2	6.5	74.7	1	1129	1296	1	20641	SS
"												3	2	6.5	98.4	2	1296	1296	0.33	0	Unst by Sta. 4
"												3	2	6.5	111.9	1					
1435	10.0	29.0	71.0	18.8	5Sq	3	Ti	Ti	112.0	12.5	42%	3	2	6.5	74.5	1	1133	1291	1	19520	SS
"												3	2	6.5	100.7	2	1291	1301	0.4	3303	Unst by Sta.5
"												3	2	6.5	110.4	1					
1434	10.0	29.0	71.0	18.8	5Sq	3	Ti	Ti	112.8	12.5	42%	3	2	6.5	75.6	3	1150	1578	3	19837	SS
"												3	2	6.5	109.4	1	1578	1578	0.2	0	Unst by Sta. 10
1433	10.0	29.0	71.0	18.8	5Sq	3	Al	Al	113.4	12.5	42%	3	2	6.5	75.4	3	1157	1640	3	22952	SS
"												3	2	6.5	109.1	1	1640	1716	0.7	18571	Unst by Sta. 12
1432	10.0	29.0	71.0	18.8	5Sq	3	Al	Al	113.3	12.5	42%	3	2	6.5	76.9	1	1145	1257	1	13712	SS
"												3	2	6.5	109.8	2	1257	1291	0.2	22077	Unst by Sta. 4
1431	10.0	29.0	71.0	18.8	5Sq	3	Al	Al	113.5	12.6	42%	3	2	6.5	75.7	1	1163	1306	1	17995	SS
"												3	2	6.5	99.7	2	1306	1610	2	22591	Ran out
1430	10.0	29.0	71.0	18.8	5Sq	3	Al	Al	113.9	12.6	42%	3	2	6.5	73.9	1	1146	1291	1	18010	SS
"												0	0	1.0	99.8	2	1291	1327	0.5	9607	Unst by Sta. 5
1429	10.0	29.0	71.0	18.8	5Sq	3	Al	Al	113.5	12.6	42%	3	2	6.5	72.6	1	1158	1266	1	13343	SS
"												0	0	1.0	100.5	2	1266	1316	0.7	9400	Unst by Sta. 6
1428	10.0	29.0	71.0	18.8	5Sq	3	Al	Al	113.3	12.5	42%	3	2	6.5	84.1	1	1116	?	0.5	?	Unst by Sta. 2
"												0	0	1.0	100.0	2					
1427	10.0	29.0	71.0	18.8	5Sq	3	Al	Al	113.4	12.5	42%	3	2	6.5	73.2	1	1129	1261	1	16080	SS
"												0	0	1.0	111.8	2	1261	1261	0.33	0	Unst by Sta.4
1426	10.0	29.0	71.0	18.8	5Sq	3	Al	Al	113.6	12.6	42%	3	2	6.5	73.3	1	1085	1095	0.33	3367	SDU by Sta. 1
"												0	0	1.0	110.5	2					
1425	10.0	29.0	71.0	18.8	5Sq	3	Al	Al	113.6	12.5	42%	3	2	6.5	68.8	1	1154	1286	1	16416	SS
"												4	2	5.7	110.9	2	1286	1316	0.33	12056	Unst by Sta. 4
1424	10.0	29.0	71.0	18.8	5Sq	3	Al	Al	113.5	12.5	42%	3	2	5.7	49.9	1	1108	1252	1	17321	SS
"												4	0	7.7	100.0	2	1252	1258	0.33	2326	Unst by Sta. 4
1423	10.0	29.0	71.0	18.8	5Sq	3	Al	Al	113.7	12.6	42%	3	2	6.5	69.2	1	1120	1261	1	17111	SS
"												4	0	7.7	107.3	2	1261	1261	0.2	0	Unst by Sta. 4
1422	10.0	29.0	71.0	18.8	5Sq	3	Al	Al	113.6	12.6	42%	3	2	6.5	63.5	1	1125	1207	1	9746	SS
"												4	0	7.7	113.9	2	1207	1207	0.2	0	Unst by Sta. 4
1421	10.0	29.0	71.0	18.8	5Sq	3	Al	Al	113.3	12.5	42%	3	2	6.5	59.2	1	1150	1257	1	13127	SS
"												4	0	7.7	119.6	2	1257	1257	0.2	0	Unst by Sta. 4
1420	10.0	29.0	71.0	18.8	5Sq	3	Al	Al	113.5	12.6	42%	3	2	7.2	58.6	1	1154	1140	1	-1637	WFO
"												4	0	7.7	118.6	2	1140	1140	0.2	0	Unst by Sta. 4

1419	10.0	29.0	71.0	18.8	5Sq	3	Al	Al	113.5	12.6	42%	3	2	5.7	49.8	1	1154	1281	1	15762	SS
"												4	0	7.7	124.5	2	1281	1281	0.2	0	Unst by Sta. 4
1418	10.0	29.0	71.0	18.8	5Sq	3	Ti	Ti	120.6	12.5	42%	3	2	5.7	49.6	1	1158	1276	1	14639	SS
"												4	2	5.7	123.5	2	1276	1276	0.2	0	Unst by Sta. 4
1417	10.0	29.0	71.0	18.8	5Sq	3	Al	Al	114.0	12.4	42%	3	2	5.7	46.9	1	1143	1270	1	15619	SS
"												3.9	2	5.8	87.6	2	1270	1586	2	22999	Ran out
"												3.9	2	5.8	107.9	1	1586	1632	0.2	37724	Unst by Sta. 10
1416	10.0	29.0	71.0	18.8	5Sq	3	Al	Al	113.3	12.5	42%	3	2	5.7	49.6	1	1108	1233	1	14915	SS
"												3	2	8.0	124.0	3	1233	1233	0.2	0	Unst by Sta. 4
1415	10.0	29.0	71.0	18.8	5Sq	3	Al	Al	112.6	12.5	42%	3	2	5.7	49.6	1	1120	1224	1	12425	SS
"												3	2	5.7	116.6	3	1224	1224	0.2	0	Unst by Sta. 4
1414	10.0	29.0	71.0	18.8	5Sq	3	Al	Al	113.3	12.5	42%	3	2	5.7	49.9	1	1120	1257	1	16598	SS
"												3	2	5.7	98.3	3	1257	1796	3	27957	Ran out
1413	10.0	29.0	71.0	18.8	5Sq	3	Al	Al	112.3	12.5	42%	3	2	5.7	49.6	1	1125	1261	1	16539	SS
"												3	2	5.7	75.7	3	1261	1669	3	20310	Ran out
1412	10.0	29.0	71.0	18.8	5Sq	3	Al	Al	112.5	12.5	42%	3	2	5.7	47.3	1	1133	1305	1	21373	SS
"												3	2	5.7	46.2	3	1305	1597	3	14397	Ran out